2006

Expanding our knowledge of protein tyrosine phosphatase-like phytases : mechanism, substrate specificity and pathways of myo-inositol hexakisphosphate dephosphorylation

Puhl, Aaron A.

Lethbridge, Alta. : University of Lethbridge, Faculty of Arts and Science, 2006

EXPANDING OUR KNOWLEDGE OF PROTEIN TYROSINE PHOSPHATASE-LIKE PHYTASES: MECHANISM, SUBSTRATE SPECIFICITY AND PATHWAYS OF *MYO*-INOSITOL HEXA*KIS*PHOSPHATE DEPHOSPHORYLATION

AARON A. PUHL
Bachelor of Science, University of Lethbridge, 2006

A Thesis
Submitted to the School of Graduate Studies
of the University of Lethbridge
in Partial Fulfillment of the
Requirements for the Degree

MASTER OF SCIENCE
(Molecular Biology/ Biochemistry)

Department of Biological Sciences
University of Lethbridge
LETHBRIDGE, ALBERTA, CANADA

EXPANDING OUR KNOWLEDGE OF PROTEIN TYROSINE PHOSPHATASE-LIKE PHYTASES: MECHANISM, SUBSTRATE SPECIFICITY AND PATHWAYS OF *MYO*-INOSITOL HEXA*KIS*PHOSPHATE DEPHOSPHORYLATION

AARON A. PUHL

Approved:

(Print Name)	(Signature)	(Rank)	(Highest Degree)	(Date)
Supervisor				
Thesis Examination Committee Member				
Thesis Examination Committee Member				
External Examiner				
Chair, Thesis Examination Committee				

ABSTRACT

Expanding our knowledge of protein tyrosine phosphatase-like phytases: mechanism, substrate specificity and pathways of *myo*-inositol hexa*kis*phosphate dephosphorylation

A novel bacterial protein tyrosine phosphatase (PTP)-like enzyme has recently been isolated that has a PTP-like active site and fold and the ability to dephosphorylate *myo*-inositol hexa*kis*phosphate. In order to expand our knowledge of this novel class of enzyme, four new representative genes were cloned from 3 different anaerobic bacteria related to clostridia and the recombinant gene products were examined. A combination of site-directed mutagenesis, kinetic, and high-performance ion-pair chromatography studies were used to elucidate the mechanism of hydrolysis, substrate specificity, and pathways of Ins P_6 dephosphorylation. The data indicate that these enzymes follow a classical PTP mechanism of hydrolysis and have a general specificity for polyphosphorylated *myo*-inositol substrates. These enzymes dephosphorylate Ins P_6 in a distributive manner, and have the most highly ordered pathways of sequential dephosphorylation of $InsP_6$ characterized to date. Bioinformatic analyses have indicated homologues that are involved in the regulation of cellular function.

ACKNOWLEDGEMENTS

This work was carried out in the laboratory of Dr. L. Brent Selinger at the University of Lethbridge during the years 2004 - 2006. Dr. Selinger receives funding from the Natural Sciences and Engineering Research Council of Canada. I am grateful to my supervisor Dr. Selinger for giving me this opportunity, as well as for his positive and encouraging attitude towards my work and for providing an excellent working environment. My sincere thanks are due to my full committee; Dr. Selinger, Dr. James Thomas, and Dr. Steven Mosimann, for their guidance in the fields of microbiology, biochemistry and molecular biology. Also, thanks to Dr. Marie Fraser for acting as external examiner and for your helpful comments.

My thanks are also due to Dr. Ralf Greiner at the Centre for Molecular Biology of the Federal Research Centre for Nutrition and Food (Karlsruhe Germany) for collecting all of the HPIC data and for help with interpretation of that data. Analysis of the isomers of the individual *myo*-inositol phosphate derivatives by N.-G. Carlsson, Chalmers University of Technology (Göteborg, Sweden), is also gratefully acknowledged.

I am also grateful to Dr. H. J. Wieden for the use of his stopped-flow spectrophotometer, FPLC system, and size-exclusion chromatography column, as well as assistance with interpretation of results.

Finally, I wish to express my deepest gratitude to my family and to all my friends for their support and tolerance during my studies and life. To my best friend Saikat Basu, thanks for putting up with me never having time for my friends. Most importantly, I would like to thank my wife Christine Reinhart, for putting up with the countless hours I spent in the lab. I thank you for the patience, understanding, support, love and tolerance that you extend to me daily.

TABLE OF CONTENTS

LIST OF TABLES

LIST OF FIGURES

Chapter 1.

Chapter 2.

Chapter 3.

LIST OF ABBREVIATIONS

ADP   Adenosine 5'-Diphosphate
ATP   Adenosine 5'-Triphosphate
BCIP   5-bromo-4-chloro-3-indolyl phosphate
bp   Base Pairs
EDTA   EthyleneDiaminetetra-acetic acid
FPLC   fast protein liquid chromatography
HPIC   High Performance Ion-Pair Chromatography
Ins P_6 *myo*-Inositol Hexa*kis*phosphate
IPP   Inositol Polyphosphate
IPPase   Inostitol Polyphosphate Phosphatase
IPTG   Isopropyl β-D-thiogalactopyranoside
Lower IPP   IPP with < 6 phosphates
MALDI-TOF   Matrix-Assisted Laser Desorption Ionization-Time Of Flight
MIPP   (rat hepatic) Multiple Inositol Polyphosphate Phosphatase
M_r Molecular Weight
PCR   Polymerase Chain Reaction
PhyAme   PTP-Like Phytase from *Megasphaera elsdenii*
PhyAsl   PTP-Like Phytase from *Selenomonas lacticifex*
PhyAsr   PTP-Like Phytase from *Selenomonas ruminantium*
PhyAsrl   PTP-Like Phytase from *Selenomonas ruminantium* subsp. *lactilytica*
PhyBsl   PTP-Like Phytase from *Selenomonas lacticifex*
PIP_3 Phosphatidylinositol-3,4,5-triphosphate
ρNPP   ρ-nitrophenyl phosphate
PTP   Protein Tyrosine Phosphatase
R_h Hydrodynamic Radius
SDS-PAGE Sodium Dodecyl Sulfate – Polyacrylamide Gel Electrophoresis

NOTE

myo-inostiol phosphate isomers are abbreviated according to IUPAC rules of nomenclature. D/L – prefix is noted to indicate that the two stereoisomers are not discriminated. In those cases where no prefix is listed the compound is a symmetric meso-compound. Where enantiomers are not known, possible isomers are given and separated by a slash.

INTRODUCTION

myo-inositol polyphosphates (IPPs) make up a group of phosphorylated inositols which are recognized as storage molecules in plants and transmembrane signaling molecules in animals (Sasakawa *et al.*, 1995; Shears, 1998;2001; Raboy, 2003). IPPs have been implicated in *myo*-inositol, phosphate and cation storage (Lott and Buttrose, 1978a;1978b; Batten and Lott, 1986; Chen and Lott, 1992; Hawkins *et al.*, 1993; Wada and Lott, 1997), dsDNA break repair (Hanakahi *et al.*, 2000), clathrin-coated vesicular recycling and control of neurotransmission (Fukuda and Mikoshiba, 1997; Gaidarov *et al.*, 2001; Rizzoli and Betz, 2002; Brailoiu *et al.*, 2003), cell proliferation (Orchiston *et al.*, 2004) and increased natural killer cell activity in the blood of rats (Zhang *et al.*, 2005). The most abundant IPPs in most cells are the higher inositol polyphosphates, *myo*-inositol hexa*kis*phosphate (Ins P_6) and *myo*-inositol penta*kis*phosphate (Ins P_5) (Sasakawa *et al.*, 1995).

Enzymes that can catalyze the release of orthophosphate from Ins P_6 have been grouped together as phytases (myo-inositol hexa*kis*phosphate phosphohydrolases) (Mullaney and Ullah, 2003). Four distinct classes of phosphatases have been characterized in the literature as having phytase activity; *i.e.*, histidine acid phosphatases, ß-propeller phytases, purple acid phosphatases (Mullaney and Ullah, 2003) and most recently, a protein tyrosine phosphatase (PTP)-like enzyme from *Selenomonas ruminantium* (Chu *et al.*, 2004).

Phytate is the salt of Ins P_6 and the principal storage form of phosphorus in plant seeds (Reddy *et al.*, 1989). Non-ruminants are unable to metabolize phytate, making a majority of phosphorus in seed unavailable to these animals. The addition of phytase to the diet of monogastric livestock has been examined as a way to reduce phosphorus pollution resulting from intensive livestock operations (Reddy *et al.*, 1989). Phytate can also act as an antinutrient, chelating important minerals and proteins (Maga, 1982). The addition of phytase to the diet allows an animal to access more of the plant phytate phosphorus and increase bioavailability of essential minerals (Konietzny and Greiner, 2002). Despite the fact that ruminants are known to metabolize Ins P_6, there have been a limited number of studies addressing the genetic and enzymatic properties of phytases found in the rumen (Yanke *et al.*, 1998; Yanke *et al.*, 1999; Chu *et al.*, 2004).

More recently, inositol polyphosphate phosphatases (IPPases), including phytases, have become of interest for their ability to produce lower IPPs for kinetic and physiological studies. IPPs have been recognized as having novel metabolic effects, and the growing list of research and pharmaceutical applications for specific IPPs has increased interest in the preparation of these compounds (Greiner *et al.*, 2002b). The chemical synthesis of individual IPPs includes difficult synthetic steps, is performed at extreme conditions (Billington, 1993) and the separation of individual isomers is problematic with most analytical approaches (Greiner *et al.*, 2002b). Since phytases hydrolyze Ins P_6 in an ordered and stepwise manner, the production of IPPs and free *myo*-inositol using phytase is a promising alternative to chemical synthesis (Greiner and Konietzny, 1996; Greiner *et al.*, 2000a).

PTP superfamily enzymes have been discovered in a range of prokaryotes, and most appear to serve roles which mimic their better-known eukaryotic counterparts as regulators of cellular function (Shi *et al.*, 1998; Kennelly and Potts, 1999). The recently described PTP-like phytase from *S. ruminantium*, PhyAsr, contains a PTP-like active site signature sequence (HCEAGVGR), but lacks significant overall primary sequence identity with known phytases and PTPs (< 20%). While its biological function is unclear, it is the first example of a PTP-like enzyme with activity towards Ins P_6. A number of putative PTP-like PhyAsr homologues have since been partially cloned from a range of bacteria isolated from the rumen and other anaerobic sources (Nakashima *et al.*, 2006).

The primary aim of the present study was to use cloned representatives of this novel class (*i.e.*, PTP-like phytases) to expand our understanding of its properties and to examine the natural variability in both primary structure and functional characteristics. In particular, it was of interest to examine the functional relationship between these enzymes and PTPs. Mutation and chemical modification studies were performed to determine 1) if these enzymes use a classical PTP mechanism for dephosphorylation, and 2) if these enzymes display other properties characteristic of PTP superfamily enzymes. It was thought that this would give us a basic understanding of this novel class by establishing a functional relatedness with the well characterized PTPs. The enzymes from *S. ruminantium*, *S. ruminantium* subsp *lactilytica, S. lacticifex*, and *Megashaera elsdenii* were chosen for cloning because it was known from the literature that these enzymes displayed some sequence similarity to PhyAsr but represented unique proteins (<50% identity). Moreover, the genes encoding PTP-like phytases from these bacteria had neither been fully cloned nor recombinantly expressed and the enzymes had not been characterized. Finally, an attempt was made to expand our understanding of this class of phytases by identifying eukaryotic homologues.

CHAPTER ONE

Literature Review

1. *myo*-Inositol Hexa*kis*phosphate

myo-inositol hexa*kis*phosphate is the most abundant phosphorylated derivative of *myo*-inositol found in nature and has been more commonly referred to as phytic acid (Figure 1.1). Phytic acid is chemically described as *myo*-inositol 1,2,3,4,5,6-hexa*kis* dihydrogen phosphate or Ins P_6 (IUPAC-IUBMB, 1992a). Phytate is the salt of phytic acid and functions as the major storage form of phosphorus in plant seeds. Inositol polyphosphates (IPPs), including Ins P_6, have been found to play diverse roles in nature and thus their cellular functions, as well as their metabolism, has been the focus of many studies.

1.1. Structure and Chemistry

In the early 1900's, the molecular structure of Ins P_6 was correctly proposed by empirical determination of the molecular composition (Suzuki *et al.*, 1907; Anderson, 1914). This was verified 60 years later with ^{31}P-NMR, demonstrating the *myo*-inositol hexa-orthophosphate structure (Johnson and Tate, 1969). This, along with a more recent structure also derived using NMR, indicated a ring structure existing in a chair conformation with five equatorial phosphate groups and one axial (C-2) (Costello *et al.*, 1976). X-ray diffraction data suggested a five axial and single equatorial phosphate group conformation was favoured when stabilized by particular cations (Blank *et al.*, 1971). More recently still, ^{13}C NMR, ^{31}P NMR and Raman spectroscopy have been used to conclude that Ins P_6 exists in aqueous solution as a 1-axial/5-equatorial conformer at low pH (<9.2) and a 5-axial/1-equatorial conformer at high pH (>9.6) (Isbrandt and Oertel, 1980). Between pH 9.2–9.6 (the pKa range of the three least acidic protons) both conformations are in a dynamic equilibrium. ^{1}H NMR experiments have since further verified these conformations, as well as those of some lesser phosphorylated IPPs (Barrientos and Murthy, 1996). They showed that the conformational preferences of IPPs at different pHs are unique to a particular isomer and do not parallel the behaviour of Ins P_6.

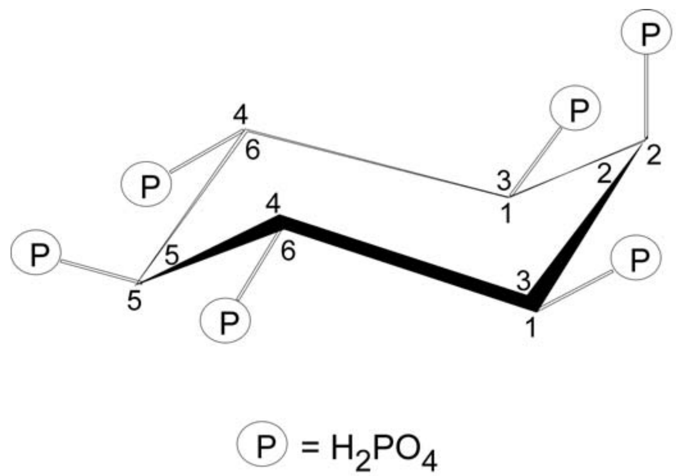

Figure 1.1. The most energetically favourable conformation of *myo*-inositol hexa*kis*phosphate, displaying 5 equatorial and 1 axial phosphate groups. The carbon atoms are numbered for the D-configuration (outside the ring) and L-configuration (inside the ring).

There are 12 proton dissociation sites on the Ins P_6 molecule, six of which are strongly acidic with approximate pK_a values of 1.8; three sites are weakly acidic with pK_a values between 5.7 and 7.6, and the remaining three sites are very weakly acidic, with pK_a values between 9.2 and 9.6 (Isbrandt and Oertel, 1980). The exact pK_a values were found to be dependent on the counterion species present and their concentration. Proton dissociation can leave the molecule with several negative charges over a broad pH range, which may attract positively charged molecules, and thus confers on Ins P_6 a high chelation capacity for multivalent cations and proteins. The conformational flexibility of Ins P_6 has a major impact on all of its binding interactions with both enzymes and cations.

The nomenclature of inositols has been an ongoing source of confusion and conflict. Ins P_6 is a *myo* compound with a plane of symmetry that crosses through C2 and C5 (Fig. 1). The remaining four carbon atoms consist of two prochiral pairs, C1/C3 and C4/C6. If the carbon ring is numbered counterclockwise, as shown by numbers outside the ring, assignment of a single substituent on carbon 1 is 1D. Conversely, if the carbon ring is numbered clockwise the assignment is 1L, as shown by numbers inside the ring (IUPAC-IUBMB, 1992b).

1.2. Occurrence and Distribution

It was discovered as early as 1872 that subcellular particles in wheat endosperm contain a calcium/magnesium salt of organic phosphate (Pfeffer, 1872). Since then it has been revealed that IPPs commonly form one to several percent of the dry weight of plant seeds (Lott, 1984). In mature seeds the IPPs are almost exclusively in the Ins P_6 form (Lott *et al.*, 2000). Phytate is the mixed cation salt of Ins P_6, and can often account for 50–80% of the total phosphorus in seeds (Cosgrove, 1966). The seeds of cereal grains and legumes show the highest content of phytate among plants (Reddy *et al.*, 1989). Ins P_6 has also been found in pollen (Jackson and Linskens, 1982a;1982b; Helsper *et al.*, 1984), spores (DeMaggio and Stetler, 1985), and vegetative tissues, such as roots, stems and leaves (Roberts and Loewus, 1968; Campbell *et al.*, 1991).

During the late 1970's, the presence of organic phosphates in red blood cells of birds, reptiles, and fish was discovered (Bartlett, 1976;1978; Isaacks *et al.*, 1978). Then, higher IPPs, including Ins P_6, were identified in mammalian GH_4 pituitary cells using metabolic labeling techniques with [^{3}H] inositol (Heslop *et al.*, 1985). Mammalian neural tissue was also shown to produce small amounts of Ins P_6, and other IPPs, upon exposure to bradykinin (Jackson *et al.*, 1987). These are but a few examples. Until recently, Ins P_6 was thought to be restricted to plants, but later studies have revealed that higher inositol polyphosphates are widespread and perhaps ubiquitous among eukaryotes (Sasakawa *et al.*, 1995).

1.3. Physiological Functions

Several physiological roles have been suggested for Ins P_6 in plant seeds and seedlings. The clearest role is as a store of *myo*-inositol (a cell wall precursor), phosphate and cations (Mg^{2+}, Ca^{2+}, Mn^{2+}, Fe^{3+} and Zn^{2+}) for use by seedlings (Lott and Buttrose, 1978a;1978b; Batten and Lott, 1986; Chen and Lott, 1992; Hawkins *et al.*, 1993; Wada and Lott, 1997). It has been suggested that Ins P_6 also has an antioxidant function in seeds during dormancy (Graf *et al.*, 1987). This assumption was based on the finding that Ins P_6 effectively blocks iron-driven hydroxyl radical formation. The role of Ins P_6 in plants has been exhaustively reviewed (Reddy *et al.*, 1982; Reddy *et al.*, 1989).

Due to the widespread discovery of IPPs across the eukaryotic kingdom, Ins P_6 and its lower IPP derivatives have become connected with a much wider array of important intracellular physiological functions. For example, stress was found to enhance Ins P_6 levels in yeast (Ongusaha *et al.*, 1998). Genetic studies have suggested that yeast might target Ins P_6 synthesis near the site of nuclear mRNA export (York *et al.*, 1999). Yeast mutants were identified that shared the common phenotypes of impaired mRNA export and restricted Ins P_6 synthesis. This led to the identification of a defective gene which normally encoded a I(1,3,4,5,6)P_5 2-kinase located on the nuclear periphery. A reasonable conclusion may be, that under stress, yeast increase their Ins P_6 pool in localized regions to signal export of specific mRNAs, that when translated into proteins counteract the stressful stimulus. Evidence has also been presented in the literature to suggest that IPPs may be directly involved with the regulation of transcription (Odom *et al.*, 2000). More recently, Ins P_6 has been shown to be required for the RNA editing activity of human ADAR2, possibly contributing to regulation of specific protein expression (Macbeth *et al.*, 2005).

Regulation of protein expression is but a single example of the possible roles of Ins P_6 and other IPPs; they have also been implicated in dsDNA break repair (Hanakahi *et al.*, 2000), clathrin-coated vesicular recycling and control of neurotransmission (Fukuda and Mikoshiba, 1997; Gaidarov *et al.*, 2001; Rizzoli and Betz, 2002; Brailoiu *et al.*, 2003), cell proliferation (Orchiston *et al.*, 2004) and increased natural killer cell activity in the blood of rats (Zhang *et al.*, 2005), among other functions. Additionally, cellular Ins P_6 and other IPPs are often precursors for other metabolites which also have roles in important physiological processes. Therefore, these *myo*-inositol phosphates can be used as enzyme substrates for metabolic investigation, as pathway inhibitors and therefore potentially as drugs (Laumen and Ghisalba, 1994). The abundance of possible roles for Ins P_6 and other higher IPPs in eukaryotes has been extensively reviewed (Sasakawa *et al.*, 1995; Chi and Crabtree, 2000; Shears, 2001; Michell *et al.*, 2003; Raboy, 2003).

It is becoming evident that maintenance of cellular metabolic reservoirs of IPPs is an important physiological activity in itself. There are a number of IPP phosphatases that have been implicated in the regulation of IPPs inside and outside the cell (Damen *et al.*, 1996; Lee *et al.*, 1999; Konietzny and Greiner, 2002; Michell, 2002; Deleu *et al.*, 2006).

1.4. Nutrition and the Environment

It was recently suggested that the majority of the extracellular Ins P_6 found in organs, tissues and biological fluids of mammals has a dietary origin and is not a consequence of endogenous synthesis, whereas intracellular Ins P_6 probably originates in the cell (Grases *et al.*, 2002; Grases *et al.*, 2005). Thus, health benefits linked to extracellular Ins P_6 are likely related to dietary phytate.

Phytate has been connected with a variety of health benefits when taken as a dietary supplement. For example, oral feeding of phytate can inhibit advanced human prostate cancer (PCA) xenograft growth in nude mice without toxicity (Singh and Agarwal, 2005). Phytate has also been found to contribute to the cholesterol lowering effect of soy protein in rats fed a cholesterol-enriched diet (Koba *et al.*, 2003). Moderate amounts of dietary phytate have also been implicated in a reduction of hepatic concentrations of total lipids and triglycerides in rats fed a high sucrose diet (Onomi *et al.*, 2004).

Conversely, phytate is not a good source of phosphorus for non-ruminant animals such as humans, chickens and pigs, as they are unable to metabolize it (Nelson, 1967; Nelson *et al.*, 1968b; Cromwell, 1980; Sandberg and Andersson, 1988). Additionally, due to proton dissociation, Ins P_6 carries several negative charges and will readily chelate divalent and trivalent cations such as Ca^{2+}, Zn^{2+}, Mg^{2+} and Fe^{3+}, as well as other trace minerals (Nelson, 1967; Nelson *et al.*, 1968a; Maga, 1982). A recent study determined that 50 mg or more of phytate in the diet of humans significantly reduced zinc absorption and calcium retention; this effect was shown to be strongly dose dependent (Fredlund *et al.*, 2006). Furthermore, Ins P_6 is known to bind with proteins, especially in an environment below the pI of the protein, maximizing the protein's positive charge. A decrease in the activity of the digestive enzymes trypsin and trypsinogen has been attributed to interaction with Ins P_6 (Caldwell, 1992).

2. Phytases

Biological systems rely on the hydrolysis of phosphate monoesters as part of many crucial processes, including energy metabolism, metabolic regulation, and many signal-transduction pathways. Because the hydrolysis of Ins P_6 is of great importance in biological systems, a specific class of enzymes hydrolysing this compound has evolved. Phytases (Ins P_6 phosphohydrolase), a special group of phosphatases, are the primary enzymes responsible for the sequential hydrolysis of Ins P_6 to inorganic monophosphate and lower IPPs. Thus, phytases are IPP degrading phosphatases which have the ability to hydrolyze Ins P_6.

2.1. Sources of Phytases

Microbial Sources

Phytate degrading enzymes have been most commonly found in fungi, particularly from the *Aspergillus* species (Konietzny and Greiner, 2002). The phytase from *A. ficuum* was the first studied for use as a commercial product (Wodzinski and Ullah, 1996). Phytate degrading enzymes have also commonly been found in many bacteria. The enzymes from *Bacillus* (Kerovuo *et al.*, 1998; Kim *et al.*, 1998a; Kim *et al.*, 1998b) and *Escherichia coli* (Greiner *et al.*, 1993) have been well characterized, structures determined (Ha *et al.*, 1999; Lim *et al.*, 2000) and can be found described in many reviews (Mullaney and Ullah, 2003; Oh *et al.*, 2004). Both intracellular and extracellular phytases have been purified from microbial sources (Oh *et al.*, 2004).

Plant Sources

Phytase activity has been found in many plants, such as maize (Laboure *et al.*, 1993), barley (Greiner *et al.*, 2000b), rye (Greiner *et al.*, 1998), spelt (Konietzny *et al.*, 1995), canola seed (Houde *et al.*, 1990) and lily pollen (Scott and Loewus, 1986). Unlike the phytases produced by microorganisms, it has been more difficult to purify plant phytases from contaminating nonspecific phosphatases (Laboure *et al.*, 1993); thus, only a few phytases from plant sources have been purified to homogeneity and extensively characterized.

Animal Sources

Phytate-degrading enzymes have been isolated from the intestinal mucosae of some monogastric animals (Bitar and Reinhold, 1972; Copper and Gowing, 1983; Yang *et al.*, 1991; Chi *et al.*, 1999). A multiple inositol polyphosphate phosphatase (MIPP) displaying phytate-degrading activity was also identified in rat hepatic tissue, localized in the ER lumen. Although the MIPP mRNA could be found ubiquitously in rat tissues, it was most highly expressed in the kidney and liver (Craxton *et al.*, 1997). More recently, MIPP homologues have been cloned from mice and humans (Chi *et al.*, 1999). A phytate-degrading enzyme has also been purified and characterized from the protozoan *Paramecium* (Freund *et al.*, 1992).

2.2. Classes of Phytases

It is becoming evident that phytate degrading enzymes are widespread in nature. To date, the characterized phytases include representatives of histidine acid phosphatases (HAP), purple acid phosphatases (PAP), and β propeller phytases (BPP) (Mullaney and Ullah, 2003). The X-ray structure of a novel phytate-degrading enzyme from *Selenomonas ruminantium* has recently been determined and suggests a new class of phytase; *i.e.*, the protein tyrosine phosphatase (PTP)-like phytases (Chu *et al.*, 2004).

Histidine Acid Phytases

The majority of cloned and characterized phytases share a common signature sequence and catalytic mechanism, and are members of a single class of phosphatase; *i.e.*, high molecular weight, histidine acid phosphatases (HAPs) (Konietzny and Greiner, 2002; Mullaney and Ullah, 2003). HAPs share a highly conserved RHGXRXP sequence motif for catalysis and a HD sequence motif which facilitates substrate binding and product leaving (Schneider *et al.*, 1993; Kostrewa *et al.*, 1997; Kostrewa *et al.*, 1999).

It was proposed that members of the HAP class follow a two step mechanism of dephosphorylation (van Etten, 1982), which has been investigated with site-directed mutagenesis studies (Ostanin *et al.*, 1992; Ostanin and van Etten, 1993) and crystal structures of transition-state complexes (Lim *et al.*, 2000; Liu *et al.*, 2004). These results indicate that: (1) the positive charge on the guanidinium group of arginine in the tripeptide RHG interacts directly with the phosphate group of the substrate, making it more susceptible to nucleophilic attack, (2) the histidine residue serves as a nucleophile in the formation of a covalent phosphohistidine intermediate, and (3) the aspartic acid residue from the C-terminal HD sequence motif protonates the leaving group. Both prokaryotic and eukaryotic HAPs are known and they share little sequence homology other than the conserved active site sequence motif. HAPs are unable to hydrolyze a metal-Ins P_6 complex (Lim *et al.*, 2000).

Purple Acid Phosphatases

Phytate-degrading enzymes have been cloned from *Aspergillus niger* (Mullaney and Ullah, 1998) and soybean seedlings (Hegeman and Grabau, 2001) which contain sequence motifs in conserved positions relative to kidney bean PAPs, which are members of a dimetal-containing phosphoesterase (DMP) family. PAPs share conserved metal-ligating residues which form binuclear Fe(III)-Me(II) centers, where Me is Fe, Mn, or Zn (Strater *et al.*, 1995; Klabunde *et al.*, 1996; Schenk *et al.*, 1999). The metal ions are coordinated by seven invariant amino acids, which are essential features of the active site found in all PAP sequences. A metal-bridging, or metal coordinated hydroxide ion in the metal centers has been suggested to directly attack the phosphorus atom of the substrate (Kimura, 2000). There has been debate over the precise mechanism of PAPs, but recent mutagenesis experiments have begun to identify the roles of key active site residues (Funhoff *et al.*, 2005; Truong *et al.*, 2005).

β Propeller Phytases

Phytases were cloned from *Bacillus* species independently by two groups. These enzymes are not related to any other phytases or phosphatases in sequence databanks, nor do they contain the conserved HAP active site sequence motif RHGXRXP (Kerovuo *et al.*, 1998; Kim *et al.*, 1998a; Kim *et al.*, 1998b). Unlike HAPs, these enzymes are dependent on Ca^{2+} ions for stability and activity, implying a different mode of Ins P_6 hydrolysis (Kerovuo *et al.*, 2000). X-ray diffraction data of the *B. amyloliquefaciens* phytate-degrading enzyme has revealed a six-bladed propeller structure which has been found in a range of proteins and exhibits a notable functional diversity (Ha *et al.*, 2000). There are six calcium-binding sites in each protein molecule. Calcium ions facilitate the binding of substrate by providing a favorable electrostatic environment (Oh *et al.*, 2001). BPPs have two phosphate binding sites, a cleavage site and an affinity site (Shin *et al.*, 2001). The phosphate in the cleavage site is hydrolyzed, while the affinity site enhances binding of substrates containing adjacent phosphate groups, such as Ins P_6.

2.3. A Novel Class of Phytase, Protein Tyrosine Phosphatase-like Phytases

A novel Ins P_6-degrading enzyme has recently been cloned from an anaerobic ruminal bacterium, *Selenomonas ruminantium* (Cheng et al., 1999; Selinger et al., 1999; Selinger et al., 2000). The primary sequence of this enzyme contains a PTP-like signature sequence ($C(X)_5R$), which is ubiquitous among members of the PTP superfamily (Figure 1.2) (Zhang, 2002). The structure of this enzyme consists of two domains, the larger having a protein tyrosine phosphatase (PTP)-like fold (Chu *et al.*, 2004). The PTP-like domain most closely resembles members of the dual-specificity PTPs and the PTP-like inositol/inositide phosphatase PTEN (Chu *et al.*, 2004). The sequence and structure of this enzyme suggests that it is distantly related to PTPs and shares a common mechanism of catalysis.

PTP Superfamily Phosphatases

The $C(X)_5R$ active site signature sequence is characteristic of enzymes belonging to the PTP superfamily (Denu and Dixon, 1998; Zhang, 2002). These enzymes are a diverse group found in both prokaryotes and eukaryotes, which include tyrosine-specific, dual specificity (DSP), low-molecular-weight (LMW), Cdc25, and phosphoinositide/IPP phosphatases (Taylor and Dixon, 2003; Zhang, 2003). These enzymes are key mediators of a wide variety of cellular processes, including growth, metabolism, gene transcription, differentiation, motility, apoptosis, cell-cell interactions and tumor suppression (Zhang, 1998;2002;2005).

```
PTP1B  : VPESPASFLNFLFKVRESGSLSPEHGPVVVHCSAGIGRSGTFCLADTCLLLMDKRKDPSS
DSPTP  : DRAVPEDLPTFTAFLDEVMEQLLDGRTVVVHCRGGLGRAGLTAACLLTQAGMPPEQAIAR
LMWPTP : ---MMILREWFQGSKQVLPRSSEDKIGVLFVCMANFCRSPMAKGLFQQLVAHHHLSHAIF
CDC25  : NLHSQKELLHEFFLRKPVLPLDIQKRVIIVFLCEFSSERGPRMCRSLREKDRALNQYPALY
PTEN   : HNPPQLELIKPFCEDLDQWLSEDDNHVAAIHCKAGKGRTGVMICAYLLHRGKFLKAQEAL
PhyAsr : ATDHVWPTPENIDRFLAFYRTLPQDAWLHFHCEAGVGRTTAFMVMTDMLKNPSVSLKDIL
                                        *     *
```

Figure 1.2. The C(X)$_5$R motif of different members of the PTP superfamily. The alignment of the region containing the P-loop was generated with GeneDoc (Nicholas *et al.*, 1997) according to alignment consensus (black = 100%; dark grey = 75%; light grey = 50%) with similarity groups enabled. The catalytically relevant Cys and Arg of the P-loop are identified with asterisks. The protein abbreviation, PTP family, GenBank accession number and residues included in the alignment are as follows: PTP1B, tyrosine-specific phosphatase, P18031, 184-243; DSPTP, dual-specificity phosphatase, YP_604354, 96-155; LMWPTP, low molecular weight phosphatase, YP_344818, 1-57; CDC25, M-phase inducer phosphatase, AAA74912, 319-378; PTEN, phosphoinositide/phosphoinositol phosphatase, AAD13528, 93-152; PhyAsr, phytate-degrading enzyme, AAQ13669, 221-280.

Most PTP superfamily enzymes hydrolyze phosphoryl groups from protein substrates, specifically, phosphotyrosine, -threonine and -serine containing peptides (Figure 1.3) (Zhang, 2002). Recently, PTP-like enzymes have been characterized which specifically hydrolyze phosphoinositides and IPPs, such as PTEN (Maehama and Dixon, 1998; Deleu *et al.*, 2006) and the phytate-degrading enzyme from *S. ruminantium* (Chu *et al.*, 2004) (Figure 1.3). The principal biological substrate for many PTP superfamily enzymes still remains unknown (Zhang, 2002).

All PTPs have similar core structures, consisting of a central parallel ß-sheet with flanking α-helices, and a single catalytic pocket which contains the PTP signature sequence at its base (Figure 1.4). The active site pocket of PTP superfamily enzymes is variable in size and shape, and may be responsible for the different substrate specificities found within this superfamily. For example, the deeper active site pocket of tyrosine-specific phosphatases (9 Å) selects phosphotyrosine containing substrates exclusively (Jia *et al.*, 1995; Dunn *et al.*, 1996), whereas the more shallow active site pocket of dual-specificity phosphatases (6 Å) can accommodate phosphotyrosine, -threonine and –serine containing substrates (Yuvaniyama *et al.*, 1996; Stewart *et al.*, 1999). Each group within the PTP superfamily has evolved distinct structural components peripheral to the conserved PTP-core which are responsible for the variability found in the catalytic pocket (Figure 1.4). Non-catalytic regions that flank the catalytic core of PTP superfamily enzymes often contribute to their diverse cellular functions (Mauro and Dixon, 1994; Andersen *et al.*, 2001b; Tonks and Neel, 2001). Regardless of the size or shape of the catalytic pocket, or the substrate hydrolyzed, all PTP superfamily enzymes characterized to date proceed through similar steps of catalysis (Zhang, 2003).

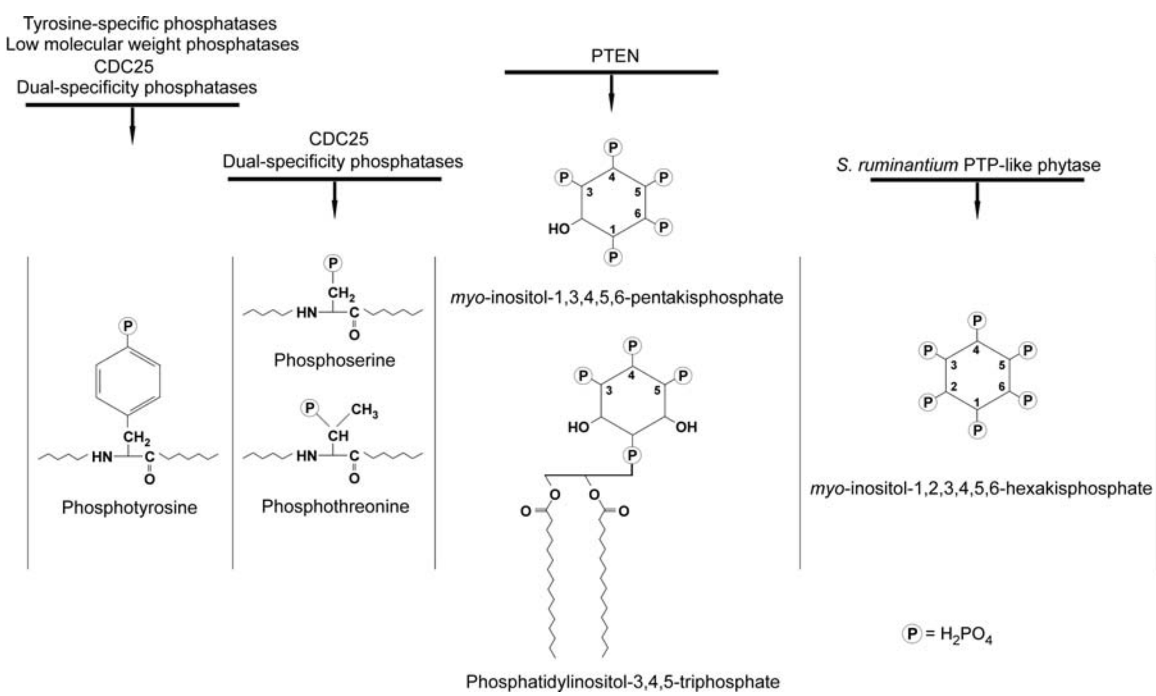

Figure 1.3. Two-dimensional illustrations of the various biological substrates hydrolyzed by members of the PTP superfamily.

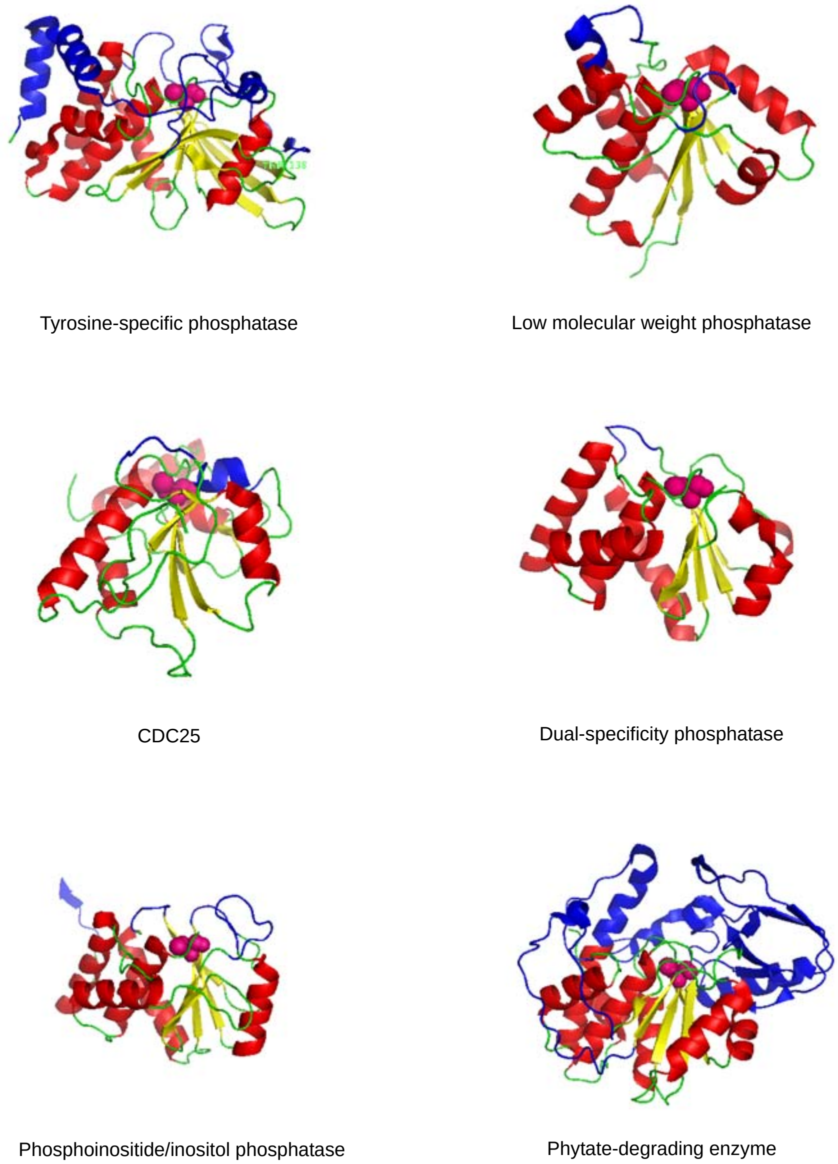

Figure 1.4. Three-dimensional structures of representatives of the six groups of enzymes belonging to the PTP superfamily. The group, description and PDB accession numbers are as follows: tyrosine-specific phosphatase, human PTP1B, 2CM2; low molecular weight phosphatase, human B-form PTP, 1XWW; CDC25, human CDC25B, 1CWT; dual-specificity phosphatase, human MAP kinase phosphatase 5, 1ZZW; phosphoinositide/inositol phosphatase, PTP domain of human PTEN, 1D5R; phytate-degrading enzyme, *Selenomonas ruminantium* PhyA, 1U24. PTP superfamily core structures are coloured green for loops, red for helices and yellow for strands. The invariant, catalytic cysteines are displayed as spheres colored magenta. Blue regions indicate structural variability contributing to the shape and depth of the catalytic pocket.

Catalytic Mechanism

Site-directed mutagenesis, mechanistic studies and crystal structures have greatly improved our understanding of the PTP catalytic mechanism. The core structure, as well as the mechanism for PTP-catalyzed phosphate monoester hydrolysis, is conserved across the PTP superfamily.

All PTPs have a phosphate-binding loop (P-loop) at the base of their active site which contains the characteristic PTP signature sequence $C(X)_5R$ (refer to Figure 1.2) (Denu and Dixon, 1998; Zhang, 2003). Site-directed mutagenesis studies have determined that the cysteine residue present in the P-loop is absolutely required for PTP activity (Guan and Dixon, 1990; Pot *et al.*, 1991; Cirri *et al.*, 1993; Zhou *et al.*, 1994). Cysteine is a strong nucleophile, and is easily modified by thiol reagents (Salvatore and Chait, 1998). Chemical modification experiments with alkylating agents also indicate that the P-loop cysteine is required for PTP activity (Pot *et al.*, 1991; Pot and Dixon, 1992; Zhang and Dixon, 1993; Zhou *et al.*, 1994). PTPs use the nucleophilic cysteine residue to bind the phosphate monoester of the substrate, forming a thiol-phosphate intermediate (Guan and Dixon, 1991; Pannifer *et al.*, 1998).

The main chain nitrogens of the P-loop residues in combination with the guanidinium group of the invariant arginine side chain have been suggested to coordinate the oxygens of the phosphate group into an optimal orientation and stabilize the highly negative charge of the substrate (Barford *et al.*, 1994). The guanidinium group is ideally suited for a coplanar bidentate complex with two of the phosphate oxygens during catalysis (Cotton *et al.*, 1973). Indeed, mutational analysis of the *Yersinia* PTPase (Zhang *et al.*, 1994c) and PTP1B (Flint *et al.*, 1997) indicate that the signature sequence arginine has a critical role in catalysis, most likely to stabilize the transition state, and to a smaller extent, influences substrate binding.

PTP superfamily enzymes have been shown to follow a general acid-base mechanism of dephosphorylation. Mutagenesis studies with the *Yersinia* PTP have suggested that an aspartic acid residue located upstream of the PTP signature sequence is responsible for the basic limb of the pH vs. rate of substrate hydrolysis profile (Zhang *et al.*, 1994b). This was an indication that the aspartic acid must be protonated for optimal hydrolytic activity. Accordingly, the PTP mechanism was suggested to utilize the aspartic acid as a general acid, donating a proton to the ester oxygen of the substrate leaving group to facilitate bond cleavage (Zhang *et al.*, 1994b; Jia *et al.*, 1995). Cleavage of the scissile bond results in a thiol-phosphate intermediate and a free substrate product (Guan and Dixon, 1991). The equivalent aspartic acid residue from a dual-specificity phosphatase has also been implicated in activation of a water molecule, thought to be responsible for hydrolysis of the enzyme-phosphate intermediate (Denu and Dixon, 1995). The importance of an aspartic acid acting as a general acid has similarly been shown in the low-molecular-weight PTPase from yeast (Wu and Zhang, 1996) and mammalian PTP1B (Lohse *et al.*, 1997).

PTEN: a PTP-like IPP/Phosphoinositide Phosphatase

The structure of the phytate-degrading enzyme from *S. ruminantium* suggests that it is distantly related to the PTP superfamily and shares a common mechanism of catalysis. It contains a PTP-like $C(X)_5R$ active site signature sequence and has a common fold with dual-specificity PTPs and the phosphoinositide/inositol phosphatase PTEN (Chu *et al.*, 2004).

The synthesis and turnover of phosphoinositides in a cell are regulated by lipid kinases, lipid phosphatases, and phospholipases. The discovery of new families of phosphatases that specifically hydrolyze phosphoinositides has paralleled the elucidation of a variety of complex cellular processes in which these molecules play crucial roles (reviewed by: (Zhang and Majerus, 1998; Takenawa and Itoh, 2001; Deleris *et al.*, 2006; Takenawa and Itoh, 2006). One such phosphatase, PTEN, is structurally related to the DSP family of PTPs, and is well known for its actions as a tumor suppressor (Li *et al.*, 1997; Myers *et al.*, 1997). This action is believed to arise from its ability to hydrolyze the 3-phosphate from the membrane-bound lipid PtdIns(3,4,5)P_3, which is a signal in the regulation of apoptosis, cell proliferation and cell migration (Maehama and Dixon, 1998; Myers *et al.*, 1998; Maehama and Dixon, 1999; Sulis and Parsons, 2003; Leslie and Downes, 2004; Leslie *et al.*, 2005).

There is good evidence that PTEN association with cellular membranes is required for activation of its PtdIns(3,4,5)P_3 phosphatase activity (McConnachie *et al.*, 2003; Iijima *et al.*, 2004). The significance of the large reservoir of free cytoplasmic PTEN has therefore been questioned. PTEN was found to dephosphorylate the 3-phosphate group of soluble inositol polyphosphates (Maehama and Dixon, 1998; Caffrey *et al.*, 2001). The functional significance of soluble PTEN has thus been implied from its ability to regulate cellular levels of Ins(1,3,4,5,6)P_5, a mammalian signaling molecule (Caffrey *et al.*, 2001; Deleu *et al.*, 2006). Ins(1,3,4,5,6)P_5 has been implicated in regulation of viral assembly (Campbell *et al.*, 2001), chromatin remodeling (Steger *et al.*, 2003) and the activity of L-type Ca^{2+} channels (Quignard *et al.*, 2003). It has also been shown to be involved with anchorage-independent colony formation and anchorage-dependent proliferation in human glioblastoma cells as well as with modulation of apoptotic responses (Orchiston *et al.*, 2004; Piccolo *et al.*, 2004).

2.4. Enzmatic Properties of Phytases

The majority of the characterized phytases are monomeric proteins, but both homo- and hetero-oligomers have been found (Konietzny and Greiner, 2002). The molecular mass of these phytases is variable; most monomeric proteins are in the range of 40–70 kDa. Most phytases have an optimal temperature for Ins P_6 hydrolysis between 40–80°C (Konietzny and Greiner, 2002).

pH Optima

Phytases can be divided into two major groups, acid and alkaline, based on their optimal pH for catalysis. Since most interest in phytases has focused on finding an enzyme that would function in the digestive tract of monogastric animals, most studies have focused on acid phytases (Mullaney and Ullah, 2003).

Acid phytases include those enzymes belonging to the HAP, PAP and more recently, PTP-like classes of phosphatases. HAPs have been isolated from a variety of microbial sources such as *Aspergillus* species (Wyss *et al.*, 1999) and *E. coli* (Greiner *et al.*, 1993). HAPs can display a range of pH vs. activity profiles that can be broad or narrow in range, and have a variety of pH optima, most commonly found at pH 2.5 and/or pH 4.5-6 (Konietzny and Greiner, 2002; Mullaney and Ullah, 2003; Oh *et al.*, 2004). Two PAPs have been characterized as having phytate degrading activity. The phytase from kidney beans displays optimal activity between pH 4.5-5 (Hegeman and Grabau, 2001) and that from *A. niger*, pH 6 (Mullaney and Ullah, 1998). The phytate-degrading enzyme produced by *S. ruminantium*, PhyAsr, was reported to have substantial activity at pH 5, but no optimal pH has been reported (Chu *et al.*, 2004).

Alkaline phytases have been isolated from plants such as *Lilium longiflorum* pollen (Scott and Loewus, 1986) and some legume seeds (Scott, 1991). Alkaline phytases have also been isolated from *Bacillus* species, and more recently, purified from species of *Bifidobacterium* (Haros *et al.*, 2005). The BPPs from *Bacillus* are the only extensively characterized class of alkaline phytase (Kerovuo *et al.*, 1998; Kim *et al.*, 1998a; Tye *et al.*, 2002). Although no sequence data are available for most of the remaining alkaline phytases and primary structure comparisons are impossible, all alkaline phytases seem to share biochemical characteristics similar to BPPs from *Bacillus* species. Alkaline phytases optimally hydrolyze phytate at a pH between 7 and 8, likely due to protonation of calcium binding sites at a lower pH resulting in poor binding of Ca^{2+} (Oh *et al.*, 2001).

Substrate Specificity

Many of the characterized HAPs exhibit a broad specificity for substrates with phosphate esters. It is thought that this is due to a mechanism that conforms to nonspecific acid phosphatase properties, since both HAPs and acid-phosphatases have the ability to hydrolyze synthetic phosphorylated substrates (Gibson and Ullah, 1988). In *A. fumigatus*, the phytase crystal structure has revealed a large active site cleft (Liu *et al.*, 2004) allowing it to accommodate a wide variety of phosphate esters (Pasamontes *et al.*, 1997). In contrast, the *E. coli* phytase is more specific for phytate (Greiner *et al.*, 1993), and accordingly, the crystal structure of this enzyme reveals a smaller active site cleft (Lim *et al.*, 2000). HAPs can only hydrolyze Ins P_6 when it exists as a metal-free phytate (Maenz *et al.*, 1999; Wyss *et al.*, 1999). The positively charged active site cleft of HAPs does not favor a metal-Ins P_6 complex (Kostrewa *et al.*, 1999; Lim *et al.*, 2000; Liu *et al.*, 2004). Chelating agents such as EDTA have been shown to stimulate the phytate-degrading activity of HAPs by removing divalent metal cations (Maenz *et al.*, 1999; Wyss *et al.*, 1999).

The substrate specificity of alkaline phytases is far narrower than that of HAPs, exhibiting strict specificity towards phytate and having relatively no enzymatic activity on other phosphate esters (Kim *et al.*, 1998a; Oh *et al.*, 2001). The strict specificity of alkaline phytases is explained by the preference for phosphate bridge formation between Ca^{2+} and the two oxianions from the adjacent phosphate groups of Ins P_6 (Ha *et al.*, 2000; Oh *et al.*, 2001; Shin *et al.*, 2001). When dealing with phytate specifically, alkaline phytases require divalent cations such as Ca^{2+} or Sr^{2+} for catalytic activity (Oh *et al.*, 2001). The crystal structure of the phytase from *B. amyloliquefaciens* revealed a negatively charged active site that provides a favorable electrostatic environment for the positively charged calcium–Ins P_6 complex (Ha *et* *al.*, 2000). Consequently, EDTA strongly inhibits alkaline phytase activity by removing the required divalent metal cations (Kerovuo *et al.*, 1998; Kim *et al.*, 1998b).

Ins P_6 Hydrolysis

Based on the position of the first phosphate hydrolyzed, three types of phytases are recognized by the Enzyme Nomenclature Committee of the International Union of Biochemistry; *i.e.*, 3-phytase (EC 3.1.3.8), 6-phytase (EC 3.1.3.26) and 5-phytase (EC 3.1.3.72). Accordingly, phytases have been characterized that can initiate hydrolysis at the D-3 (L-1), L-6 (D-4) or D-6 (L-4) phosphate positions (Konietzny and Greiner, 2002). Traditionally, phytases from microorganisms have been described as 3-phytases (EC 3.1.3.8), whereas seeds of higher plants were said to contain 6-phytases (EC 3.1.3.26). The phytate-degrading enzymes from *Pseudomonas* (Cosgrove *et al*., 1970), *Bacillus* spp. (Greiner *et al.*, 2002b), *Klebsiella terrigena* (Greiner *et al*., 1997; Sajidan *et al*., 2004), *Candida krusei* (Quan *et al.*, 2003), *Pantoea agglomerans* (Greiner, 2004), *Aspergillus ficuum* (Irving and Cosgrove, 1972) and *Saccharomyces cerevisiae* (Turk *et al.*, 2000) fit this general description. Phytate-degrading enzymes isolated from many plants also fit into this general category, such as those from mung bean (Maiti *et al.*, 1974), rice (Hayakawa *et al.*, 1990), wheat (Nakano *et al.*, 2000), and a variety of other cereals (Greiner and Alminger, 2001) and legumes (Greiner *et al.*, 2002a). However, this is not an absolute rule and is becoming less applicable, as illustrated by indications of 3-phytase activity in lupine seeds (Greiner, 2002) and 6-phytase activity in *E. coli* (Greiner *et al.*, 1993). Recently characterized basidiomycete fungi have been shown to have dual pathways, hydrolyzing either the 3 or 6-position (Lassen *et al.*, 2001). Additionally, an alkaline phytase that is present in lily pollen and seeds initiates hydrolysis at the 5-phosphate of Ins P_6, a selectivity not previously displayed by phytases (Barrientos *et al.*, 1994). More recently, the extracellular phytate-degrading enzyme from *S. ruminantium*, PhyAsr, has also been described as a 5-phytase (Chu *et al.*, 2004).

To date, knowledge of the order in which phytases hydrolyze phosphate groups from phytate and the Ins P_6 derivatives they produce is limited. Most characterized phytases hydrolyze Ins P_6 in a stepwise manner, yielding *myo*-inositol penta*kis*-, tetra*kis*-, tris-, bis-and mono-phosphate products (Konietzny and Greiner, 2002). The acid phytases have generally been found to release five or even all six phosphate groups of phytate, and *myo*-inositol monophosphate and *myo*-inositol, respectively, have been detected as their final degradation products (Konietzny and Greiner, 2002). Alternatively, the alkaline phytases are poor at accepting a *myo*-inositol phosphate with three or fewer phosphate residues as a substrate, and *myo*-inositol trisphosphate has been shown to be their end product without high levels of enzyme activity and long incubation times (Greiner *et al.*, 2002b). Extensive characterization of BPPs has shown this to be a result of preference for adjacent phosphate groups on the substrate (Shin *et al.*, 2001; Greiner *et al.*, 2002b). The pathway of hydrolysis by phytate-degrading enzymes seems to be unique for each species, and may be evidence of the variety of roles played by these enzymes, Ins P_6, and its derivatives, in biological systems.

2.5. Physiological Roles of Phytases

It is becoming increasingly evident that phytate degrading enzymes are widespread in nature and the role of these enzymes in each organism varies and largely depends on the specific function attributed to the substrate Ins P_6. The presence of multiple phytases with differing specificity, pH optima, and biochemical properties within individual species suggests that hydrolysis of Ins P_6 is under the control of multiple phytases. We are likely entering a new period of research which will involve elucidating the physiological importance of multiple phytases and the biological roles of the IPPs they produce.

Microorganisms

In microorganisms, phytase expression is most frequently induced and the enzymes sometimes secreted in response to phosphate starvation. The expression of phytases can result in release of phosphate from surrounding and/or internal Ins P_6 stores. This is not the only factor affecting the production of microbial phytate-degrading enzymes. For example, the synthesis of periplasmic phytate-degrading enzymes in *E. coli* was found to drastically increase in the stationary phase and when under anaerobic conditions (Greiner *et al.*, 1993), and *K. terrigena* was found to increase phytate degrading activity when phytate was present in the cultivation medium (Greiner *et al.*, 1997). Additionally, (Chatterjee *et al.*, 2003) have suggested that phytase activity may be required for optimal virulence in *Xanthomonas oryzae*. This might suggest that many of the biological roles of phytate degrading enzymes remain unknown.

Plants

In plants, phytase is induced during germination, to degrade phytate, and thus provide the growing seedling with orthophosphate, lower IPPs, free myo-inositol and previously bound cations, such as K^+, Mg^{2+}, Zn^{2+}, and Ca^{2+} (Reddy *et al.*, 1989). These products are then utilized for the purpose of plant growth. Interestingly, the constitutive alkaline phytase that is present in lily pollen and seeds removes the 5, 4 and then 6-phosphate of Ins P_6 to yield Ins (1,2,3)P_3 as the final product. This final product has been shown to inhibit iron-catalyzed free radical formation by chelating iron (Hawkins *et al.*, 1993; Spiers *et al.*, 1995; Phillipy and Graf, 1997).

The role of *myo*-inositol phosphate intermediates in the transport of materials into the cell has been established. In particular, *myo*-inositol trisphosphates are important in transport as secondary messengers and in signal transduction (Shears, 1998). These molecules can be the products of phytate hydrolysis.

Animals

The role of phytases in animal cells is more difficult to understand. It is becoming evident that maintenance of the cell's metabolic reservoirs of Ins P_6 and other IPPs is an important physiological activity. A phytate-degrading enzyme belonging to the HAP family of phosphatases, multiple inositol polyphosphate phosphatase (MIPP), displays an ability to regulate the cellular activities of Ins P_6 and Ins(1,3,4,5,6)P_5 (Craxton *et al.*, 1997; Chi *et al.*, 2000; Deleu *et al.*, 2006). Additionally, MIPP-generated metabolites are themselves physiologically active as a Ca^{2+}-mobilizing signal (Yu *et al.*, 2003). Due to upregulation of MIPP mRNA during chondrocyte hypertrophy it was suggested that MIPP may aid bone mineralization and salvage the inositol moiety prior to apoptosis (Caffrey *et al.*, 1999). The evolutionary conservation of MIPP within the inositol phosphate pathway suggests a significant role for MIPP throughout higher eukaryotes (Chi *et al.*, 1999).

2.6. Applications of Phytases

Ins P_6 is not a good source of phosphorus for non-ruminant animals as they are unable to metabolize it (Nelson, 1967; Nelson *et al.*, 1968b). This has had considerable impact on modern intensive livestock operations due to the introduction of grain based diets, as up to 80% of phosphorus in cereal grains and legumes is present as phytate phosphorus (Reddy *et al.*, 1989). A consequence is the need to supplement monogastric livestock diets with inorganic phosphate in order to provide adequate nutrition (Nelson, 1967; Nelson *et al.*, 1968b). The Ins P_6 present in the diet is excreted in the manure and is subsequently hydrolyzed by soil and water borne microorganisms. The released phosphate moves into rivers and lakes and can result in eutrophication of water supplies (Raboy, 2001; Turner *et al.*, 2002). Supplementation of animal feed with phytase enables the utilization of organic phosphate by monogastrics and reduces the amount of phosphate in manure, preventing it from reaching the environment (Wodzinski and Ullah, 1996; Haefner *et al.*, 2005). More recently, phytate-degrading enzymes have become of interest for their ability to produce lower inositol polyphosphates (IPPs). The IPPs generated are useful for kinetic and physiological studies. IPPs have been recognized as having novel metabolic effects such as prevention of diabetes complications (Ruf *et al.*, 1991; Carrington *et al.*, 1993; Ruf *et al.*, 1994), treatment of chronic inflammation (Claxson *et al.*, 1990), reduction in the risk of colon cancer (Baten *et al.*, 1989; Graf and Eaton, 1993; Shamsuddin *et al.*, 1997) and kidney stone prevention (Modlin, 1980; Ohkawa *et al.*, 1984). Additionally, the IPPs D-*myo*-inositol (1,3,4,5) tetra*kis*phosphate and D-*myo*-inositol (1,4,5) triphosphate have been found to stimulate intracellular Ca^{2+} release which affect cellular metabolism and secretion (Potter, 1990; Harmer *et al.*, 2002; Migita *et al.*, 2005). The growing list of research and pharmaceutical applications for specific IPPs has increased interest in the preparation of these compounds. The chemical synthesis of individual IPPs includes difficult steps and is performed at extreme conditions (Billington, 1993). The separation of IPP isomers has also been reported to be difficult with most analytical approaches (Greiner *et al.*, 2002b). Since phytases hydrolyze Ins P_6 in an ordered and sequential manner, the production of IPPs and free *myo*-inositol using phytase is a potential and promising alternative to chemical synthesis (Greiner and Konietzny, 1996; Wodzinski and Ullah, 1996; Greiner *et al.*, 2000a; Haefner *et al.*, 2005).

CHAPTER TWO

PhyAsr from Selenomonas ruminantium uses a classical PTP mechanism to facilitate 3-phytase activity

ABSTRACT

PhyAsr from *Selenomonas ruminantium* is a protein tyrosine phosphatase (PTP)-like phytase with a number of unique properties inferred from structural studies. In order to elucidate its mechanism of hydrolysis and pathway of Ins P_6 dephosphorylation, a combination of site-directed mutagenesis and kinetic studies have been conducted. The data indicate PhyAsr follows a classical PTP mechanism of hydrolysis and has a general specificity for polyphosphorylated *myo*-inositol substrates. A combination of high-performance ion-pair chromatography and kinetics were used to determine that, in contrast to previous reports, PhyAsr preferentially cleaves the 3-phosphate position of Ins P_6. PhyAsr produces Ins(2)P via a highly ordered pathway of sequential dephosphorylation of $InsP_6$: D-Ins(1,2,4,5,6)P_5, Ins(2,4,5,6)P_4, D-Ins(2,4,5)P_3 and D-Ins(2,4)P_2.

2.1 INTRODUCTION

myo-inositol polyphosphates (IPPs) make up a group of phosphorylated inositols which are recognized as ubiquitous products of inositol metabolism (Sasakawa *et al.*, 1995). The most abundant IPPs in most cells are the higher inositol polyphosphates, *myo*-inositol hexa*kis*phosphate (Ins P_6) and *myo*-inositol penta*kis*phosphate (Ins P_5) (Sasakawa *et al.*, 1995). The biological importance of IPPs in eukaryotic cells has been well established (Sasakawa *et al.*, 1995; Chi and Crabtree, 2000; Shears, 2001; Raboy, 2003; Irvine, 2005). Moreover, IPPs have been recognized as having novel metabolic effects, and the growing list of research and pharmaceutical applications for specific IPPs has increased interest in the preparation of these compounds (Greiner *et al.*, 2002b).

Enzymes that can catalyze the release of orthophosphate from Ins P_6 have been grouped together as phytases (myo-inositol hexa*kis*phosphate phosphohydrolases) (Mullaney and Ullah, 2003). Four distinct classes of phosphatases have been characterized in the literature as having phytase activity; histidine acid phosphatases, ß-propeller phytases, purple acid phosphatases (Mullaney and Ullah, 2003) and most recently, a protein tyrosine phosphatase (PTP)-like enzyme from *Selenomonas ruminantium* (PhyAsr) (Chu *et al.*, 2004).

Protein tyrosine phosphatase (PTP) superfamily enzymes have been discovered in a range of prokaryotes, and most appear to serve roles which mimic their better-known eukaryotic counterparts as regulators of cellular function (Shi *et al.*, 1998; Kennelly and Potts, 1999). The recently described PTP-like phytase from *S. ruminantium*, PhyAsr, contains a PTP-like active site signature sequence (HCEAGVGR), but lacks significant primary sequence identity with known IPPases and PTPs (< 20%). While its biological function is unclear, it is the first example of a PTP-like enzyme with activity towards Ins P_6. The X-ray crystallographic structure of PhyAsr (Chu *et al.*, 2004) reveals a PTP-like fold and a number of novel catalytic properties have been inferred. In particular, it has been suggested that PhyAsr is the first example of a PTP-like enzyme to hydrolyze substrate processively, starting with the 5-phosphate position and utilizing a stand-by site to bind successive intermediates. This is novel among PTP-like enzymes and non-PTP-like IPPases. The characterized phytases are distributive enzymes, such that each myo-inositol phosphate intermediate dissociates from the enzyme and may act as a substrate in further hydrolysis reactions (Konietzny and Greiner, 2002). Further, most phytases initiate hydrolysis at the D-3 (L-1) or D-4 (L-6) phosphate positions and some at the D-6 position (Konietzny and Greiner, 2002; Oh *et al.*, 2004). Additionally, unlike other characterized PTP superfamily enzymes, the P-loop of PhyAsr was observed in both a catalytically inactive “open” form in the absence of ligand and an active “closed” form with ligand bound (Chu *et al.*, 2004).

The catalytic mechanism of PTP superfamily enzymes has been extensively studied. The active site signature sequence, $C(X)_5R$, is required for activity (Zhang *et al.*, 1994b; Zhang, 1998;2002;2003) and follows a general acid-base mechanism of dephosphorylation. The invariant Cys residue exists as a cysteinate and catalysis involves the formation of a phosphocysteine intermediate (Guan and Dixon, 1990; Cirri *et al.*, 1993; Zhang *et al.*, 1994c; Zhou *et al.*, 1994). Main-chain amines and the guanidinium group of the conserved Arg coordinate the oxygens of the phosphate group in the catalytic site and stabilize the negative charge of the substrate (Barford *et al.*, 1994) while an invariant Asp serves as the general acid (Zhang *et al.*, 1994b; Jia *et al.*, 1995; Lohse *et al.*, 1997).

Given the unique catalytic properties of PhyAsr inferred from structural studies we have investigated the catalytic mechanism using a combination of kinetic and site-directed mutant studies. We present experimental data that indicates PhyAsr follows a classical PTP mechanism of catalysis. A combination of high-performance ion-pair chromatography and kinetics were used to determine that, in contrast to previous reports, PhyAsr preferentially cleaves the D-3-phosphate position of Ins P_6. Finally, the complete Ins P_6 dephosphorylation pathway for the enzyme has been determined and is consistent with a distributive mechanism for the sequential removal of phosphate groups.

2.2 MATERIALS AND METHODS

Expression construct production

The region coding for the mature *S. ruminantium* phytase (*phyAsr*; GeneBank accession number AF177214) was amplified from genomic DNA using polymerase chain reaction (PCR). PhyAsr Forward and Reverse primers (Table 2.1) included an NdeI site (CAT ATG) for cloning and a 5’ GC cap. The signal peptide sequence was predicted using SignalP 3.0 (Nielsen *et al.*, 1997; Bendtsen *et al.*, 2004). PhyAsr numbering begins with 1 at the N-terminus of the protein sequence found in GeneBank. The PCR product was digested with *Nde*I and ligated into similarly digested pET28b vector (Novagen, San Diego, CA). Mutant proteins C252S, C252A, R258K and D223N were prepared from *phyA*sr using the QuikChange Site-Directed Mutagenesis Kit (Stratagene, La Jolla, CA) according to the manufacturer's instructions. Mutagenesis primers are listed in Table 2.1. Constructs were sequenced by automated cycle sequencing at the University of Calgary, Core DNA and Protein services facilities. Sequence data were analyzed with the aid of SEQUENCHER™ version 4.0 (Gene Codes Corp. Ann Arbor, MI) and MacDNAsis version 3.2 (Hitachi Software Engineering Co., Ltd., San Bruno, CA).

Table 2.1. Primers employed in this study.

Construct	**Primer Name**	**Primer sequence**
PhyAsr	For	GCC ATA TGG CCA AGG CGC CGG AGC AG
	Rev	GCC ATA TGG CGC CAT TTC CCT GAC TC
C252S	For	GCT CCA TTT CCA TTC TGA AGC CGG TGT CG
	Rev	CGA GGT AAA GGT AAG ACT TCG GCC ACA GC
C252A	For	GCT CCA TTT CCA TGC GGA AGC CGG TGT CG
	Rev	CGA CAC CGG CTT CCG CAT GGA AAT GGA GC
R258K	For	GCC GGT GTC GGC AAG ACG ACG GCG TTC
	Rev	GAA CGC CGT CGT CTT GCC GAC ACC GGC
D223N	For	CAT CGC GGC GAC GAA TCA CGT CTG GCC AAC GC
	Rev	GCG TTG GCC AGA CGT GAT TCG TCG CCG CGA TG

Protein production and purification

Escherichia coli BL21 (DE3) cells (Novagen Inc., Madison, WI) were transformed with the *phyAsr* expression constructs. Protein expression was accomplished according to the instructions in the pET Systems Manual (Novagen Inc.). Protein over expression was induced in cultures by adding IPTG to a final concentration of 1 mM. Incubation was continued overnight at 37^{o}C.

Induced cells were harvested and resuspended in lysis buffer: 20 mM KH_2PO_4 (pH 7), 0.3 M NaCl, 1 mM β-mercaptoethanol (BME), 5% glycerol and one Complete Mini, EDTA-free protease inhibitor tablet (Roche Applied Science; Laval, QC). Cells were lysed with a Branson (Danbury, CT) model 450 sonifier. Cell debris was removed by centrifugation at 20 000 x g. Recombinant 6xHis tagged PhyAsr was purified to homogeneity by metal chelating affinity chromatography (Ni^{2+}-NTA-agarose) according to the supplied protocol (Qiagen Corp, Mississauga, ON). Protein was washed on the column with lysis buffer containing 15 mM imidazole and eluted with lysis buffer containing 0.4 M imidazole. Purified protein was dialyzed overnight into 20 mM HEPES (pH 7), 0.3 M NaCl, 0.1 mM EDTA and 1 mM BME. The homogeneity of the purified protein was confirmed by 12% w/v SDS-polyacrylamide gel electrophoresis (Laemmli, 1970), and Coomassie Brilliant Blue R-250 staining. Protein concentrations were determined using the extinction coefficient calculated by PROT-PARAM (Gasteiger *et al.*, 2005).

Assay of enzymatic activity and quantification of the liberated phosphate

Activity measurements were carried out at 37°C. Enzyme reaction mixtures consisted of a 600 μl buffered substrate solution and 150 μl of a 25 nM enzyme solution. The buffered substrate solution contained 50 mM Na-acetate (pH 5) and 2 mM sodium phytate or a variable concentration (0.025 – 4 mM) of one of the individual IPPs used in our study. Ionic strength was held constant at 0.2 M with the addition of NaCl. Following the appropriate, empirically determined incubation period, the reactions were stopped and the liberated phosphate was quantified. Preliminary characterization, pH vs. rate and alkylation studies were done using the ammonium molybdate method previously described (Yanke *et al.*, 1998). A 750 μL aliquot of 5% (w/v) trichloroacetic acid was added to stop the reaction, followed by the addition of 750 μL of phosphomolybdate coloring reagent. The coloring reagent was prepared by the addition of 4 volumes 1.5% (w/v) ammonium molybdate solution in 5.5% (v/v) sulfuric acid to 1 volume 2.7% (w/v) ferrous sulfate solution. Liberated inorganic phosphate was measured as A_{700} on the spectrophotometer. For kinetic studies we used a modified Heinonen and Lahti method which was better suited to the range of substrate concentrations involved (Heinonen and Lahti, 1981). A 1.5 mL aliquot of a freshly prepared solution of acetone/5 N H_2SO_4/10 mM ammonium molybdate (2:1:1 v/v/v) was added to the assay mixture for stopping and detection, followed by 100 μL 1.0 M citric acid.

In order to quantify the released phosphate, a calibration curve was produced for each quantification method over a range of 5-600 nmol phosphate / 2 mL reaction mixture. Activity (U) was expressed as μmol phosphate liberated per min. Blanks were run by addition of the stop solution to the assay mixture prior to addition of the enzyme solution. The steady-state kinetic constants (K_m, k_{cat}) for the hydrolysis of Ins P_6 and its derivatives by PhyAsr were calculated from regressional analysis (Sigma-plot 8.0; Systat Software Inc.; Point Richmond, CA) of Lineweaver-Burk plots of the data.

Preparation of individual myo-inositol phosphate isomers

Lyophilized PhyAsr was shipped to Dr. Ralf Greiner at the Centre for Molecular Biology of the Federal Research Centre for Nutrition and Food in Karlsruhe Germany where HPIC, production and isolation of lower IPPs and kinetic studies with lower IPPs was performed.

D-Ins(1,2,4,5,6)P_5, D-Ins(1,2,5,6)P_4 and Ins(2,4,5,6)P_4 were obtained as described previously(Greiner *et al.*, 2002a; Greiner *et al.*, 2002b). For the production of IPP isomers generated by PhyAsr, sodium phytate (2.5 mmol) was incubated at 37°C in a mixture containing 50 mM NH_4-acetate (pH 5.0) and 10 U of the purified enzyme in a final volume of 500 μL. After an incubation period of 30 min, the reaction was stopped by heat treatment (95°C, 10 min).

The incubation mixture was lyophilised and the dry residues were dissolved in 10 mL 1.0 M NH_4-formate (pH 2.5). The solution was loaded onto a Q-Sepharose column (2.6 x 90 cm) equilibrated with 1.0 M NH_4-formate (pH 2.5) at a flow rate of 2.5 mL/min. The column was washed with 500 mL of 1.0 M NH_4-formate (pH 2.5); the bound IPPs were eluted with a linear gradient from 1.0 to 1.4 M NH_4-formate (pH 2.5) (1000 mL) at 2.5 mL/min. Fractions of 10 mL were collected. From even-numbered tubes, 100 μL aliquots were lyophilised. The residues were dissolved in 3 N H_2SO_4 and incubated for 90 min at 165°C to hydrolyse the eluted IPPs completely. The liberated phosphate was measured as previously described. The content of the fraction tubes corresponding to the individual IPPs were pooled and lyophilised until only a dry residue remained. The residue was dissolved in 10 mL of water. Lyophilisation and redissolving were repeated twice. IPP concentration was determined by High-Performance Ion-Pair Chromatography (HPIC) on Ultrasep ES 100 RP18 from Bischoff Chromatography (Leonberg, Germany) (Sandberg and Ahderinne, 1986). The purity of the IPP preparation was determined on an HPIC system (Skoglund *et al.*, 1998). D-Ins(2,4,5)P_3 and D-Ins(2,4)P_3 were obtained in the same ways by using the Ins P_6-degrading enzyme from *Klebsiella terrigena*.

Identification of enzymatically formed hydrolysis products

The enzymatic reaction was started at 37°C by addition of 50 μL of a suitable diluted solution of PhyAsr to the incubation mixtures (2 U/mL). The incubation mixture consisted of 1.250 mL 0.1M sodium acetate buffer (pH 5.0) containing 3.125 μmol sodium phytate or one of the purified individual lower IPP esters. From the incubation mixture, 100 μL samples were removed periodically and the reaction was stopped by heat treatment (95°C, 10 min). 50 μL of the heat-treated samples were resolved on an HPIC system using a Carbo Pac PA-100 (4 x 250 mm) analytical column (Dionex; Sunnyvale, CA) and a gradient of 5–98% HCl (0.5 M, 0.8 mL/min) (Skoglund *et al.*, 1998). The eluants were mixed in a post-column reactor with 0.1%

$Fe(NO_3)_3$ in a 2% $HClO_4$ solution (0.4 mL/min) (Phillippy and Bland, 1988). The combined flow rate was 1.2 mL/min.

Identification of the myo-inositol monophosphate isomer

Myo-inositol monophosphates were produced by incubation of 1.0 U of PhyAsr with a limiting amount (0.1 μmol) of the individual IPP ester (Ins(1,2,3,4,5,6)P_6, D-Ins(1,2,3,5,6)P_5, D-Ins(1,2,5,6)P_4, Ins(2,4,5,6)P_4) in a final volume of 500 μL of 50 mM NH_4-formate. After lyophilization, the residues were dissolved in 500 μL of a solution of pyridine: bis(trimethylsilyl)trifluoroacetamide (1:1 v/v) and incubated at room temperature for 24 h. The silylated products were injected at 270°C into a gas chromatograph coupled with a mass spectrometer. The stationary phase was methylsilicon in a fused silica column (0.25 mm x 15 m). Helium was used as the carrier gas at a flow rate of 0.5 m/s. The following heating program was used for the column: 100°C to 340°C, rate increase: 4°C/min. Ionisation was performed by electron impact at 70 eV and 250°C.

Enzyme modification

Alkylation of PhyAsr was carried out in 20 mM HEPES (pH 7) containing 10 mM freshly prepared iodoacetic acid (IAA) and 1 M guanidine at room temperature in the dark. The modification reaction was initiated with the addition of 1 nmol of enzyme to the reaction mixture (final volume of 500 μL). A control reaction was prepared in the same way except iodoacetate was omitted. At 10 minute intervals 50 μL aliquots were withdrawn and diluted in 700 μL of 0.05 M NaAc (pH 5). 150 μL of the diluted modification reaction was then assayed for phytase activity as described previously. The modification reaction was repeated in the presence of a range of sodium phytate concentrations. The percentage of residual phytase activity was calculated relative to the control. For samples analyzed by mass spectrometry, excess IAA was quenched with addition of 10 x molar excess dithiothreitol.

Mass spectrometry

Mass analysis was performed on both PhyAsr and the alkylation product using Matrix Assisted Laser Desorption/Ionization Time-of-Flight (MALDI-TOF) at the McGill University proteomics lab. The theoretical accuracy of this instrument is 1 for every 2000 Da, or, 0.05% of the total mass of PhyAsr. Masses were obtained for the modified and unmodified proteins followed by tryptic digestion and tandem mass spectrometry (MS/MS) analysis.

2.3 RESULTS

Recombinant PhyAsr kinetics

The catalytic properties of the recombinant wild-type PhyAsr towards Ins P_6 as a substrate were determined (Table 2.2). The rate of PhyAsr catalyzed phosphate release can be saturated by increasing concentrations of Ins P_6 and remains linear over the time period of the assay (data not shown). The initial rates of reaction as a function of Ins P_6 concentration are consistent with a classical Michaelis-Menton enzyme mechanism (data not shown). The apparent k_{cat} and K_m for wild-type PhyAsr were determined to be 264 ± 19 s^{-1} and 425 ± 28 μM respectively.

Table 2.2. Kinetic parameters for phytase activity of PhyAsr and various PhyAsr mutants. Values given are the average ± standard deviation of at least three separate experimental runs.

Construct	**k_{cat} (s^{-1})**	**K_m (µM)**
PhyAsr	264 ± 19	425 ± 28
C252S	0	-
C252A	0	-
D223N	0.84 ± 0.06	40.0 ± 9.7
R258K	0.25 ± 0.01	410 ± 131

Modification and mutational studies

Structural and bioinformatic analysis of PhyAsr have revealed a PTP-like core structure and a conserved PTP-like active site signature sequence. In order to confirm the participation of the PhyAsr Cys252 thiol group in the catalytic mechanism, chemical modification experiments using iodoacetic acid (IAA) were performed. The wild-type recombinant enzyme hydrolyzed Ins P_6 at a rate of 668.11 μmol Pi min^{-1} mg^{-1}, which was normalized to 100% activity. PhyAsr can be inactivated by IAA (Figure 2.1). Following 60 minutes of incubation with IAA, 96% of activity was lost relative to the control. Mass spectrometry was used to confirm that only the lone Cys was modified. The mass of the

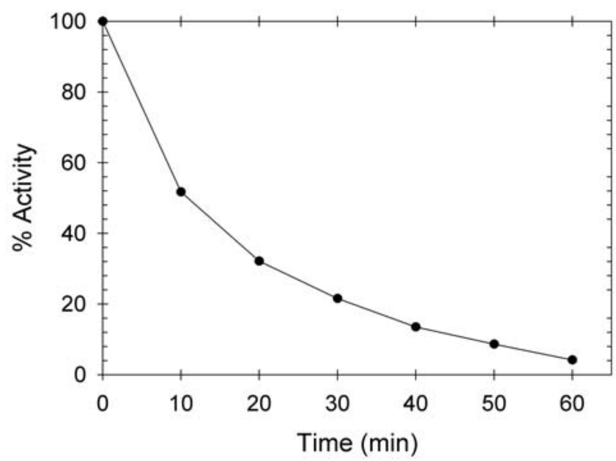

Figure 2.1. Time course of PhyAsr inactivation by 10 mM iodoacetate (IAA). Residual activity is plotted as a function of time incubated with IAA relative to a control reaction.

alkylated PhyAsr was determined to be 37,946 ± 19 Da and that of the unalkylated PhyAsr was 37,898 ± 19 Da. The difference of 48 Da is in good agreement with the expected difference of 59 Da, predicted to correspond to a single alkylation event. Whole protein analysis was followed by tryptic digestion and MS/MS fragmentation. The alkylation event was mapped to a single digest fragment containing the PTP signature sequence (underlined) and the proposed nucleophilic Cys252, TLPQDAWLHFH<u>CEAGVGR</u>. IAA can also alkylate histidine residues under the proper conditions. To confirm that Cys252 was indeed the residue modified, PhyAsr C252S mutant enzyme was similarly alkylated. Alkylation of the C252S mutant yielded a product equal in mass to that of the unalkylated enzyme, indicating that under our conditions there were no modifiable residues accessible to IAA. Additionally, Ins P_6 was found to provide concentration-dependent protection against the inactivation caused by IAA (Figure 2.2). Further, we have shown that replacement of Cys252 of PhyAsr with either Ser or Ala completely abolished IPPase activity (Table 2.2).

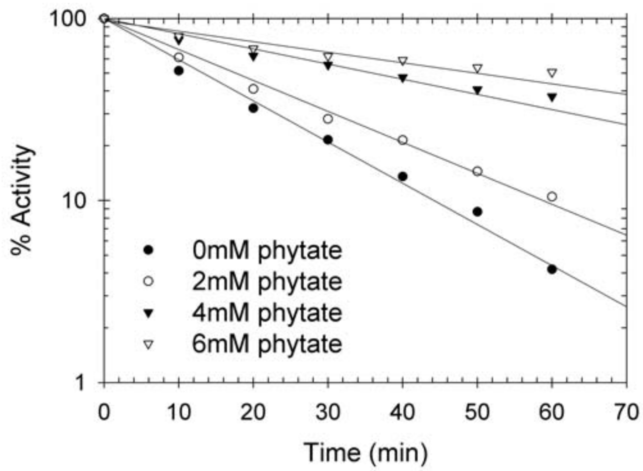

Figure 2.2 The effect of varying concentrations of Ins P_6 on the inactivation of PhyAsr by IAA. The modification reaction was repeated in the presence of 0, 2, 4 and 6 mM sodium phytate. Average activity of the protected and unprotected, modified enzyme relative to an un-alkylated control for three separate experiments is presented.

The P-loop Arg of PTP superfamily enzymes has been shown with mutational analysis to be important for optimal activity. *Yersinia* PTP (Zhang *et al.*, 1994c) and PTP1B (Flint *et al.*, 1997) have been determined to rely on the P-loop Arg for efficient catalysis and to a lesser extent, substrate binding. To determine if Arg258 of the PTP-like active site signature sequence of PhyAsr serves a similar function in catalysis it was mutated in a conservative fashion to Lys. The catalytic properties of R258K were determined (Table 2.2).

Mutation of Arg258 to a Lys reduced turnover by 99.91%, but had a negligible effect on the K_m, which was 410μM.

PTP superfamily enzymes have been shown to follow a general acid-base mechanism of dephosphorylation. The importance of an Asp located upstream of the active site has been verified in PTPs with mutational analysis (Zhang *et al.*, 1994b; Wu and Zhang, 1996; Lohse *et al.*, 1997). PhyAsr sequence and structure both suggest that Asp223 is the equivalent general acid (Chu *et al.*, 2004). To verify this, Asp223 was modified in the most structurally conservative way possible with a mutation to Asn. The D223N mutation resulted in a 99.68% decrease in turnover number, with a corresponding 10-fold decrease in K_m, which was determined to be 40 μM (Table 2.2). This mutation was also determined to alter the pH vs. activity profile relative to the profile of wild-type recombinant PhyAsr (Figure 2.3). Replacement of the carboxyl group at residue 223 caused an alkaline shift in optimal pH from five to six. The data presented is consistent with the suggestion that PhyAsr utilizes a PTP-like catalytic mechanism.

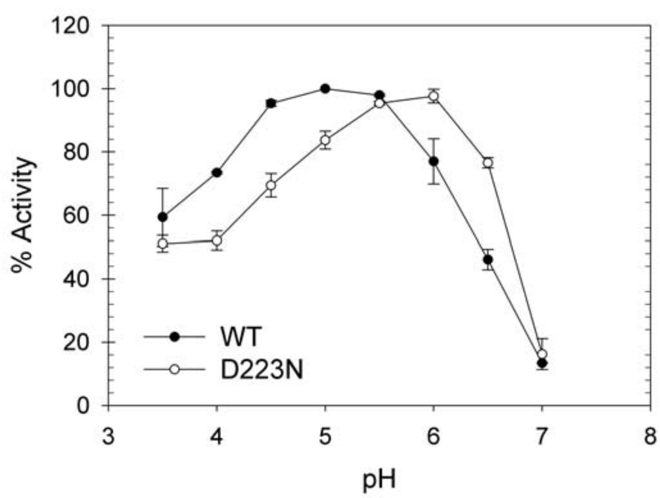

Figure 2.3. The effect of pH on phytase activity of PhyAsr and its D223N mutant. Standard phytase assays were run over a pH range of 3.5 to 7. The overlapping buffer systems used were: 50 mM formate (pH 3.5-4), 50 mM sodium acetate (pH 4-6) and 50 mM imidazole (pH 6-7). The data are mean values ± standard deviation of three separate experiments.

Preferred substrate

Purified PhyAsr was incubated with excess Ins P_6 for 30 and 90 minutes and the stopped reaction was subjected to chromatography. Results of the High-Performance Ion-Pair Chromatography (HPIC) analysis of the Ins P_6 hydrolysis products generated by PhyAsr are shown in Figure 2.4. Following 30 minutes of incubation no Ins P_6 remains and D/L-Ins(1,2,4,5,6)P_5 is the only penta*kis*phosphate degradation product observed. This indicates that PhyAsr preferentially acts on the D/L-3-phosphate position of Ins P_6 and is not consistent with a processive mechanism utilizing a stand-by site. The demonstration that PhyAsr cleaves the 3-phosphate first contradicts the existing classification inferred from the PhyAsr-hexasulphate structure (Chu *et al.*, 2004).

Hydrolysis pathway and kinetic studies

In addition to D/L-Ins(1,2,4,5,6)P_5, the other major products present after 30 minutes of incubation are Ins(2,4,5,6)P_4 and D/L-Ins(2,4,5)P_3, representing 80% of the Ins P_4 and Ins P_3 products. Minor products were D/L-Ins(1,2,5,6)P_4, D/L-Ins(1,2,4,6)P_4, D/L-Ins(1,2,6)P_3 and D/L-Ins(1,2,4)P_3. Trace amounts of D/L-Ins(2,4)P_2 and D/L-Ins(1,2)P_2 were also formed. After 90 minutes of incubation, all of the Ins P_5, and all but trace amounts of the major Ins P_4 product had been hydrolyzed to the Ins P_3 and Ins P_2 products.

The k_{cat} and K_m for the enzymatic degradation of the *myo*-inositol phosphates present in our hydrolysis pathway were determined to aid in the elucidation of the hydrolysis pathway and preferred substrates of PhyAsr. The respective kinetic parameters are given in Table 2.3. To confirm the identity of the Ins P_5 isomer, kinetic parameters were determined for the enzymatic hydrolysis of purified D-Ins(1,2,4,5,6)P_5 and the isolated Ins P_5 produced by PhyAsr. The k_{cat} and K_m for their hydrolysis were almost identical, 295 s^{-1} and 298 s^{-1} and 390 μM and 402 μM, respectively, further corroborating that PhyAsr preferentially hydrolyzes the D-3 phosphate position of Ins P_6 first. Similarly, kinetic parameters were determined for D-Ins(2,4)P_2 and D-Ins(2,6)P_2, and compared to those generated with the PhyAsr Ins P_2 product in order to confirm the isomer generated from Ins(2,4,5)P_3. The results indicate that D-Ins(2,4)P_2 is the major Ins P_2 product. The results of gas chromatography-mass spectrometry analysis indicate that the end product of Ins P_6 hydrolysis by PhyAsr is Ins(2)P.

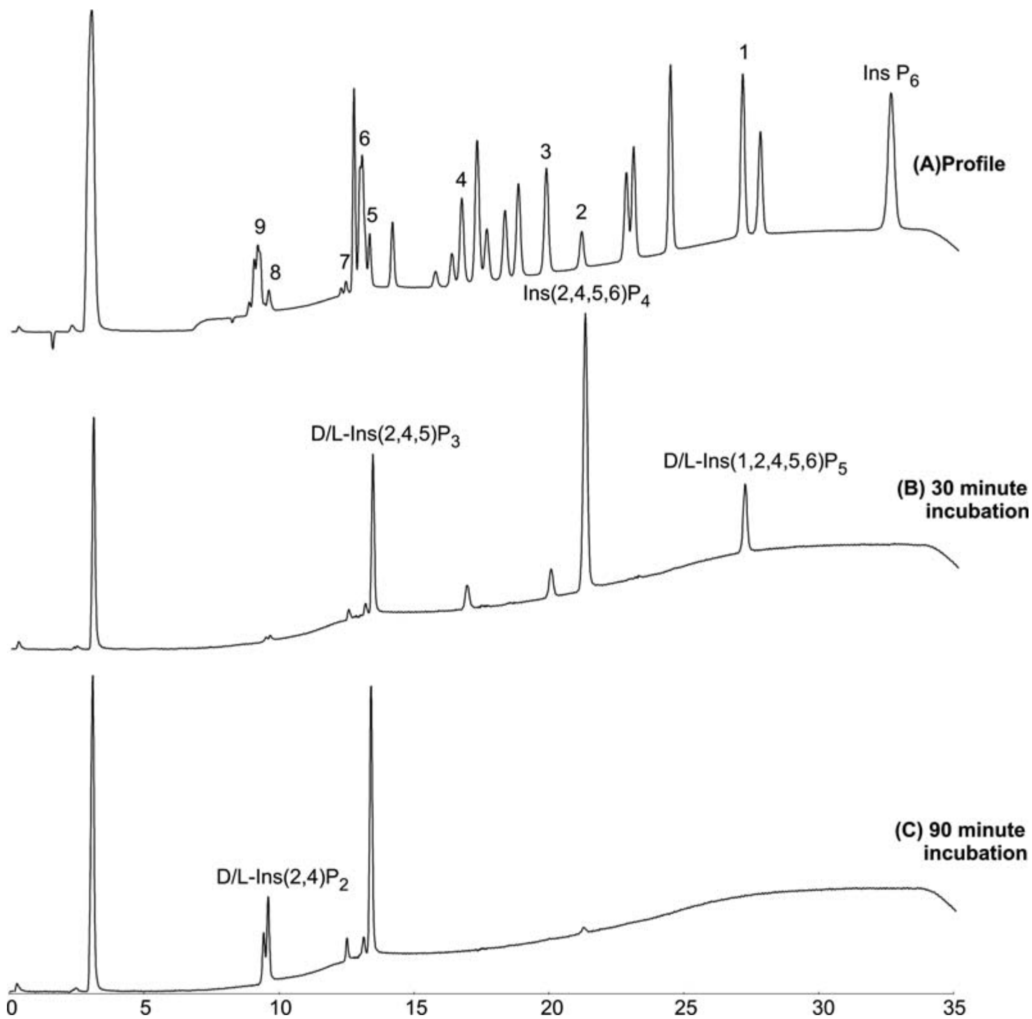

Figure 2.4. High-performance ion-pair chromatography analysis of the hydrolysis products of IPPs by PhyAsr. (A) Reference sample. The source of the reference IPPs is as indicated in Skoglund *et al.* (1998); Peaks: (1) D/L-Ins(1,2,4,5,6)P_5; (2) Ins(2,4,5,6)P_4; (3) D/L-Ins(1,2,5,6)P_4; (4) D/L-Ins(1,2,4,6)P_4; (5) D/L-Ins(1,4,5)P_3; D/L-Ins(2,4,5)P_3; (6) D/L-Ins(1,2,6)P_3, Ins(1,2,3)P_3; (7) D/L-Ins(1,2,4)P_3; (8) D/L-Ins(2,4)P_2; (9) D/L-Ins(1,2)P_2, Ins(2,5)P_2, D/L-Ins(4,5)P_2. (B) PhyAsr incubated with Ins P_6 for 30 min. (C) PhyAsr incubated with Ins P_6 for 90 min. Peaks representative of major pathway products are labelled accordingly.

Table 2.3. Kinetic parameters for enzymatic *myo*-inositol polyphosphate dephosphorylation by PhyAsr. Values given are the average ± standard deviation of at least three separate experimental runs.

Substrate	**k_{cat} (s^{-1})**	**K_m (μM)**	**k_{cat} / K_m (s^{-1} μM^{-1})**
$Ins(1,2,3,4,5,6)P_6$	264 ± 19	425 ± 28	621 ± 60
$D\text{-}Ins(1,2,4,5,6)P_5$	295 ± 24	390 ± 22	756 ± 75
$Ins(2,4,5,6)P_4$	217 ± 11	474 ± 23	457 ± 32
$D\text{-}Ins(2,4,5)P_3$	202 ± 16	493 ± 25	409 ± 38
$D\text{-}Ins(2,4)P_2$	187 ± 6	516 ± 21	362 ± 19
$D\text{-}Ins(2,6)P_2$	67 ± 6	874 ± 35	76 ± 7
$InsP_5^{*}$	298 ± 6	402 ± 17	741 ± 35
$InsP_2^{*}$	193 ± 17	521 ± 19	370 ± 35

*Generated by PhyAsr.

2.4 DISCUSSION

PTP-like mechanism

PhyAsr is the first example of an enzyme with a PTP-like core structure exhibiting phytase activity (Chu *et al.*, 2004) and accordingly this suggests that it is the first IPPase with a PTP-like mechanism of catalysis. Kinetic properties of PhyAsr catalyzed Ins P_6 hydrolysis are consistent with the kinetic properties of other PTP superfamily enzymes towards the commonly used phosphatase substrate *p*-nitrophenyl phosphate (pNPP) (Zhang *et al.*, 1992; Guo *et al.*, 2002). Sequence alignments of PhyAsr with known PTP superfamily enzymes indicates low similarity with known PTPs, but shows a PTP-like active site signature sequence with a conserved Cys and Arg. PTPs use the nucleophilic Cys residue to bond the phosphate monoester of the substrate, forming a thiol-phosphate intermediate (Guan and Dixon, 1991; Pannifer *et al.*, 1998).

The only Cys present in the mature PhyAsr is located in the PTP-like signature sequence, making it an ideal candidate for chemical modification experiments. To confirm the participation of the Cys252 thiol group in the catalytic mechanism, PhyAsr was alkylated with IAA. We have shown that PhyAsr can be inactivated by IAA, and that the loss of enzymatic activity is due to the single and specific modification of Cys252 in the PTP-like active site signature sequence. The inactivation of PhyAsr by IAA was inhibited by the presence of the substrate Ins P_6. These data are consistent with Cys252 being a nucleophilic thiol within the substrate binding site, and supports the PTP-like mechanism. Similar chemical modification experiments with alkylating agents have been used to indicate that the PTP active site signature sequence Cys is required for the activity of other PTP superfamily enzymes (Pot *et al.*, 1991; Pot and Dixon, 1992; Zhang and Dixon, 1993; Zhou *et al.*, 1994).

We have also verified previous results that substitution of Cys252 causes a complete loss of IPPase activity. Our results are similar to those obtained with both the mammalian receptor-like PTP LAR (Pot *et al.*, 1991) and with a PTP from *Yersinia* (Guan and Dixon, 1990), and further suggest that the lone Cys of PhyAsr is directly involved in catalysis.

To substantiate the claim that PhyAsr follows a PTP-like mechanism, Arg258 of the PTP active site signature sequence was mutated to a Lys. *Yersinia* PTP (Zhang *et al.*, 1994c) and PTP1B (Flint *et al.*, 1997) have been shown to rely on the P-loop Arg for efficient catalysis and to a smaller extent, substrate binding. We have shown that replacement of the guanidinium group with the amine group of Lys in PhyAsr reduces product turnover 1000 fold. This is consistent with results found for the *Yersinia* PTP and PTP1B, where Arg to Lys mutations caused 8200 and 5500 fold reductions in k_{cat} respectively. R258K had a negligible effect on the K_m of PhyAsr, suggesting that the P-loop Arg has a minor role in substrate binding, and a major effect on catalysis.

PTP superfamily enzymes follow a general acid-base mechanism of dephosphorylation, using an invariant Asp to act as a general acid, donating a proton to the ester oxygen of the leaving group. The importance of an Asp as a general acid has been shown in the *Yersinia* PTP (Zhang *et al.*, 1994b), a low-molecular-weight PTP from yeast (Wu and Zhang, 1996) and mammalian PTP1B (Lohse *et al.*, 1997). We have targeted and shown that Asp223 serves a comparable role in PhyAsr. The D223N mutation results in a 300-fold decrease in turnover number indicating that this residue has a major effect on catalysis. The same mutation also caused an alkaline shift in the catalytic pH optimum due to a perturbation of the pK_a value of the catalytic group of the general acid, as was determined for the *Yersinia* PTP (Zhang *et al.*, 1994a). This is likely due to a water molecule being required to act as the general acid for the D223N mutant. Surprisingly, the D223N mutation caused a reduction in K_m by 10-fold indicating that the replacement of a carboxyl group with an amide within the binding pocket of PhyAsr has a constructive effect on substrate binding, possibly due to the large negative charge associated with Ins P_6.

Preferred substrate position

Based on the position of the first phosphate hydrolyzed, three types of phytases are recognized by The Enzyme Nomenclature Committee of the International Union of Biochemistry; *i.e.*, 3-phytases (EC 3.1.3.8), that act on the D-3 phosphate position; 6-phytases (EC 3.1.3.26), that act on the L-6 or D-6 position; and 5-phytases (EC 3.1.3.72). It was recently suggested from the PhyAsr-hexasulphate structure that PhyAsr preferentially dephosphorylates Ins P_6 at the 5-phosphate position first (Chu *et al.*, 2004). In contrast, D/L-Ins(1,2,4,5,6)P_5 was the only penta*kis*phosphate product ever observed in our study of the PhyAsr mediated dephosphorylation of Ins P_6. Kinetic parameters determined for the enzymatic hydrolysis of D-Ins(1,2,4,5,6)P_5 and the Ins P_5 isomer produced by PhyAsr were compared to confirm the identity of the Ins P_5 isomer as D-Ins(1,2,4,5,6)P_5. HPIC and kinetic analysis thus indicate that PhyAsr initiates hydrolysis at the D-3 phosphate position. The structure reported by Chu *et al* (2004) was determined at a pH of 9, and utilized the inhibitor inositol hexasulfate, which might affect the conformational and charged state of the substrate and thus its interaction with the binding pocket of PhyAsr. Of note, PhyAsr's closest structural homologue, the inositide/inositol phosphatase PTEN, acts only on the 3-phosphate position of the lipid substrate PtdIns(3,4,5)P_3 and the IPPs Ins(1,3,4,5,6)P_5 and Ins(1,3,4,5)P_4 (Maehama and Dixon, 1998; Caffrey *et al.*, 2001).

Hydrolysis pathway

The characterized phytases all remove phosphate from Ins P_6 in a distributive manner, such that each myo-inositol phosphate intermediate is released from the enzyme and may act as a substrate in further hydrolysis reactions (Konietzny and Greiner, 2002). It was recently suggested from the structure that PhyAsr utilizes a stand-by site to bind substrate between successive hydrolysis reactions (Chu *et al.*, 2004). In contrast, our HPIC analysis indicates that PhyAsr hydrolyzes Ins P_6 in a distributive fashion similar to other phytases.

Kinetic parameters (k_{cat}/K_m) were used to determine the preferred IPP substrate. There is a slight but consistent preference for a more highly phosphorylated substrate and a slight overall preference for the Ins P_5 tested (Ins P_5>Ins P_6>Ins P_4>Ins P_3>Ins P_2). This preference is likely due to the favourable electrostatic effect between the positively charged binding pocket of the enzyme (Chu *et al.*, 2004) and the negative phosphate groups on the substrate.

Despite the similar kinetic parameters found for the individual IPPs, PhyAsr was determined to dephosphorylate Ins P_6 via a largely ordered, sequential fashion. PhyAsr initiates hydrolysis of Ins P_6 exclusively at the D-3 position and produces Ins(2)P predominantly (>80%) via D-Ins(1,2,4,5,6)P_5, Ins(2,4,5,6)P_4, D-Ins(2,4,5)P_3 and D-Ins(2,4)P_2, (3,1,6,5,4; Figure 2.5).

The final end product of Ins P_6 hydrolysis by PhyAsr is Ins(2)P. Therefore, PhyAsr has a preference for the equatorial phosphate groups, and is able to remove all five. Many phytases that have the ability to remove all five equatorial phosphates from Ins P_6 also exhibit low specific activities (Wyss *et al.*, 1999; Konietzny and Greiner, 2002). PhyAsr represents a general IPPase that has a relatively high specific activity. PhyAsr's highly-ordered pathway makes it a good candidate for IPP production.

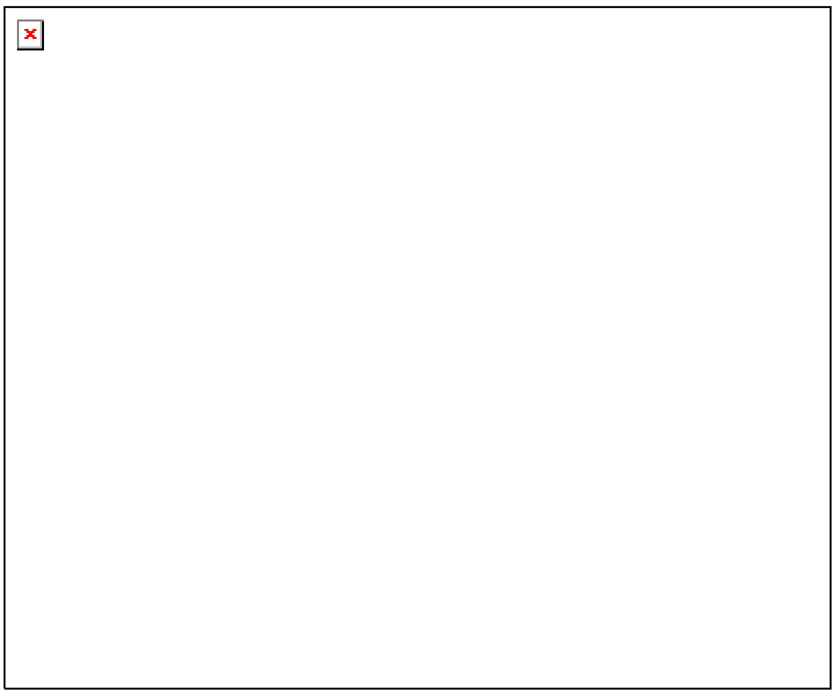

Figure 2.5. The dephosphorylation pathways of Ins P_6 by PhyAsr as determined by high-performance ion-pair chromatography (HPIC) and kinetic analysis. Larger arrows indicate major pathway, smaller arrows indicate minor pathways. The major pathway accounts for approximately 80% of degradation products.

CHAPTER THREE

Cloning and characterizing PhyAsrl from *Selenomonas ruminantium* subsp. *lactilytica***,** a PTP-like 5-phytase

ABSTRACT

PhyAsrl from *Selenomonas ruminantium* subsp *lactilytica* is a protein tyrosine phosphatase (PTP)-like phytase with a number of unique properties. In order to elucidate its substrate specificity and pathway of Ins P_6 dephosphorylation, a combination of kinetic and high-performance ion-pair chromatography studies were conducted. The data indicate that PhyAsrl has a general specificity for polyphosphorylated *myo*-inositol substrates but can also dephosphorylate adenosine triphosphate (ATP) *in vitro*. PhyAsrl preferentially cleaves the 5-phosphate position of Ins P_6 and produces Ins(2)P via a highly ordered pathway of sequential dephosphorylation; *i.e.*, Ins P_6, Ins(1,2,3,4,6)P_5, D-Ins(1,2,3,6)P_4, Ins(1,2,3)P_3, and D/L-Ins(1,2)P_2.

3.1 INTRODUCTION

Phytases (*myo*-inositol hexa*kis*phosphate phosphohydrolases) are enzymes that can catalyze the release of orthophosphate from *myo*-inositol hexa*kis*phosphate (Ins P_6) (Mullaney and Ullah, 2003). Four distinct classes of phosphatases have been characterized in the literature as having phytase activity; *i.e*., histidine acid phosphatases, β-propeller phytases, purple acid phosphatases (Mullaney and Ullah, 2003) and most recently, protein tyrosine phosphatase (PTP)-like phytases (Chu *et al.*, 2004; refer, Chapter 2). Based on the position of the first phosphate hydrolyzed, three types of phytases are recognized by The Enzyme Nomenclature Committee of the International Union of Biochemistry; *i.e*., 3-phytase (EC 3.1.3.8), 6-phytase (EC 3.1.3.26) and 5-phytase (EC 3.1.3.72). Phytases hydrolyze Ins P_6 in a sequential and stepwise manner, yielding lower inositol polyphosphates (IPPs) which may again become substrates for further hydrolysis (Konietzny and Greiner, 2002). This occurs at different rates and in different orders among phytases, and may be evidence of the variety of biological roles played by these enzymes, Ins P_6, and Ins P_6 derivatives.

Phytases are widespread in nature, and have been found in many plants and microorganisms (Wodzinski and Ullah, 1996), and more recently, mammals (Craxton *et al.*, 1997; Chi *et al.*, 1999). A number of microbial phytase genes have been cloned and sequenced (Konietzny and Greiner, 2002; Vats and Banerjee, 2004). Phytases from *Bacillus* species (Kerovuo *et al.*, 1998; Ha *et al.*, 1999; Greiner *et al.*, 2002b), *Escherichia coli* (Greiner *et al.*, 1993; Greiner *et al.*, 2000a; Lim *et al.*, 2000) and *Aspergillus* species (Ullah *et al.*, 2000; Liu *et al.*, 2004) have been purified and their biochemical and catalytic properties, structures and stereospecificities have been reported. Despite the fact that ruminants are known to metabolize Ins P_6, there is a limited number of papers addressing the genetic and enzymatic properties of Ins P_6-degrading enzymes found in the rumen.

An enzyme belonging to the protein tyrosine phosphatase (PTP) superfamily has been characterized from the anaerobic, ruminal bacterium *Selenomonas ruminantium* (PhyAsr). PhyAsr has a PTP-like fold and a conserved PTP-like active site signature sequence ($C(X)_5R$) which facilitates a classical PTP mechanism of dephosphorylation (Chu *et al.*, 2004; refer, Chapter 2). This enzyme is unique among PTP superfamily enzymes as it displays the ability to dephosphorylate Ins P_6, as well as other IPPs (Chu *et al.*, 2004; refer, Chapter 2). A number of putative PTP-like phytase homologues have been partially cloned from a range of anaerobic bacteria found in the rumen (Nakashima *et al.*, 2006). To date, little information is available in the literature regarding the biochemical characteristics of this novel class of enzyme. Here we report the cloning and sequencing of the full gene encoding a PTP-like phytase from *S. ruminantium* subsp. *lactylitica* (*phyAsrl*). We present the biochemical and kinetic parameters of the gene product and investigate its substrate specificity. Finally, we give experimental data that elucidates the stereospecificity of PhyAsrl and its major pathway of Ins P_6 hydrolysis.

3.2 MATERIALS AND METHODS

Gene cloning

Selenomonas ruminantium subsp. *lactilytica* (ATCC 19205) was cultured anaerobically (100% CO_2) at 39°C in Hungate tubes with 5 mL of modified Scott and Dehority medium (Scott and Dehority, 1965) containing 10% (v/v) rumen fluid, 0.2% (w/v) glucose, 0.2% (w/v) cellobiose and 0.3% (v/v) starch. Isolation of total DNA was performed as described previously (Priefer *et al.*, 1984). Genomic DNA was partially digested with *Eco*RI or *Pst*I. The relative sizes of the fragments containing the gene coding for phytase (*phyAsrl)* were determined by Southern blot hybridization using the DIG DNA Labeling and Detection Kit (Boehringer; Mannheim, Germany) and a probe. The probe was a polymerase chain reaction (PCR) product corresponding to a previously determined sequence fragment (GeneBank accession number DQ257442; Nakashima *et al*., 2006). Digested DNA corresponding to the approximate size of the *phyAsrl* containing fragments was gel purified (MinElute Gel Extraction Kit; Qiagen Inc.; Mississauga, ON), and ligated into the equivalent dephosphorylated *Eco*RI or *Pst*I pBluescript II SK (+) (Stratagene, La Jolla, CA). PCR primers (Table 3.1) were generated from the known internal *phyAsrl* sequence fragment (Nakashima *et al.*, 2006) and were used in conjunction with M13 and T7 universal primers to generate PCR products from the ligation product corresponding to regions of *phyA*srl straddling the known sequence (Figure 3.1). The PCR products were then ligated into pGEM-T Easy (Promega Corp., Madison, WI) and sequenced by automated cycle sequencing at the University of Calgary Core DNA and Protein services facilities. Sequence data was analyzed with the aid of SEQUENCER™ version 4.0 (Gene Codes Corp. Ann Arbor, MI) and

MacDNAsis version 3.2 (Hitachi Software Engineering Co., Ltd., San Bruno, CA). Similarity searches in GenBank (Fassler *et al.*, 2000; Benson *et al.*, 2006) were done using BLAST (Altschul *et al.*, 1990) and preliminary sequence alignments were generated using CLUSTAL W 1.82 (Higgins *et al.*, 1994; Chenna *et al.*, 2003). Alignment optimization was carried out with GeneDoc (Nicholas *et al.*, 1997) using methods for comparative structure-based sequence alignments (Greer, 1981) and the experimentally determined structure of the PTP-like Ins P_6-degrading enzyme from *S. ruminantium* JY35 (PDB accession: 1U24; Chu *et. al.*, 2004).

Table 3.1. Primers used in this study. Restriction sites are underlined.

Primer Name	Primer Sequence
19205 For	ACA TTT GTG CCG ATG GGT AA
19205 For N	ATA AGA GCC TGC CGA AAA AT
19205 Rev	TGC CCT CGA CCT GCT TT
19205 Rev N	GCT TAC GGG AAT GTC ACC A
*Nde*I Exp	GC<u>C ATA TG</u>A AAC AAG AAG AAG CCG TCT T
*Xho*I Exp	GC<u>C TCG AG</u>T TAT CTT TGT GCT TTC ACC C

Recombinant phyAsrl expression construct

The region coding for the mature *S. ruminantium* subsp. *lactilytica* phytase (PhyAsrl; GeneBank accession number EF016752; residues 33-321) was amplified from genomic DNA using PCR. The predicted signal peptide sequence was determined with SIGNAL P 3.0 (Nielsen *et al.*, 1997; Bendtsen *et al.*, 2004). PhyAsrl forward and reverse primers (Table 3.1) included an *Nde*I and *Xho*I site, respectively, for cloning and a 5’ GC cap. The PCR product was digested with *Nde*I and *Xho*I and ligated into similarly digested pET28b vector (Novagen Inc., San Diego, CA). Constructs were verified with automated cycle sequencing.

Protein production and purification

Escherichia coli BL21 (DE3) cells (Novagen Inc.) were transformed with the *phyAsrl* expression constructs. Over expression was carried out according to the instructions in the pET Systems Manual (Novagen Inc.). Cultures were induced with the addition of IPTG to a final concentration of 1 mM. Incubation was continued for four hours at 37^{o}C. Induced cells were harvested and resuspended in lysis buffer: 20 mM KH_2PO_4 (pH 7), 300 mM NaCl, 1 mM β-mercaptoethanol (BME), 5% glycerol and one Complete Mini, EDTA-free protease inhibitor tablet (Roche Applied Science; Laval, QC). Cells were sonicated and debris was removed by centrifugation at 20 000 x g for 45 minutes. The protein was purified to homogeneity using Ni^{2+}-NTA spin columns according to the supplied protocol (Qiagen Corp.). Protein was washed on the column with lysis buffer containing 15 mM imidazole and subsequently eluted with lysis buffer containing 0.4 M imidazole. Purified protein was dialyzed with three buffer changes into 500 mL of 25 mM Tris (pH 7), 0.3 M NaCl, 0.1 mM EDTA and 5 mM BME. Homogeneity of the purified protein was confirmed by 12% (w/v) SDS-polyacrylamide gel electrophoresis (SDS-PAGE)(Laemmli, 1970), and Coomassie Brilliant Blue R-250 staining. The theoretical M_r and extinction coefficient of PhyAsrl were determined using PROT PARAM (Gasteiger *et al.*, 2005). Protein concentrations were determined by monitoring the A_{280}. For storage, purified protein was dialyzed into 20 mM ammonium bicarbonate (pH 8) with 3 buffer changes, lyophilized, and stored at -20^{o}C.

Assay of enzymatic activity

Activity measurements were carried out at 37°C. Enzyme reaction mixtures consisted of a 600 μL buffered substrate solution and 150 μL of a 200 nM enzyme solution. The buffered substrate solution contained 50 mM sodium acetate (pH 4.5) and 2 mM sodium phytate, or another of the substrates used in our study. Ionic strength (I) was held constant at 0.2 M with the addition of NaCl except for in those assays examining the effect of I, where NaCl concentrations were varied from 0 to 0.8 M. Phytase activity was determined at different pH with overlapping buffer systems: 50 mM glycine (pH 2-3), 50 mM formate (pH 3-4), 50 mM sodium acetate (pH 4-6), 50 mM imidazole (pH 6-7), and 50 mM Tris (pH 7-8). Phytase activity was also determined at incremental temperatures from 10 to 70 degrees.

PhyAsrl's substrate specificity was determined with the replacement of sodium phytate in the standard phosphatase assay (37^{o}C with 50 mM sodium acetate, pH 4.5) for other phosphoester containing substrates. The I of the reactions was adjusted to 0.2 M with NaCl accordingly. Phosphoester containing substances examined included: Ins P_6, phosphatidylinositol-3,4,5-triphosphate (PIP_3), β-glycerophosphate, D/L-α-glycerophosphate, α-naphthyl phosphate, phospho (enol) pyruvate, phenolphthalein diphosphate, O-nitophenyl-β-D-galactopyranoside 6-phosphate, phenyl phosphate, ρ-nitrophenyl phosphate (ρNPP), 5-bromo-4-chloro-3-indolyl phosphate (BCIP), O-phospho-L-tyrosine, O-phospho-L-threonine, O-phospho-L-serine, adenosine 5'-triphosphate (ATP), adenosine 5'-diphosphate (ADP), D-fructose-1,6-diphosphate, D-fructose-6-phosphate, D-glucose-6-phosphate, D-ribose-5-phosphate. All substrates tested for hydrolysis were present at 2 mM with the exception of PIP_3 which was 500 μM.

Quantification of the liberated phosphate

Following the appropriate, empirically determined incubation period, the reactions were stopped and the liberated phosphate was quantified. Biochemical characterization was done using the ammonium molybdate method previously described (Yanke *et al.*, 1998). A 750 μL aliquot of 5% (w/v) trichloroacetic acid was added to stop the reaction, followed by the addition of 750 μL of phosphomolybdate coloring reagent. The coloring reagent was prepared by the addition of 4 volumes 1.5% (w/v) ammonium molybdate solution in 5.5% (v/v) sulfuric acid to 1 volume 2.7% (w/v) ferrous sulfate solution. Liberated inorganic phosphate was measured as A_{700} on the spectrophotometer. For kinetic studies we utilized a modified Heinonen and Lahti method which was better suited to the range of substrate concentrations involved (Heinonen and Lahti, 1981). A 1.5 mL aliquot of a freshly prepared solution of acetone/5 N H_2SO_4/10 mM ammonium molybdate (2:1:1 v/v/v) was added to the assay mixture for stopping and detection, followed by 100 μl 1.0 M citric acid. Any cloudiness was removed by centrifugation prior to measurement of the absorbance at 355 nm.

In order to quantify the released phosphate, a calibration curve was produced for each quantification method over a range of 5-600 nmol phosphate / 2 mL reaction mixture. Activity (U) was expressed as μmol phosphate liberated per min. Blanks were run by addition of the stop solution to the assay mixture prior to addition of the enzyme solution. The steady-state kinetic constants (K_m, k_{cat}) for the hydrolysis of Ins P_6, its derivatives, and ATP by PhyAsrl were calculated from Michaelis-Menton plots. The data were analyzed with non-linear regression using SIGMA-PLOT 8.0 (Systat Software Inc.; Point Richmond, CA).

Preparation of individual myo-inositol phosphate isomers

Lyophilized PhyAsr was shipped to Dr. Ralf Greiner at the Centre for Molecular Biology of the Federal Research Centre for Nutrition and Food in Karlsruhe Germany where HPIC, production and isolation of lower IPPs and kinetic studies with lower IPPs was performed.

The production of *myo*-inositol phosphate isomers (D-Ins(1,2,3,4)P_4, D-Ins(1,2,3,6)P_4 and the Ins P_4 generated by PhyAsrl) was done as described previously (Greiner *et al.*, 2002a; Greiner *et al.*, 2002b; refer, Chapter 2). The source of the Ins P_6-degrading enzymes and the respective products generated was *Megasphaera elsdenii* (Puhl, A.; personal communication), to produce D-Ins(1,2,3,4)P_4, *Klebsiella terrigena* (Greiner *et al.*, 1997), to produce D-Ins(1,2,3,6)P_4 and PhyAsrl to produce the unknown isomer D/L-Ins(1,2,3,4)P_4. Sodium phytate (2.5 mmol) was incubated at 37°C in a mixture containing 50 mM NH_4-acetate, pH 5.0 (*K. terrigena* and *M. elsdenii*) or pH 4.5 (*S. ruminantium* subsp. *lactilytica*) and 10 U of the appropriate enzyme in a final volume of 500 μL.

Identification of enzymatically formed hydrolysis products

Standard phytase assays were run at 37°C by addition of 50 μL of a suitably diluted solution of PhyAsrl to the incubation mixtures. Periodically stopped reactions were resolved on a High-Performance Ion Chromatography system (HPIC) using a Carbo Pac PA-100 (4 x 250 mm) analytical column (Dionex; Sunnyvale, CA) and a gradient of 5–98% HCl (0.5 M, 0.8 mL/min) as previously described (Skoglund *et al.*, 1998). The eluants were mixed in a post-column reactor with 0.1% $Fe(NO_3)_3$ in a 2% $HClO_4$ solution (0.4 mL/min)(Phillippy and Bland, 1988). The combined flow rate was 1.2 mL/min. *myo*-inositol monophosphates were produced by incubation of 1.0 U of PhyAsrl with a limiting amount (0.1 μmol) of sodium phytate in a final volume of 500 μL of 50 mM NH_4-formate. The end products were identified using a gas chromatograph coupled with a mass spectrometer as previously described (Greiner *et al.*, 2002a; Greiner *et al.*, 2002b; refer, Chapter 2).

3.3 RESULTS

Sequence analysis

A 1.9 kbp DNA fragment was isolated from the genome of *S. ruminantium* subspecies *lactilytica* (GeneBank Accession Number DQ257442) by cloning regions up and downstream of the sequence fragment determined by Nakashima *et al*. (2006). BLAST X analysis of the sequenced product indicated the presence of two open reading frames (ORFs; phyAsrl and *orf2*) and one partial ORF (*orf3*) with homologues in GeneBank (Figure 3.1). *Orf2* is located 200 bp downstream of *phyAsrl* and its deduced product is similar to putative Trp repressors found in several clostridial species. The partial ORF, o*rf3*, is located 90 bp downstream of *orf2* and its product shows similarity to various putative prokaryotic histidyltRNA synthetases, tRNA ligases and ATP phosphoribosyltransferases. The first ORF, *phyAsrl*, encodes a 322 amino acid protein that contains a PTP-like signature sequence with an invariant Cys and Arg, H<u>C</u>HAGHG<u>R</u>. The sequence also includes a predicted N-terminal signal peptide sequence. Several PhyAsrl homologues were found in GenBank using BLAST and aligned (Figure 3.2). All of the homologous proteins found are of bacterial origin. The closest homologue to PhyAsrl is the PTP-like phytase from *S. ruminantium* (30% identity). Other homologues are putative members of the PTP superfamily and display 20 to 28% identity to both PhyAsrl and the enzyme from *S. ruminantium*.

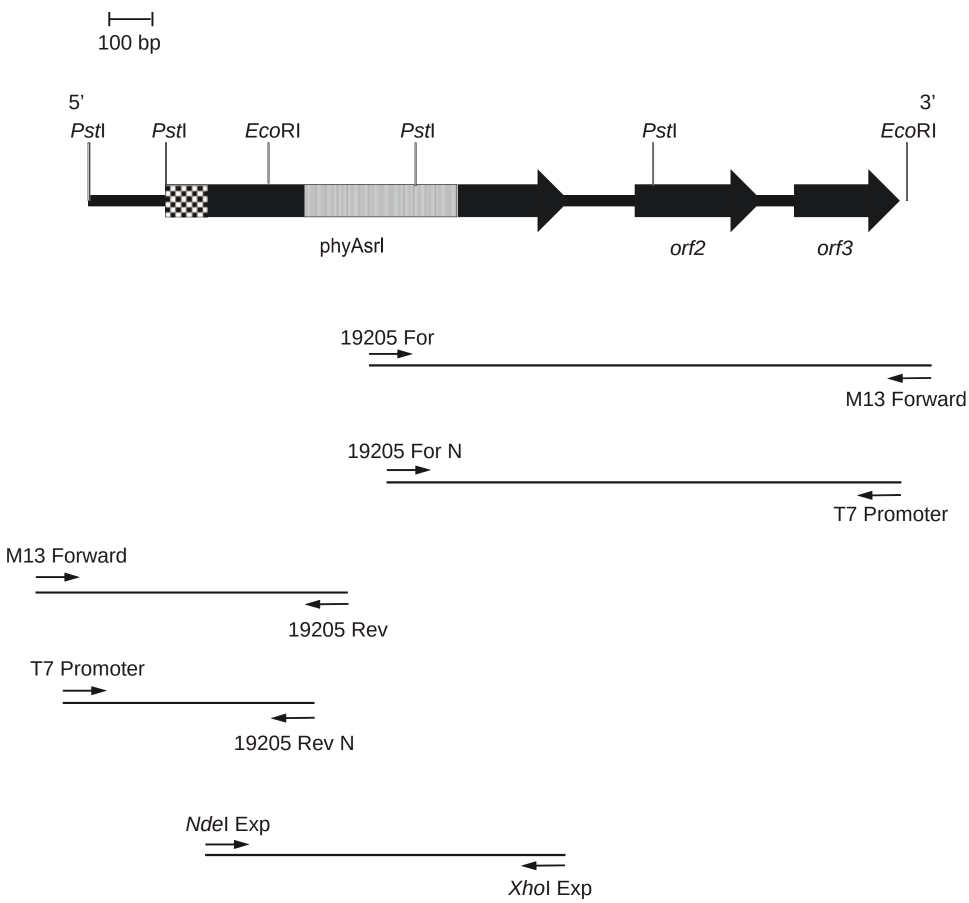

Figure 3.1. Schematic diagram representing phyAsrl and the steps involved in its PCR cloning. The relative positions of the primers used are indicated. The 378 bp fragment cloned previously is presented as a striped box. The predicted signal peptide is indicated by checkers.

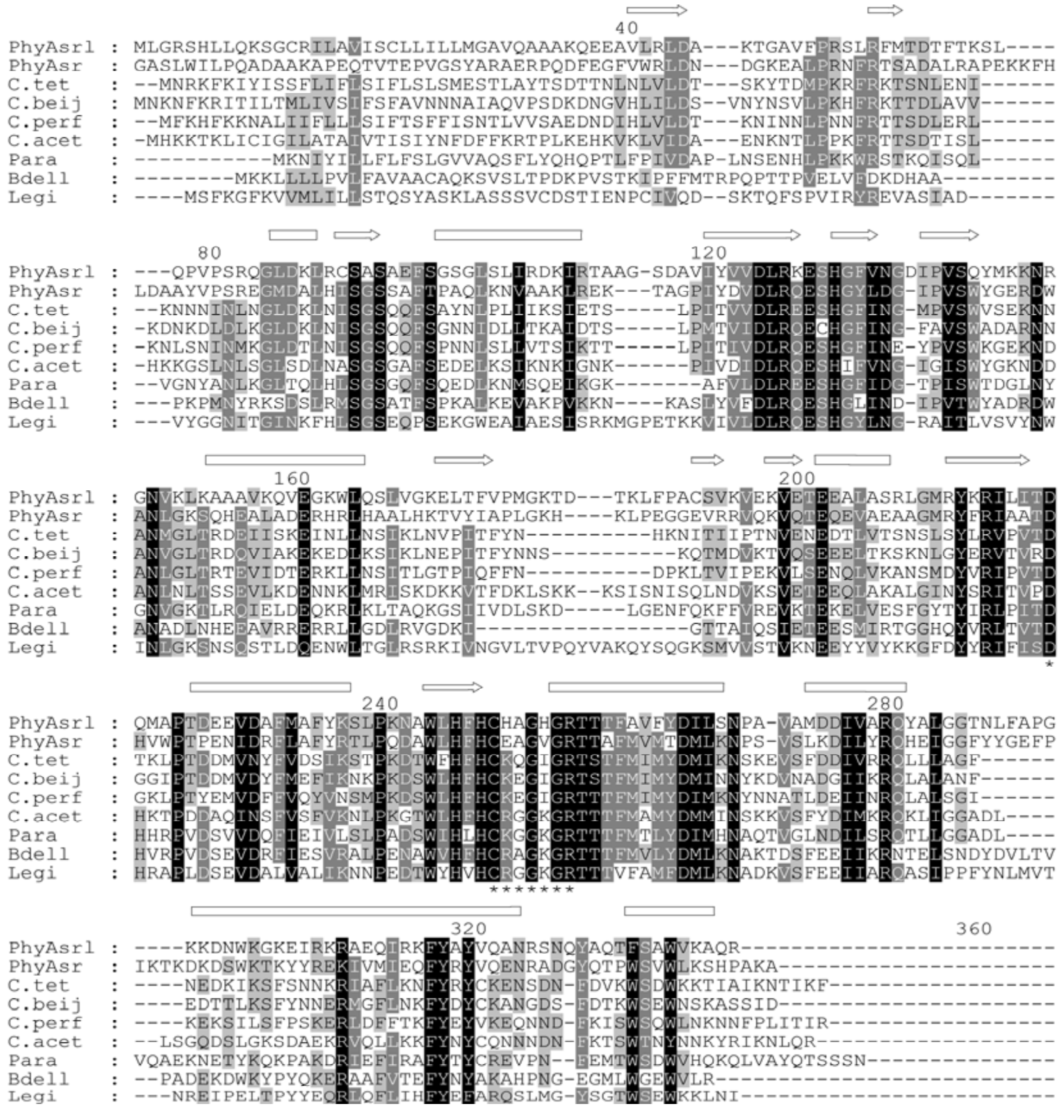

Figure 3.2. Comparative structure-based amino acid sequence alignment of the *Selenomonas ruminantium* subsp. *lactylitica* phytase and its GeneBank homologues. Shading is according to alignment consensus as given by GENE DOC (black = 100%; dark grey = 75%; light grey = 50%) with similarity groups enabled. Numbering is according to the sequence of PhyAsrl found in GeneBank. The PTP-like signature sequence and the conserved upstream aspartic acid are identified by asterisks. Secondary structures are identified for PhyAsr (PDB accession: 1U24) above the alignment with arrows indicating β-strands and cylinders indicating α-helices. The protein abbreviation, source and GenBank accession numbers are as follows: PhyAsrl, *Selenomonas ruminantium* subsp. *lactylitica*, EF016752; PhyAsr (residues 15-343), *S. ruminantium*, AAQ13669; C.tet, *Clostridium tetani* E88, NP_782216; C.beij, *C. beijerincki* NCIMB 8052, ZP_00910765; C.perf, *C. perfringens*, ABG83558; C.acet, *C. acetobutylicum*, NP_149178; Para, *Parachlamydia* sp. UWE25, CAF24552; Bdell, *Bdellovibrio bacteriovorus* HD100, CAE79111; Legi, *Legionella pneumophila* str. Lens, CAH16976.

Figure 3.2 illustrates the sequence conservation found between PhyAsrl and its homologues. The PTP signature sequence motif $C(X)_5R$ is conserved among all of the homologues and is responsible for activity amongst members of the PTP superfamily (Zhang, 2003), including the PTP-like phytase from *S. ruminantium* JY35 (refer, Chapter 2). The Asp important for acid-base catalysis in the PTP-like phytase from *S. ruminantium* (refer, Chapter 2) found upstream of the active site signature sequence is also conserved.

Expression and purification

Following induction with IPTG, overexpression of a polypeptide with an M_r of about 34 000 was observed with SDS-PAGE. This is consistent with the mass predicted from the sequence of the recombinant protein (predicted M_r = 34 633). Incubation with IPTG for periods longer than 4 hours was found to significantly reduce the protein yield due to the formation of inclusion bodies. The Ni^{2+}-NTA purification was able to produce >90% homogeneity of PhyAsrl in a single step, as determined by SDS-polyacrylamide gel electrophoresis and Coomassie Blue-250 staining (data not shown).

Enzymatic activity and substrate specificity

The activity of PhyAsrl toward Ins P_6 was examined initially. PhyAsrl can hydrolyze Ins P_6, and displays a specific activity of 16.23 U mg^{-1}. The specific activity of PhyAsrl is low compared to that of the PTP-like phytase from *S. ruminantium* which is 668.11 U mg^{-1} (refer, Chapter 2). Other characterized phytases display a range of activities (Konietzny and Greiner, 2002), from 0.5 U mg^{-1} in mung bean (Mandel *et al.*, 1972) to > 800 U mg^{-1} in *E. coli* (Greiner *et al.*, 1993; Wyss *et al.*, 1999; Golovan *et al.*, 2000).

The I, pH and temperature profiles for PhyAsrl were determined in order to establish the optimal conditions for Ins P_6 hydrolysis. The rate of hydrolysis of Ins P_6 by PhyAsrl is dependent on I (Figure 3.3) and optimal PhyAme activity occurs between 100 and 200 mM. For this reason, biochemical assays were performed under conditions of controlled I. PhyAsrl displayed activity at acidic pH values with an optimum at pH 4.5 (Figure 3.4A). Activity rapidly decreased on the acidic side of the optimum and above pH 5. No significant activity could be observed below pH 3 or above pH 7. PhyAsrl displayed significant levels of ATPase activity, thus the pH optimum for ATP as a substrate was also determined. ATPase activity had a similar pH profile to that with Ins P_6 with an optimum pH of 4.5 but a slight acidic shift overall (Figure 3.4A). The maximum phytase activity was observed at 55 ^oC (Figure 3.4B).

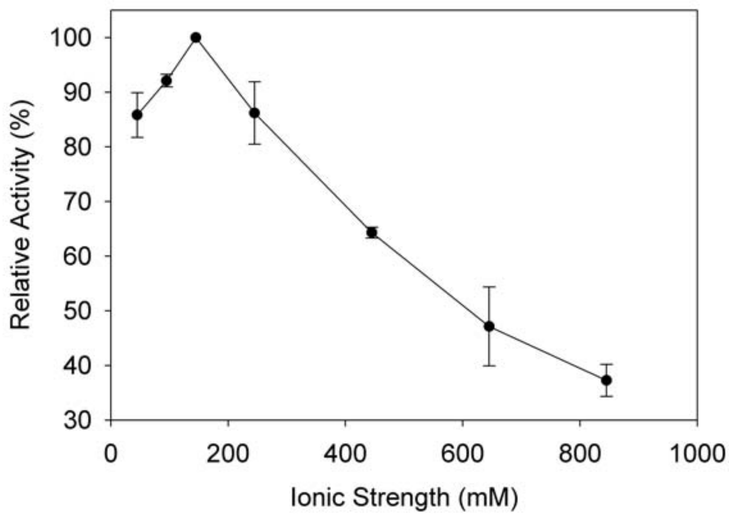

Figure 3.3. Effect of I on the activity of PhyAsrl. Standard phytase assays were run under varying NaCl concentrations. The data are mean values with error bars representing the standard deviations between three independent experiments. Values are normalized to 0.15 M.

We tested PhyAsrl's ability to hydrolyze various other phosphorylated compounds in order to characterize its specificity. The compounds that were hydrolyzed by PhyAsrl are given in Table 3.2. PhyAsrl displays narrow substrate specificity, showing significant activity towards only Ins P_6 and ATP. Ins P_6 is not the substrate with the highest rate of hydrolysis. The specific rate of hydrolysis of ATP was found to be 29.15 U mg^{-1} (179.63% relative to Ins P_6) with the next highest activity shown towards ADP (8.23% relative to Ins P_6). PhyAsrl has

100-fold lower specific activity towards commonly used phosphatase substrates pNPP and BCIP than towards Ins P_6 and very little activity on sugar phosphates.

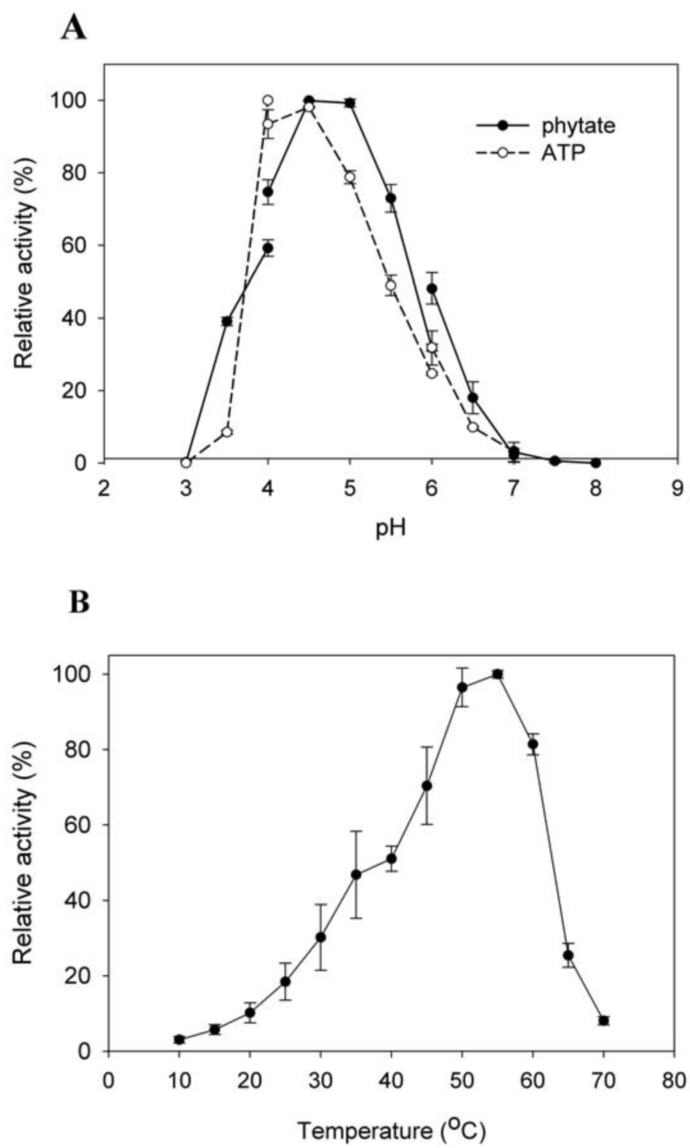

Figure 3.4. Effects of pH (A) and temperature (B) on PhyAsrl activity. (A) Standard phosphatase assays were performed with either 2 mM sodium phytate or ATP, at 37°C, over a pH range of 2 to 8. (B) To determine the optimum temperature for catalysis, standard phytase assays were performed with the temperature of the assays adjusted incrementally from 10 to 70 °C. The data presented in (A) and (B) are mean values with error bars representing the standard deviation between three independent experiments.

Table 3.2. Substrate specificity of PhyAsrl. For determination of relative activity, hydrolysis rate of Ins P_6 was taken as 100%. All substrates were tested at 2 mM with the exception of PIP_3 which was tested at 500μM.

Substrate	**Specific activity ($U\ mg^{-1}$)**	**Relative activity (%)**
ATP	29.15	179.63
Ins P_6	16.23	100.00
ADP	1.34	8.23
Phospho (enol) pyruvate	0.73	4.50
PIP_3	0.42	2.59
O-phospho-L-tyrosine	0.29	1.77
BCIP	0.15	0.91
ρNPP	0.12	0.77
Phenolphthalein diphosphate	0.08	0.52
D-fructose-1,6-diphosphate	0.08	0.47
O-phospho-L-serine	0.03	0.18

Table 3.3. Kinetic parameters of the recombinant PhyAsrl. Standard phosphatase assays were run (50 mM NaAc (pH 4.5); 0.2 M I with NaCl; 37°C) containing a varying amount of substrate. Data given is the average ± standard deviation of three independent experiments.

Substrate	**K_m (μM)**	**k_{cat} (s^{-1})**	**k_{cat}/K_m ($mM^{-1}\ s^{-1}$)**
Ins P_6	65 ± 14	6.644 ± 0.41	102.22 ± 22.77
ATP	195 ± 16	14.648 ± 0.84	75.12 ± 7.51

In an effort to elucidate the enzyme-substrate affinity and the preferred substrate, ATP or Ins P_6, we determined the catalytic properties of the recombinant wild-type PhyAsrl (Table 3.3). The rate of PhyAsrl catalyzed phosphate release can be saturated by increasing the concentrations of either substrate, and remains linear over the time period of the assay (data not shown). The initial rates of reaction as a function of Ins P_6 or ATP concentration are consistent with a classical Michaelis-Menton enzyme mechanism (data not shown). The apparent k_{cat} with Ins P_6 as a substrate is 2-fold lower than the k_{cat} with ATP; conversely, the apparent K_m for Ins P_6 is three-fold lower than that of ATP. The resulting specificity constants (k_{cat}/K_m), 102 mM^{-1} s^{-1} for the hydrolysis of Ins P_6 and 75 mM^{-1} s^{-1} for the hydrolysis of ATP, indicate that Ins P_6 is the preferred substrate (Konietzny and Greiner, 2002). The PTP-like phytase from *S. ruminantium* displays k_{cat} and K_m values towards Ins P_6 of 264 s^{-1} and 425 μM (refer, Chapter 2), 40 and six-fold higher than that of PhyAsrl, respectively.

Hydrolysis pathway

Isomer-specific HPIC analysis was utilized to identify the hydrolysis products generated by PhyAsrl. Purified PhyAsrl was incubated with excess sodium phytate for 30, 90 and 300 minutes and the stopped reaction was resolved by HPIC (Figure 3.5). Following 30 minutes of incubation, the quantity of Ins P_6 had decreased, and Ins(1,2,3,4,6)P_5 appeared as the major degradation product (90%), along with trace amounts of D/L-Ins(1,2,3,4,5)P_5 and D/L-Ins(1,2,4,5,6)P_5.

Following 90 minutes of incubation, no Ins P_6 or Ins P_5 products remained and D/L-Ins(1,2,3,4)P_4 was present as the major product (90%), along with small amounts of D/L-Ins(1,2,4,6)P_4 and D/L-Ins(1,2,5,6)P_4. Also detectable after 90 minutes was D/L-Ins(1,2,6)P_3 and/or Ins(1,2,3)P_3 and following 300 minutes of incubation these were found as the major product (90%), accompanied by trace amounts of D/L-Ins(1,2,4)P_3. The Ins P_2 products generated by 300 minutes of incubation were D/L-Ins(1,2)P_2 and/or Ins(2,5)P_2 and/or D/L-Ins(4,5)P_2, but can be narrowed to D/L-Ins(1,2)P_2 because no phosphates remain in the 5-position on any of the Ins P_3 hydrolysis products.

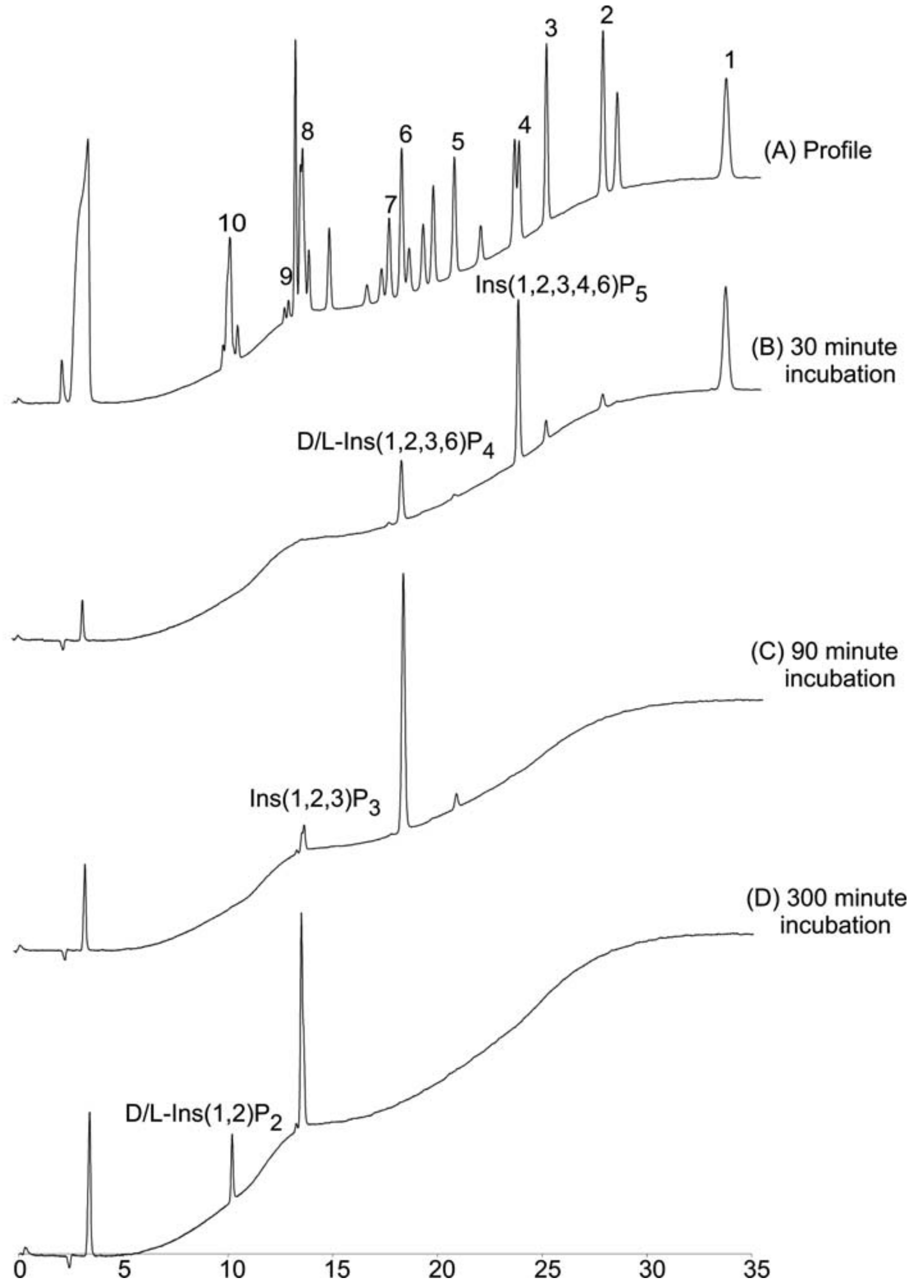

Figure 3.5. High-Perfomance Ion Chromatography analysis of hydrolysis products of *myo*-inositol polyphosphates by PhyAsrl. (A) Reference sample. The source of the reference *myo*-inositol phosphates is as indicated in Skoglund *et al.* (1998); Peaks: (1) Ins(1,2,3.4,5,6)P_6; (2) D/L-Ins(1,2,4,5,6)P_5; (3) D/L-Ins(1,2,3,4,5)P_5; (4) Ins(1,2,3,4,6)P_5; (5) D/L-Ins(1,2,5,6)P_4; (6) D/L-Ins(1,2,3,4)P_4; (7) D/L-Ins(1,2,4,6)P_4; (8) D/L-Ins(1,2,6)P_3, Ins(1,2,3)P_3; (9) D/L-Ins(1,2,4)P_3; (10) D/L-Ins(1,2)P_2, Ins(2,5)P_2, D/L-Ins(4,5)P_2. (B) PhyAsrl incubated with Ins P6 for 30 min. (C) PhyAsrl incubated with Ins P6 for 90 min. (D) PhyAsrl incubated with Ins P6 for 300 min. Peaks representative of major pathway products are labelled accordingly.

The kinetic parameters of lyophilized PhyAsrl were determined with different IPP substrates in order to identify the Ins P_4 hydrolysis products and to determine the specific isomer generated. The k_{cat} and K_m for the hydrolysis of D-Ins(1,2,3,4)P_4 and D-Ins(1,2,3,6)P_4 were 1.3 s^{-1} and 127.8 μM and, 2.3 s^{-1} and 96.3μM, respectively. The k_{cat} and K_m for the enzymatic hydrolysis of the purified Ins P_4 isomer generated by PhyAsrl were 2.2 s^{-1} and 97.1 μM, respectively. The similarity of the kinetic constants with D-Ins(1,2,3,6)P_4 as a substrate and those with the purified Ins P_4 generated by PhyAsrl suggests that D-Ins(1,2,3,6)P_4 was the isomer generated. Additionally, to determine the Ins P_3 isomer produced, kinetic parameters were compared for the hydrolysis of D-I(1,2,6)P_3 and the purified Ins P_3 produced by PhyAsrl. The k_{cat} and K_m values for the hydrolysis of D-I(1,2,6)P_3 were 3.4 s^{-1} and 167.6 μM, respectively, and for the hydrolysis of the purified Ins P_3 produced by PhyAsrl, 1.6 s^{-1} and 108.3 μM, respectively. The differing values suggest that D-I(1,2,6)P_3 is not the Ins P_3 isomer produced by PhyAsrl but rather Ins(1,2,3)P_3.

The end products of phytic acid degradation were determined by incubating excess protein with a limiting substrate concentration. The results of a gas chromatography-mass spectrometry analysis of the end products revealed that the end product is Ins(2)P.

3.4 DISCUSSION

Sequence analysis

We have cloned a gene (*phyAsrl*) encoding phytase from *Selenomonas ruminantium* subsp. *lactylitica.* This is the second full-length PTP-like phytase to be examined in the literature. The deduced amino acid sequence shows significant similarity to the recently characterized PTP-like phytase from *S. ruminantium* (Chu *et al.*, 2004; refer, Chapter 2), most notably in the PTP-like active site signature sequence (Figure 3.2). The Ins P_6-degrading enzyme from *S. ruminantium* has been shown to have a PTP-like core structure and catalytic mechanism similar to that of members of the PTP superfamily (Chu *et al.*, 2004; refer, Chapter 2). The sequence identity, conservation of the active site signature sequence and similar ability to hydrolyze Ins P_6 allows us to suggest that these enzymes may have a similar three-dimensional structure and a common mechanism of catalysis. Further, several bacterial putative PTPs have comparable sequence similarity to PhyAsrl (Figure 3.2), but unknown enzymatic properties. It is possible that these proteins also have the ability to hydrolyze Ins P_6.

Enzymatic activity and substrate specificity

The gene product of *phyAsrl* was expressed, purified and characterized. The catalytic activity of PhyAsrl was found to be influenced by the I of the assay mixture. The *Yersinia* PTP and mammalian PTP1-catalyzed hydrolysis of pNPP were also sensitive to the I of the reaction medium, which was suggested to be due to electrostatic interactions between the protein and its substrate (Zhang *et al.*, 1992; Zhang, 1995). The active site region of PhyAsrl's homologue from *S. ruminantium* is highly positively charged (Chu *et al.*, 2004), similar to Yersinia PTP and PTP1 (Barford *et al.*, 1994; Stuckey *et al.*, 1994). This implies that electrostatic interactions are similarly important for PhyAsrl activity.

Phytases can be divided into two major groups, acid and alkaline, based on their optimal pH for catalysis (Konietzny and Greiner, 2002). Since most interest in phytase has traditionally focused on finding an enzyme that would function in the digestive tract of monogastric animals, most studies have focused on acid phytases (Mullaney and Ullah, 2003). Acid phytases include those enzymes belonging to the HAP, PAP and PTP superfamily classes of phosphatases (Mullaney and Ullah, 2003; refer, Chapter 2). PhyAsrl shows optimal phytase activity at pH 4.5 and is thus an acid phytase. This is comparable to the previously characterized PTP-like phytase from *S. ruminantium* which showed optimal phytase activity at pH 5 (refer, Chapter 2). Of note, the PTP from *Yersinia* and mammalian

PTP1 both display optimal activity at similar pHs (*i.e.*, pH 5 and 5.5, respectively) towards the artificial phosphatase substrate ρNPP (Zhang *et al.*, 1992; Zhang, 1995).

PhyAsrl exhibits narrow substrate specificity with significant levels of activity being shown towards only Ins P_6 and ATP. Although Ins P_6 is not the compound with the highest relative rate of hydrolysis, it does exhibit the highest specificity constant (k_{cat}/K_m) for Ins P_6, indicating that it is the preferred substrate (Konietzny and Greiner, 2002). ATPase activity may be indicative of the ablitity to dephosphorylate pyrophosphate groups on biologically relevant 'higher' phosphoinositol substrates such as Ins P_7 (Raboy, 2003). Most acid phytases exhibit a broad specificity for substrates with phosphate esters (Konietzny and Greiner, 2002). PhyAsrl displays narrow specificity, but its activity is in the low end of the range of characterized phytases, whereas most phytases with strict substrate specificity show higher activity than those with broad specificity (Konietzny and Greiner, 2002). To date, the phytases that display the greatest substrate specificity have been isolated from *Bacillus* sp. (Shimizu, 1992) and *E. coli* (Greiner et al., 1993).

Hydrolysis pathway

To date, most of the known phytases initiate hydrolysis of Ins P_6 at the D-3 (L-1) or D-4 (L-6) phosphate positions, several also cut at the D-6 position first (Konietzny and Greiner, 2002). The PTP-like phytase from *S. ruminantium* hydrolyzes the D-3-phosphate position of Ins P_6 first (refer, Chapter 2). One previous exception is the alkaline phytase purified from lily pollen, which is a 5-phytase belonging to the class of HAPs (Barrientos *et al.*, 1994; Mehtaa *et al.*, 2006). HPIC analysis indicates that PhyAsrl primarily (90%) initiates hydrolysis at the 5-phosphate position, making it a 5-phytase. Since all the theoretically existing myo-inositol penta*kis*phosphate isomers are well resolved on the HPIC system, the identity of the penta*kis*phosphate isomer generated by PhyAsrl is well established. We have thus characterized the first microbial phytase to display specificity for the 5-phosphate ester bond of Ins P_6.

PhyAsrl displays the ability to cleave all five equatorial phosphate groups of Ins P_6, a characteristic common to many acid phytases (Konietzny and Greiner, 2002). PhyAsrl can produce Ins(2)P via the routes indicated in Figure 3.6. The HPIC and kinetic results indicate that about 90% of the Ins P_6 is hydrolyzed according to a single pathway, Ins P_6, Ins(1,2,3,4,6)P_5, D-Ins(1,2,3,6)P_4, Ins(1,2,3)P_3, D/L-Ins(1,2)P_2 finally to Ins(2)P (Figure 3.6). The order in which PhyAsrl removes phosphate groups has little resemblance to that of the Ins P_6-degrading enzyme from *S. ruminantium* (refer, Chapter 2) except that both enzymes have the ability to cleave all five equatorial phosphate groups of Ins P_6.

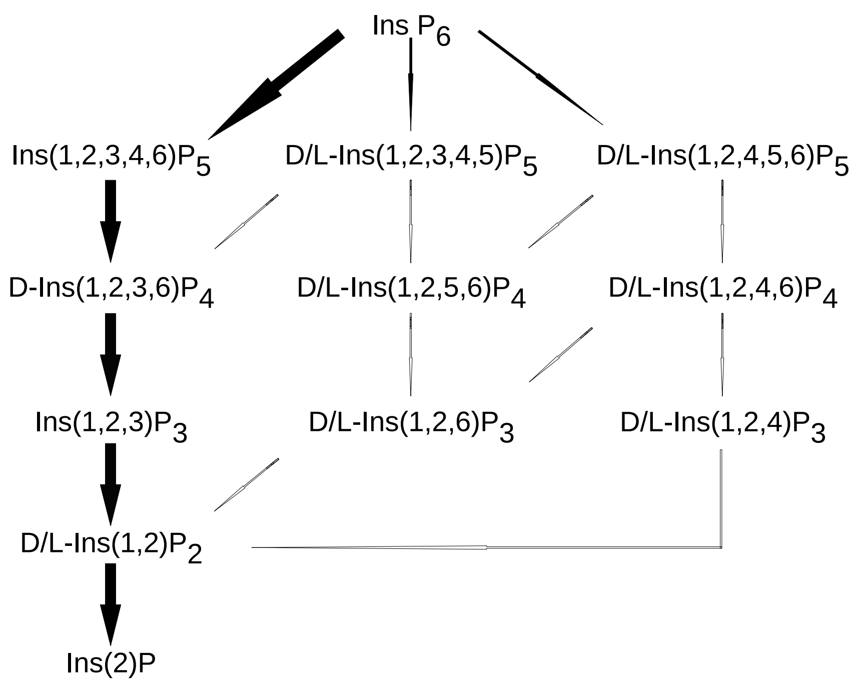

Figure 3.6. The dephosphorylation pathways of Ins P_6 by PhyAsrl as determined by high-performance ion-pair chromatography (HPIC) and kinetic analysis. Larger arrows indicate major pathway, smaller arrows indicate minor pathways. Open arrows are possible routes of hydrolysis, solid arrows represent routes supported with kinetic data. The major pathway accounts for approximately 90% of degradation products.

CHAPTER FOUR

Cloning and characterizing PhyAme from *Megasphaera elsdenii*, a PTP-like phytase with mixed 3- or 6-phosphate position specificity

ABSTRACT

PhyAme from *Megasphaera elsdenii* is a protein tyrosine phosphatase (PTP)-like phytase with a number of unique properties. In order to elucidate its substrate specificity and pathway of Ins P_6 dephosphorylation, a combination of kinetic and high-performance ion-pair chromatography studies were conducted. The data indicate that PhyAme has a general specificity for polyphosphorylated *myo*-inositol substrates *in vitro*. PhyAme preferentially cleaves Ins P_6 at one of two phosphate positions; *i.e.*, the D-3- or D-4-phosphate positions. This enzyme predominantly degrades Ins P_6 to Ins(2)P via: (A) D-Ins(1,2,4,5,6)P_5, D-Ins(1,2,5,6)P_4, D-Ins(1,2,6)P_3 and D-Ins(1,2)P_2, and (B) D-Ins(1,2,3,5,6)P_5, D-Ins(1,2,3,6)P_4, Ins(1,2,3)P_3 and D/L-Ins(1,2)P_2 (60% and 30% respectively). Finally, bioinformatic analysis and the identification of a functionally characterized homologue have been used to speculate a biological role.

4.1 INTRODUCTION

Protein tyrosine phosphatase (PTP) superfamily enzymes have been discovered in a range of prokaryotes, and most appear to serve roles which mimic their better-known eukaryotic counterparts as regulators of cellular function (Shi *et al.*, 1998; Kennelly and Potts, 1999). Some bacteria have adapted PTPs as ‘molecular missiles’, secreted into the infected host where they assist in the progression of infection (Bliska *et al.*, 1991; Fu and Galan, 1998; Bretz *et al.*, 2003). Enzymes belonging to the PTP superfamily have been isolated from the anaerobic ruminal bacteria *Selenomonas ruminantium* (PhyAsr)(Chu *et al.*, 2004; refer, Chapter 2) and *S. ruminantium* subsp. *lactilytica* (PhyAsrl)(refer, Chapter 3) and characterized. These enzymes also contain a conserved PTP-like active site signature sequence ($C(X)_5R$) that facilitates a classical PTP mechanism of dephosphorylation (Chu *et al.*, 2004; refer, Chapter 2). The X-ray structure of PhyAsr reveals a PTP-like domain as well as a smaller β-barrel domain, a structural feature not found in other known PTP-like enzymes (Chu *et al.*, 2004). These enzymes are also unique among PTPs in that they have the ability to dephosphorylate *myo*-inositol hexa*kis*phosphate (Ins P_6).

All enzymes that can hydrolyze Ins P_6 have been grouped together as phytases (*myo*-inositol hexa*kis*phosphate phosphohydrolases). Four distinct classes of phosphatases have been characterized in the literature as having phytase activity; *i.e.*, histidine acid phosphatases, β-propeller phytases, purple acid phosphatases (Mullaney and Ullah, 2003), and most recently, PTP-like phytases (Chu *et al.*, 2004; refer, Chapter 2;Chapter 3). Based on the position of the first phosphate hydrolyzed, three types of phytases are recognized by the Enzyme Nomenclature Committee of the International Union of Biochemistry; *i.e.*, 3-phytase (EC 3.1.3.8), 6-phytase (EC 3.1.3.26) and 5-phytase (EC 3.1.3.72). Phytases hydrolyze Ins P_6 in a sequential and stepwise manner, yielding lower inositol polyphosphates (IPPs) which may again become substrates for further hydrolysis (Konietzny and Greiner, 2002). This occurs at different rates and in different orders among phytases, and may be evidence of the variety of biological roles played by these enzymes, as well as their substrates, Ins P_6 and lower IPPs.

Phytases have been the focus of countless studies due to interest in: 1) their ability to reduce the metabolically unavailable organic phosphate content of livestock feedstuffs (Reddy *et al.*, 1989; Konietzny and Greiner, 2002), and 2) their ability to produce lower IPPs for pharmaceutical applications (Greiner *et al.*, 2002b). IPPs have been implicated in *myo*-inositol, phosphate and cation storage (Lott and Buttrose, 1978a;1978b; Batten and Lott, 1986; Chen and Lott, 1992; Hawkins *et al.*, 1993; Wada and Lott, 1997), dsDNA break repair

(Hanakahi *et al.*, 2000), clathrin-coated vesicular recycling and control of neurotransmission (Fukuda and Mikoshiba, 1997; Gaidarov *et al.*, 2001; Rizzoli and Betz, 2002; Brailoiu *et al.*, 2003), cell proliferation (Orchiston *et al.*, 2004) and increased natural killer cell activity in the blood of rats (Zhang *et al.*, 2005). The chemical synthesis of individual IPPs involves difficult steps, is performed at extreme conditions (Billington, 1993) and the separation of individual isomers is problematic with most analytical approaches (Greiner *et al.*, 2002b). Since phytases hydrolyze Ins P_6 in an ordered and stepwise manner, the production of IPPs and free *myo*-inositol using phytase is a promising alternative to chemical synthesis (Greiner and Konietzny, 1996; Greiner *et al.*, 2000a). Interestingly, PhyAsr and PhyAsrl display relatively ordered and specific pathways of Ins P_6 dephosphorylation, a unique feature among characterized phytases.

A number of putative PTP-like PhyA homologues have been partially cloned from a range of bacteria isolated from the rumen and other anaerobic sources (Nakashima *et al.*, 2006). This paper describes the cloning and sequencing of the full gene encoding a novel PTP-like phytase from *Megasphaera elsdenii* (*phyAme*), as well as the overexpression, purification, and detailed physicochemical and stereospecific characterization of the recombinant gene product. Additionally, bioinformatic analysis has been used to speculate a biological role.

4.2 MATERIALS AND METHODS

Gene cloning

Megasphaera elsdenii YR60 was cultured anaerobically (100% CO_2) at 39°C in Hungate tubes with 5 mL of modified Scott and Dehority medium (Scott and Dehority, 1965) containing 10% (v/v) rumen fluid, 0.2% (w/v) glucose, 0.2% (w/v) cellobiose and 0.3% (v/v) starch. Isolation of total DNA was performed as described previously (Priefer *et al.*, 1984).

Genomic DNA was digested with *Hin*dIII. The relative size of the fragment containing the gene coding for phytase (*phyAme)* was determined by Southern blot hybridization using the DIG DNA Labeling and Detection Kit (Boehringer; Mannheim, Germany) and a probe. The probe was a polymerase chain reaction (PCR) product corresponding to the previously determined sequence fragment (GeneBank accession number DQ257441; Nakashima et al. 2006). Digested DNA corresponding to the approximate size of the *phyAme* containing fragment was gel purified (MinElute Gel Extraction Kit; Qiagen Inc.; Mississauga, ON), and ligated into dephosphorylated *Hin*dIII pBluescript II SK (+) (Stratagene, La Jolla, CA). PCR primers (Table 4.1) were generated from the known internal *phyAme* partial sequence (Nakashima *et al.*, 2006). These were used in conjunction with M13 and T3 universal primers to generate PCR products from the ligation mix corresponding to regions of *phyAme* adjacent to the known sequence. The PCR products were ligated into pGEM-T Easy (Promega Corp., Madison, WI) and sequenced by automated cycle sequencing at the University of Calgary Core DNA and Protein services facilities. Sequence data was analyzed with the aid of SEQUENCHER™ version 4.0 (Gene Codes Corp. Ann Arbor, MI) and MacDNAsis version 3.2 (Hitachi Software Engineering Co., Ltd., San Bruno, CA). Homology searches in GenBank (Fassler *et al.*, 2000; Benson *et al.*, 2006) were done using BLAST (Altschul *et al.*, 1990) and preliminary sequence alignments were generated using CLUSTAL W 1.82 (Higgins *et al.*, 1994; Chenna *et al.*, 2003). Alignment optimization was carried out with GeneDoc (Nicholas *et al.*, 1997) using methods for comparative structure-based sequence alignments (Greer, 1981) and the experimentally determined structure of the PTP-like phytase from *S. ruminantium* (PhyAsr; PDB accession: 1U24; Chu *et. al.*, 2004). Secondary structure predictions were generated with SSpro (Pollastri *et al.*, 2002) on the SCRATCH web server (Baldi and Pollastri, 2003; Cheng *et al.*, 2005).

Table 4.1. Primers used in this study. Restriction sites are underlined.

Primer Name	**Primer Sequence**
060 For	CGA TTT GCC CAT TCA TCC TC
060 Rev	CCT TTC CCC TGG TCG TAG AC
060 Rev N	AGA CGG CCG TCG GAG ATT T
*Nde*I Exp	GCC ATA TGG TTT TTT CGG CCA TGG GTA T
*Eco*RI Exp	GCG AAT TCT CAA CGG TTA TTG ACT CTC A

Recombinant phyAme expression construct

The region coding for the mature *Megasphaera elsdenii* phytase (*phyAme*; GeneBank accession number EF025174; residues 26-360 of gene product) was amplified from genomic DNA using PCR. The predicted signal peptide sequence was determined with SIGNAL P 3.0 (Nielsen *et al.*, 1997; Bendtsen *et al.*, 2004). PhyAme forward (*Nde*I Exp) and reverse (*Eco*RI Exp) primers (Table 4.1) included an *Nde*I and *Eco*RI site, respectively, for cloning and a 5' GC cap. The PCR product was digested with *Nde*I and *Eco*RI and ligated into similarly digested pET28b vector (Novagen Inc., San Diego, CA). Constructs were verified with automated cycle sequencing.

Protein production and purification

Escherichia coli BL21 (DE3) cells (Novagen Inc.) were transformed with the *phyAme* expression constructs. Over expression was carried out according to the instructions in the pET Systems Manual (Novagen Inc.). Cultures were induced with the addition of IPTG to a final concentration of 1 mM and incubated for 4 hours at 37^{o}C. Induced cells were harvested by centrifugation and resuspended in lysis buffer: 20 mM KH_2PO_4 (pH 7), 0.6 M NaCl, 1 mM β-mercaptoethanol (BME), and one Complete Mini, EDTA-free protease inhibitor tablet (Roche Applied Science; Laval, QC). Cells were sonicated and debris was removed by centrifugation at 20 000 x g for 45 minutes. The protein was purified to homogeneity using Ni^{2+}-NTA spin columns according to the supplied protocol (Qiagen Corp.). Protein was washed on the column with lysis buffer containing 15 mM imidazole (wash buffer #1) and then with wash buffer #2 (20 mM PO_4 (pH 7), 0.3 M NaCl, 10% glycerol, 15 mM imidazole, and 1 BME). Protein was subsequently eluted with lysis buffer containing 0.35 M imidazole. Purified protein was dialyzed with three buffer changes into 500 mL of 20 mM Tris (hydroxymethyl) aminomethane (Tris; pH 7), 0.3 M NaCl, 0.1 mM EDTA and 5 mM BME. The homogeneity of the purified protein was confirmed by 12% (w/v) SDS-polyacrylamide gel electrophoresis (SDS-PAGE)(Laemmli, 1970), and Coomassie Brilliant Blue R-250 staining. The theoretical M_r and extinction coefficient of PhyAme were determined using PROT PARAM (Gasteiger *et al.*, 2005). Protein concentrations were determined by monitoring the A_{280}. For storage, purified protein was dialyzed into 50 mM ammonium bicarbonate (pH 8) with 3 buffer changes, lyophilized and stored at -20^{o}C.

Gel Filtration

Molecular mass was determined by fast protein liquid chromatography (FPLC) on a Superdex 75 (Pharmacia Biotech, St Albans, UK) preparative column (2.5 X 100 cm), equilibrated with one of the buffers tested: 25 mM NaAc (pH 5), pyridine (pH 5), histidine (pH 6), imidazole (pH 6), phosphate (pH 7), Tris (pH 7.5), HEPES (pH 8) containing 0.3 M I with NaCI, 1 mM EDTA, 1 mM BME, at 8^{o}C. 1 mL of protein solution (25 μM), in the corresponding filtration buffer, was loaded on the column. The flow rate was 2 mL/min, and the elution was monitored by absorbance at 280 nm. The column was standardized using elongation factor EF-Tu (M_r = 48 kDa), bovine serum albumin (M_r = 66 kDa), and elongation factor EF-G (M_r = 78 kDa).

Dynamic light scattering

Light scattering data for PhyAme (6-25 μM) were collected with a DynaPro Dynamic Light Scattering Instrument (Protein Solutions Inc., High Wycombe, UK) and analyzed with DYNAMICS ™ (version 5.24.02, Protein Solutions Inc.). The hydrodynamic radius (R_h) of

PhyAme was determined in solution with 25 mM NaAc (pH 5) or Tris (pH 7.5), 0.2 M I with NaCI, 1 mM EDTA, 1 mM BME, at 21^{o}C. Molecular weight (M_r) was estimated with a standard protein curve, where M_r = (R_h factor * R_h) ^ power, R_h factor = 1.549, and power = 2.426. Each result presented is an average of at least 20 readings between two separate experiments.

Assay of enzymatic activity

Activity measurements were carried out at 37°C. Enzyme reaction mixtures consisted of a 600 μL buffered substrate solution and 150 μL of a 0.5 μM enzyme solution. The buffered substrate solution contained 50 mM sodium acetate (pH 5) and 2 mM sodium phytate, or another of the substrates used in our study. I was held constant at 0.2 M with the addition of NaCl except in those assays examining the effect of I, where NaCl concentrations were varied from 0 to 0.8 M. Phytase activity was determined at different pH's with overlapping buffer systems: 50 mM glycine (pH 2-3), 50 mM formate (pH 3-4), 50 mM sodium acetate (pH 4-6), 50 mM imidazole (pH 6-7), and 50 mM Tris (pH 7-8). Phytase activity was also determined at incremental temperatures from 10 to 70^{o}C. Following the appropriate empirically determined incubation period the reactions were stopped and the liberated phosphate was quantified with the ammonium molybdate methods previously described (refer, Chapter 2;Chapter 3). Activity (U) was expressed as μmol phosphate liberated per min. The steady-state kinetic constants (K_m, k_{cat}) for the hydrolysis of Ins P_6 and other lower IPPs by PhyAme were calculated from Michaelis-Menton plots. The data was analyzed with non-linear regression using SIGMA-PLOT 8.0 (Systat Software Inc.; Point Richmond, CA).

PhyAme's substrate specificity was determined by replacing Ins P_6 in the standard phosphatase assay (37^{o}C with 50 mM sodium acetate, pH 5) with other phosphoester containing substrates. The I of the reactions was adjusted to 0.2 M with NaCl accordingly. Phosphoester containing substances examined included: sodium phytate, phosphatidylinositol-3,4,5-triphosphate (PIP_3), β-glycerophosphate, D/L-α-glycerophosphate, α-naphthyl phosphate, phospho (enol) pyruvate, phenolphthalein diphosphate, O-nitophenyl-β-D-galactopyranoside 6-phosphate, phenyl phosphate, ρ-nitrophenyl phosphate (ρNPP), 5-bromo-4-chloro-3-indolyl phosphate (BCIP), O-phospho-L-tyrosine, O-phospho-L-threonine, O-phospho-L-serine, adenosine 5'-triphosphate (ATP), adenosine 5'-diphosphate (ADP), D-fructose-1,6-diphosphate, D-fructose-6-phosphate, D-glucose-6-phosphate, D-ribose-5-phosphate. All substrates tested for hydrolysis were present at 2 mM with the exception of PIP_3 which was 500 μM.

The effect of enzyme concentration on the hydrolysis of Ins P_6 was investigated with standard phytase assays at pH 5.0, 37 ^oC**,** in 50 mM NaAc, I = 0.2 M using NaCl with limiting substrate. The reaction was started by adding enzyme, to a final concentration of 1.5 to 100 nM protein, to a 0.05 mM substrate solution. In all cases, assay tubes were pre-incubated with 1 mg/mL BSA to minimize irreversible enzyme absorption.

Preparation of individual myo-inositol phosphate isomers

Lyophilized PhyAsr was shipped to Dr. Ralf Greiner at the Centre for Molecular Biology of the Federal Research Centre for Nutrition and Food in Karlsruhe Germany where HPIC, production and isolation of lower IPPs and kinetic studies with lower IPPs was performed.

Phytases from *Aspergillus niger*, *E. coli*, and rye were used to generate D-Ins(1,2,4,5,6)P_5, D-Ins(1,2,3,4,5)P_5, and D-Ins(1,2,3,5,6)P_5. These isomers and the Ins P_5 generated by PhyAme were prepared as described previously (Greiner *et al.*, 2002a; Greiner *et al.*, 2002b; refer, Chapter 2;Chapter 3). Sodium phytate (2.5 mmol) was incubated at 37°C in a mixture containing 50 mM NH_4-acetate, pH 4.5 (*A. niger and E. coli*), pH 5 (*M. elsdenii*) or pH 6 (rye) and 10 U of the appropriate enzyme in a final volume of 500 μL.

Identification of enzymatically formed hydrolysis products

Standard phytase assays were run at 37°C by addition of 50 μL of a suitably diluted solution of PhyAme to the incubation mixtures. Periodically stopped reactions were resolved on a High-Performance Ion Chromatography system (HPIC) using a Carbo Pac PA-100 (4 x 250 mm) analytical column (Dionex; Sunnyvale, CA) and a gradient of 5–98% HCl (0.5 M, 0.8 mL/min) as previously described (Skoglund *et al.*, 1998). The eluants were mixed in a post-column reactor with 0.1% $Fe(NO_3)_3$ in a 2% $HClO_4$ solution (0.4 mL/min) (Phillippy and Bland, 1988). The combined flow rate was 1.2 mL/min. *myo*-inositol monophosphates were produced by incubation of 1.0 U of PhyAme with a limiting amount (0.1 μmol) of Ins P_6 in a final volume of 500 μL of 50 mM NH_4-acetate. The end products were identified using a gas chromatograph coupled with a mass spectrometer as previously described (Greiner *et al.*, 2002a; Greiner *et al.*, 2002b).

4.3 RESULTS

Sequence analysis

A 1.8 kbp DNA fragment was isolated from the genome of *Megaspaera elsdenii* YR60 (GeneBank accession number: DQ257441) by cloning regions up and downstream of a sequence fragment determined by Nakashima *et al,* (2006). BLAST X analysis of the sequenced product indicated the presence of one open reading frame (ORF; *phyAme*) and one partial ORF (*orf2*) with homologues in GeneBank (Figure 4.1). O*rf2* is located 200 nucleotides downstream of *phyAme* and its product is similar (33/55 identities) to the N-terminus of a major envelope protein of *Selenomonas ruminantium* (GeneBank accession number AB252707). The complete *phyAme* ORF encodes a 360 amino acid protein (PhyAme) that contains a PTP-like signature sequence, CEAGAGR. Several PhyAme homologues were found in GenBank with BLAST and all are of bacterial origin. The homologues with the highest sequence identity to PhyAme are the PTP-like phytases from *S. ruminantium* (PhyAsr; 50% identity) and *S. ruminantium* subsp. *lactilytica* (PhyAsrl; 34% identity; Figure 4.2). Other homologues are putative members of the PTP superfamily and display 20 to 27% identity to PhyAme (Table 4.2).

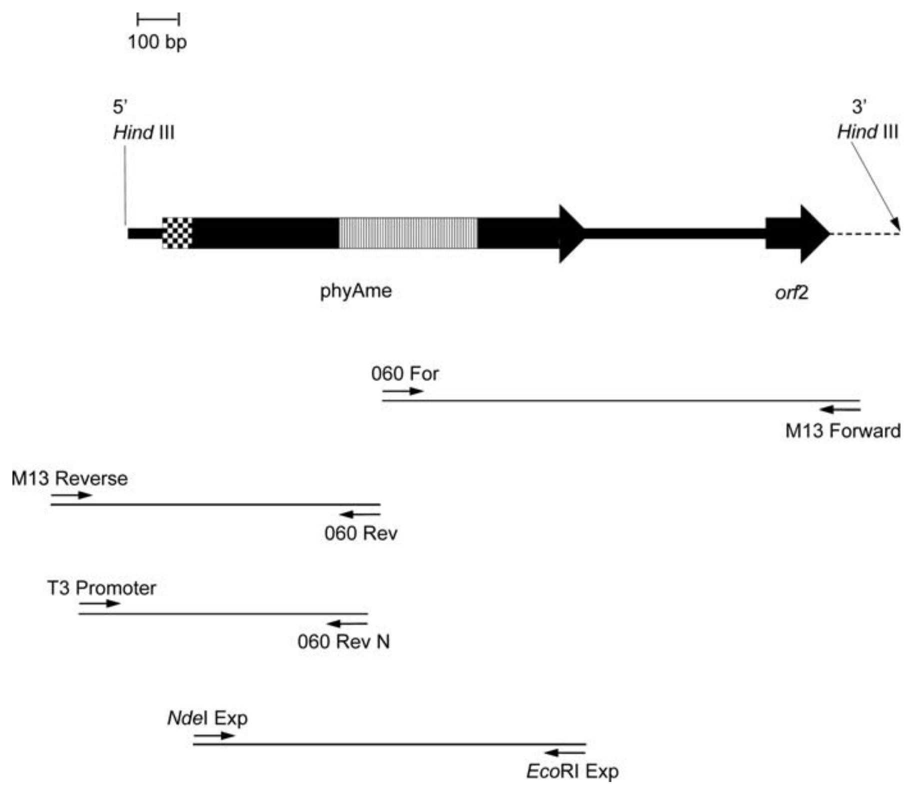

Figure 4.1. Schematic diagram representing *phyAme* and the steps involved in its PCR cloning. The relative positions of the primers used are indicated. The 380 bp fragment cloned previously is presented as a striped box. The predicted signal peptide is indicated by a checkered box. A dashed line represents unsequenced regions.

Interestingly, the PTP-like domain of a type III-secreted protein HopPtoD2 from *Pseudomonas syringae* also shows some similarity to PhyAme (18% identity; Figure 4.2). Although the overall sequence identity is low, the identities between the 230 C-terminal residues of PhyAme and HopPtoD2 are significant (25%). Additionally, secondary structure predictions were performed for HopPtoD2 using Recurrent Neural Networks (Baldi and Pollastri, 2003) (Figure 4.2) and these align well with the experimentally determined structure of PhyAsr on the sequence alignment. Perhaps most notable is the sequence and predicted structural similarity within the region corresponding to the small, partial β-barrel domain found in PhyAsr, a novel feature amongst PTP-like enzymes (Chu *et al.*, 2004).

Table 4.2. Similarity of PTP-like phytase sequence from *Megasphaera elsdenii* to PTP-like phytase and putative PTP homologoues found in GeneBank using BLAST. Similarity scores were determined with GeneDoc and the structure based sequence alignment described in materials and methods.

Source	**GeneBank accession**	**Description**	**% Identity PhyAme**
S. ruminantium	AAQ13669	PTP-like IPPase	44
S. ruminantium subsp. *lactylitica*	EF016752	PTP-like IPPase	29
Parachlamydia sp. UWE25	CAF24552	Putative PTP	27
Clostridium acetobutylicum	NP_149178	Putative PTP	26
Clostridium perfringens	ABG83558	Putative PTP	26
Bdellovibrio bacteriovorus	CAE79111	Putative PTP	26
Acidovorax avenae subsp. *citrulli*	ZP_01403063	Putative PTP	24
Clostridium beijerincki	ZP_00910765	Putative PTP	24
Xanthomonas campestris	AAM41387	Putative PTP	24
Clostridium tetani	NP_782216	Putative PTP	21
Legionella pneumophila	CAH16976	Putative PTP	20
Pseudomonas syringae	Q79LY0	PTP-like; HopPtoD2	17

Expression and purification of PhyAme

Following induction with IPTG, overexpression of a polypeptide with an M_r of about 39 kDa was observed with SDS-polyacrylamide gel electrophoresis (PAGE). This is consistent with the mass predicted from the sequence of the recombinant protein (predicted M_r = 40 561 Da). The Ni^{2+}-NTA purification was able to produce > 95% homogeneity of

PhyAme in a single step, as determined by SDS-PAGE and Coomassie Brilliant Blue R-250 staining (data not shown). The specific activity of PhyAme toward Ins P_6 as a substrate was examined. PhyAme can hydrolyze Ins P_6, and displays a maximum specific activity of 269.3 U mg^{-1}. The specific activity of PhyAme is average amongst PTP-like phytases when compared to the relatively high activity of PhyAsr (668.11 U mg^{-1}) (refer, Chapter 2) and the relatively low activity of PhyAsrl (16.23 U mg^{-1}) (refer, Chapter 3).

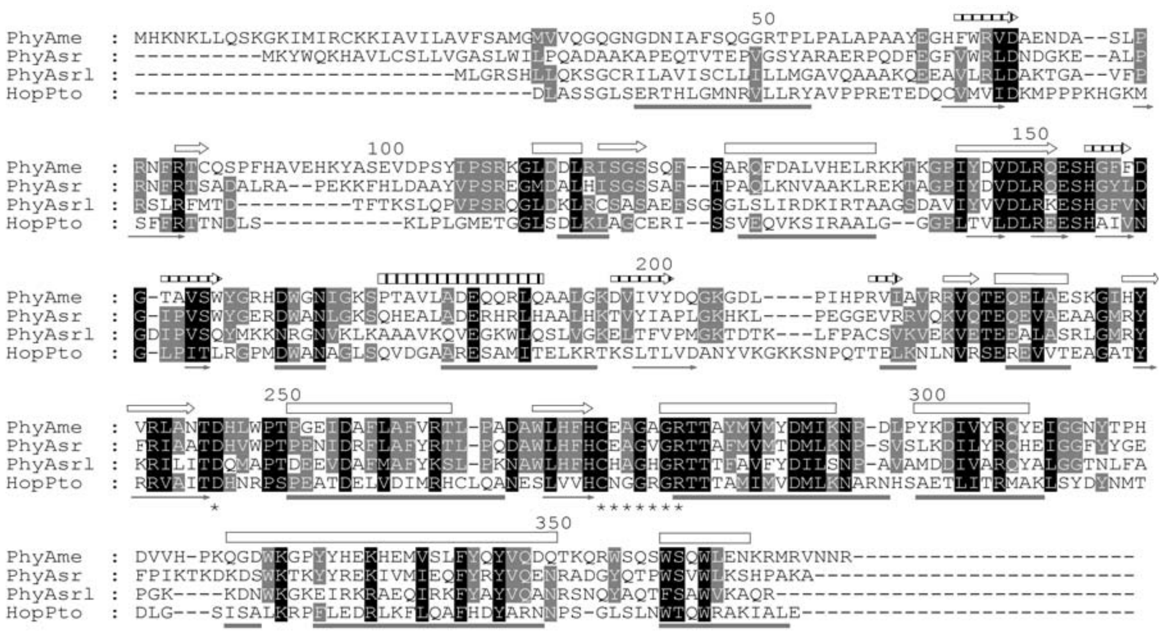

Figure 4.2. Comparative structure-based amino acid sequence alignment of the *M. elsdenii* PTP-like enzyme and its characterized GeneBank homologues. Shading is according to alignment consensus as given by GENE DOC (black = 100%; dark grey = 75%) with similarity groups enabled. The protein abbreviation, source and GenBank accession numbers are as follows: PhyAme, *M. elsdenii*, EF025174; PhyAsr, *S. ruminantium* JY35, AAQ13669; PhyAsrl, *S. ruminantium* subsp. *lactylitica*, EF016752; HopPtoD2, *Pseudomonas syringae*, AAO43976 (residue numbers 152-468). Numbering is according to the sequence of PhyAme found in GeneBank. The PTP-like signature sequence and the conserved upstream aspartic acid are identified by asterisks. Secondary structures are identified for PhyAsr (PDB accession: 1U24) above the sequences with hollow arrows representing β-strands and hollow boxes indicating α-helices. The secondary structures corresponding to the partial β-barrel domain of PhyAsr (Chu *et al.*, 2004) are indicated by vertical stripes. Below the sequences are the predicted secondary structures for hopPtoD2 according to Recurrent Neural Networks (Baldi and Pollastri, 2003), where solid arrows represent β-strands and solid boxes indicate α-helices.

Biochemical profiles and substrate specificity

The I, pH, and temperature dependence of PhyAme activity were determined in order to establish the optimal conditions for Ins P_6 hydrolysis. Optimal PhyAme activity was displayed at I of 0.2 - 0.3 M and activity quickly decreased as I was increased above 0.4 M (Figure 4.3). PhyAme is active under a narrow range of acidic pHs and optimal activity occurrs at pH 5 (Figure 4.4A). Previously characterized PhyAsr and PhyAsrl show optimal activity at pH 5 and 4.5, respectively (refer, Chapter 2;Chapter 3). PhyAme displayed maximum activity at 60^{o}C and activity decreased sharply at higher temperatures (Figure 4.4B).

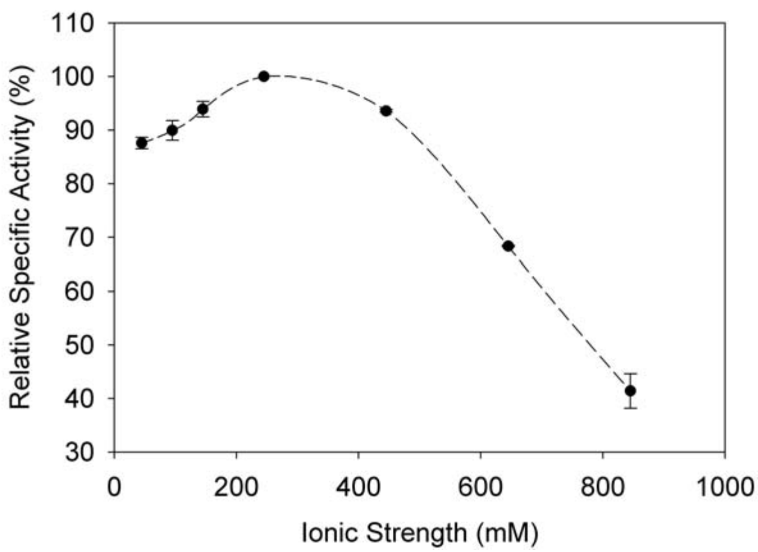

Figure 4.4. Effect of I on the activity of PhyAme. Standard assays were run under varying I controlled with NaCl. The data are mean values with error bars representing the standard deviations between three independent experiments. Values are normalized to 0.25 M.

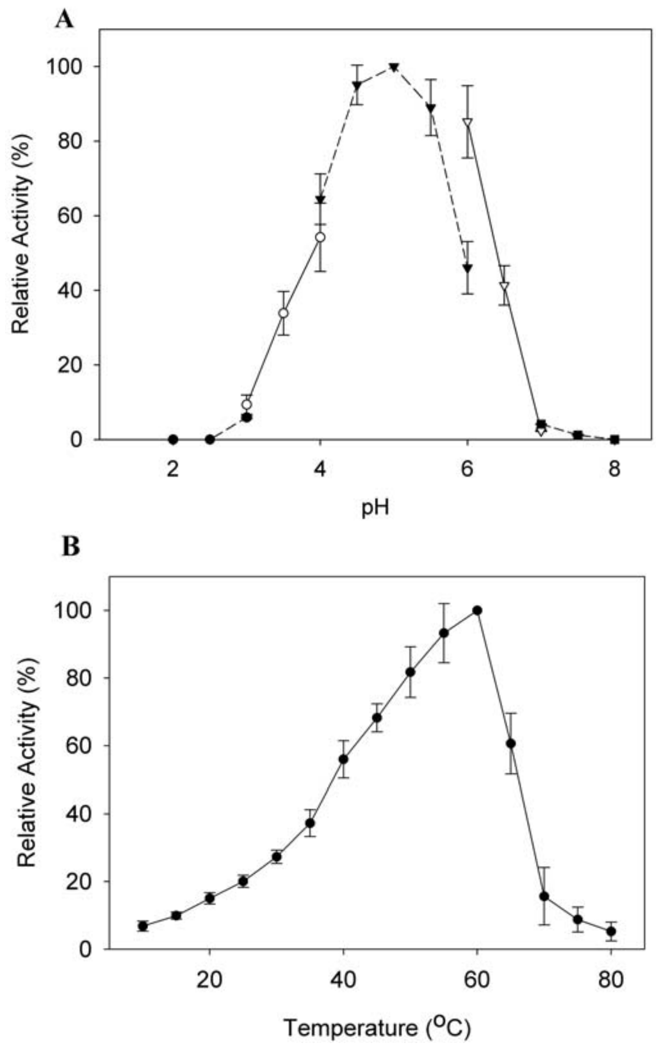

Figure 4.3. Effects of pH (A) and temperature (B) on PhyAme activity. (A) Standard phytase assays were performed with 2 mM sodium phytate over a pH range of 2 to 8. (B) To determine the optimum temperature for catalysis, standard phytase assays were performed with the temperature of the assays adjusted incrementally from 10 to 80 °C. The data presented in (A) and (B) are mean values with error bars representing the standard deviation between three independent experiments.

We tested PhyAme's ability to hydrolyze various other phosphorylated compounds in order to characterize its specificity. The compounds that were hydrolyzed by PhyAme are given in Table 4.3. PhyAme displays extremely narrow substrate specificity, showing significant activity only towards IPP substrates. Besides IPPs, PhyAme could hydrolyze the phosphoinositide PIP_3 with a specific activity of 1.26 U mg^{-1}, 0.66% relative to the activity displayed towards Ins P_6. PhyAme displayed very little activity towards the commonly used phosphatase substrates pNPP and BCIP or towards any of phosphorylated amino acids tested.

Table 4.3. Substrates that were dephosphorylated by PhyAme. For determination of relative activity hydrolysis rate of Ins P_6 was taken as 100%. All substrates were tested at 2 mM with the exception of PIP_3 which was tested at 500 μM. A full list of substrates tested is presented in '*Materials and Methods*'.

Substrate	**Specific activity ($U\ mg^{-1}$)**	**Relative activity (%)**
Ins P_6	190.75	100.00
PIP_3	1.26	0.66
ATP	0.97	0.51
D-fructose-1,6-diphosphate	0.57	0.30
α-naphthyl acid phosphate	0.56	0.29
pNPP	0.55	0.29
Phospho (enol) pyruvate	0.54	0.28
BCIP	0.52	0.27
O-phospho-L-tyrosine	0.49	0.26
D-ribose-5-phosphate	0.27	0.14
O-phospho-L-threonine	0.25	0.13
Phenolphthalein diphosphate	0.20	0.10

Oligomeric nature of PhyAme

Size estimates of PhyAme were performed by gel filtration on a Superdex 75 (2.5 X 100 cm) column. The column was calibrated with molecular mass (M_r) standards as outlined under "*Materials and methods*". In Tris (pH 7.5) PhyAme eluted as two peaks, one at an elution position similar to EF-Tu, corresponding to an M_r of 48 kDa, and the second at a position similar to EF-G, corresponding to an M_r of 78 kDa (Figure 4.5). Elution fractions corresponding to each individual peak were isolated, concentrated, and re-run through a Superdex 75 column; both samples similarly displayed elution of two peaks. This suggests that PhyAme can form a self-association state in solution. To test the suggested association state under the conditions of our assays, gel filtration was repeated in NaAc (pH 5). An acetate buffer caused elution of a single peak equivalent to an M_r of about 55 kDa, suggesting that the monomer is the preferred state (Figure 4.5). Size estimates were repeated in a range of buffers to test if the phenomenon was sensitive to pH or the buffer species present. Gel filtration experiments indicate that the suggested association state of PhyAme is largely sensitive to the pH of the medium. The elution of a peak corresponding to a PhyAme homodimer only occurred at pH ≥7.5. Additionally, increasing I was found to significantly increase the elution ratio of dimer to monomer (data not shown).

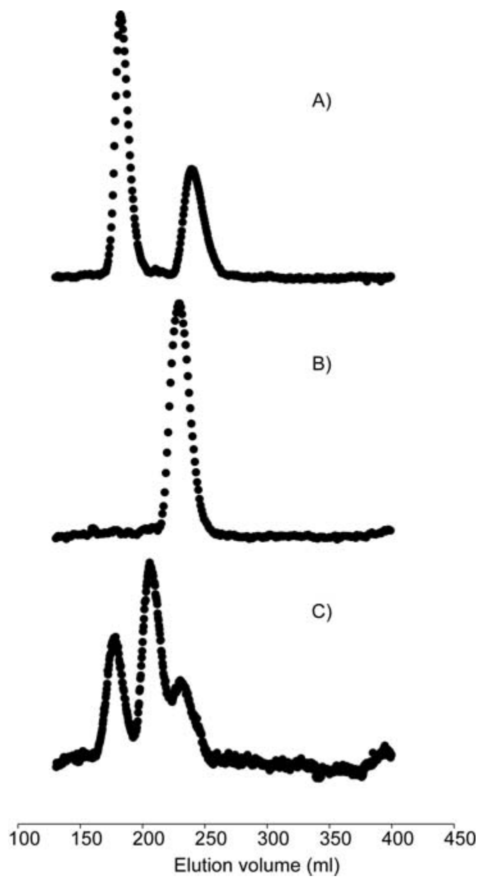

Figure 4.5. Size exclusion FPLC analysis of PhyAme in A) Tris pH 7.5 and B) NaAc pH 5 with 0.3 M I applied to 2.5 X 100-cm Superdex 75 column, monitored at 280 nm. Shown in C) are the elution positions for the protein standards used: elongation factor EF-Tu (M_r = 48 kDa), bovine serum albumin (M_r = 66 kDa), and elongation factor EF-G (M_r = 78 kDa)

Since PhyAme eluted as two peaks on a Superdex 75 preparative column, one with a higher than expected M_r, we further explored its oligomeric nature by determining the hydrodynamic radius in solution with dynamic light scattering (DLS). In 25 mM Tris (pH 7.5), PhyAme (6 μM) displays a hydrodynamic radius of 3.9 nm, corresponding to a predicted M_r of 78.4 kDa and in good agreement with the theoretical dimer M_r (81 kDa). In 25 mM NaAc (pH 5) PhyAme (25 μM) displays a hydrodynamic radius of 3.31 nm, corresponding to a predicted M_r of 52.7 and in agreement with the theoretical monomer M_r (40.6 kDa).

Monomer and dimer equilibrium can also be probed through enzyme concentration dependence of enzyme activity (Zhang *et al.*, 1991; Zhang *et al.*, 1992). Under standard assay conditions of 50 mM NaAc (pH 5), I = 0.2 M with NaCl, 37°C and limiting substrate (0.05 mM), we found that at enzyme concentration between 1.5 and 100 nM, the specific activity of PhyAme remains constant (data not shown). These data are also consistent with the conclusion that PhyAme exists as an enzymatically active monomer in solution with acetate.

Pathway of Ins P_6 dephosphorylation

Isomer-specific HPIC analysis was used to identify the hydrolysis products generated by PhyAme. Purified PhyAme was incubated with excess sodium phytate for 60, 120 and 300 minutes and the stopped reactions were resolved by HPIC (Figure 4.6). Following 60 minutes of incubation, the quantity of Ins P_6 had decreased, and D/L-Ins(1,2,4,5,6)P_5 and D/L-Ins(1,2,3,4,5)P_5 appeared as the major Ins P_5 degradation products (65% and 30%, respectively), along with very small amounts of Ins(1,2,3,4,6)P_5. This indicates that PhyAme initiates hydrolysis of Ins P_6 at one of three possible positions, with the 3 and 6 posphate positions being favoured and to a much lesser extent, the 5 phosphate position. Significant quantities of D/L-Ins(1,2,5,6)P_4, D/L-Ins(1,2,3,4)P_4 and Ins(1,2,3)P_3 and/or D/L-Ins(1,2,6)P_3 plus trace amounts of D/L-Ins(1,2,4,5)P_4 and D/L-Ins(1,2,4,6)P_4

were also found after 60 min. incubation. Following 120 minutes of incubation the chromatogram was similar to that after 60 minutes except the overall major product had become Ins(1,2,3)P_3 and/or D/L-Ins(1,2,6)P_3, and trace amounts of D/L-Ins(1,2)P_2 and/or D/L-Ins(4,5)P_2 and/or Ins(2,5)P_2 had been produced. After 300 minutes of incubation PhyAme had degraded all of the InsP_6 and InsP_5s. Ins(1,2,3)P_3 and/or D/L-Ins(1,2,6)P_3 were found as the major products after 300 minutes, along with significant amounts of D/L-Ins(1,2,3,4)P_4 and D/L-Ins(1,2)P_2 and/or D/L-Ins(4,5)P_2 and/or Ins(2,5)P_2.

The end products of Ins P_6 degradation were determined by incubating excess protein with a limiting substrate concentration. The results of a gas chromatography-mass spectrometry analysis revealed that the end product is Ins(2)P. Both PhyAsr and PhyAsrl were shown to similarly produce Ins(2)P as an end product (refer, Chapter 2;Chapter 3). At pH 5, Ins P_6 is expected to have 5 equatorial phosphates (positions 1,3,4,5,6) and 1 axial phosphate (position 2) (Isbrandt and Oertel, 1980), suggesting that these enzymes have the ability to cleave only equatorial phosphates from IPP substrates.

Kinetic properties

We determined the catalytic properties of the recombinant wild-type PhyAme with Ins P_6 and different Ins P_5 isomers as substrates to elucidate the enzyme-substrate affinity and to determine the specific Ins P_5 isomers generated (Table 4.4). The rate of PhyAme catalyzed phosphate release can be saturated by increasing the concentration of any of the IPP substrates tested, and remains linear over the time period of the assay (data not shown). The specific activity of PhyAme as a function of substrate concentration appears to be consistent with a classic Michaelis-Menton enzyme mechanism. The apparent k_{cat} and K_m values for PhyAme with Ins P_6 as a substrate were 122.1 s^{-1} and 64.2 μM. These values are comparable to previously characterized PhyAsr and PhyAsrl which, with Ins P_6 as a substrate, display k_{cat}

and K_m values of 264 s^{-1} and 425 μM (refer, Chapter 2) and 6.6 s^{-1} and 65 μM (refer, Chapter 3), respectively.

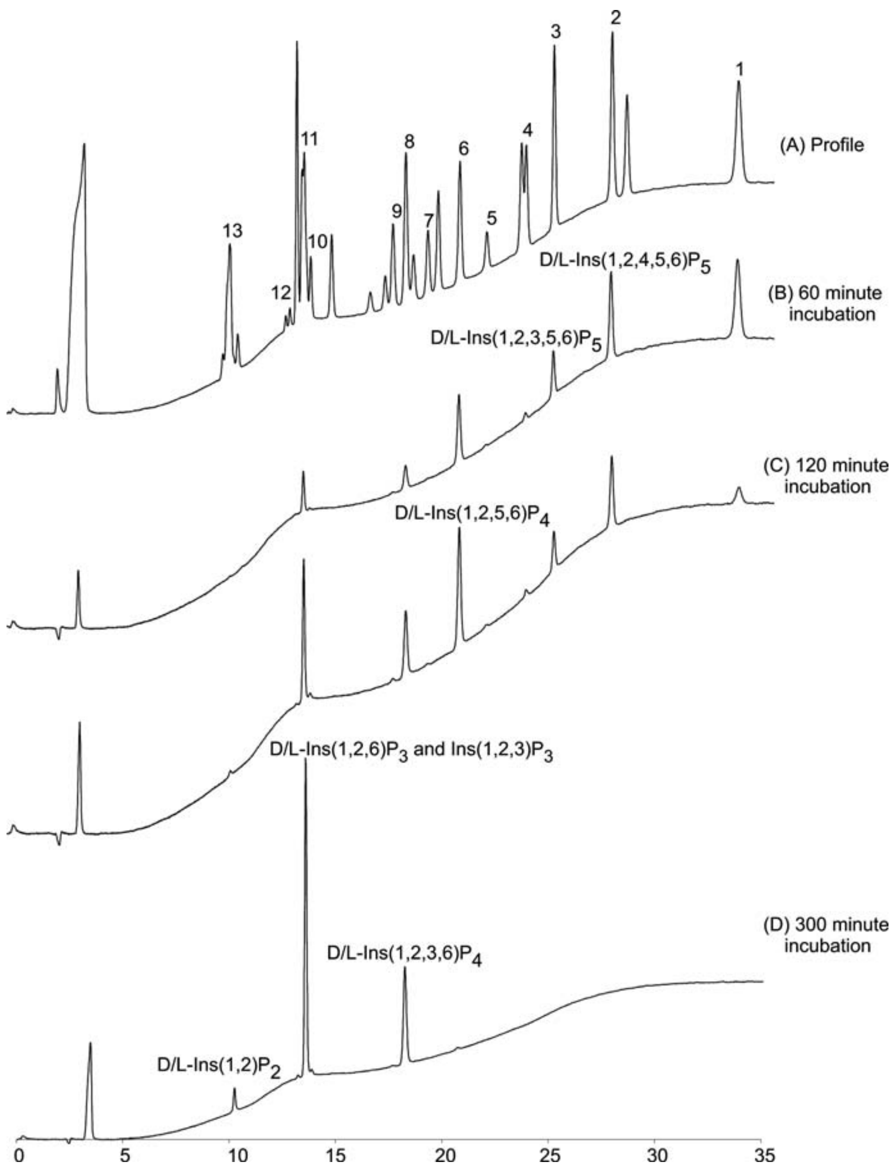

Figure 4.6. High-Perfomance Ion Chromatography analysis of hydrolysis products of *myo*-inositol polyphosphates by PhyAme. (A) Reference sample. The source of the reference *myo*-inositol phosphates is as indicated in (Skoglund *et al.*, 1998); Peaks: (1) Ins(1,2,3,4,5,6)P_6; (2) D/L-Ins(1,2,4,5,6)P_5; (3) D/L-Ins(1,2,3,4,5)P_5; (4) Ins(1,2,3,4,6)P_5; (5) Ins(2,4,5,6)P_4; (6) D/L-Ins(1,2,5,6)P_4; (7) D/L-Ins(1,2,4,5)P_4; (8) D/L-Ins(1,2,3,4)P_4; (9) D/L-Ins(1,2,4,6)P_4; (10) D/L-Ins(1,4,5)P_3, D/L-Ins(2,4,5)P_3; (11) Ins(1,2,3)P_3, D/L-Ins(1,2,6)P_3; (12) D/L-Ins(1,2,4)P_3; (13) D/L-Ins(1,2)P_2, D/L-Ins(4,5)P_2, Ins(2,5)P_2. (B) PhyAme incubated with Ins P_6 for 60 min. (C) PhyAme incubated with Ins P_6 for 120 min. (D) PhyAme incubated with Ins P_6 for 300 min.

Table 4.4. Kinetic constants for enzymatic *myo*-inositol polyphosphate dephosphorylation with recombinant PhyAme. Standard assays were run (50 mM NaAc (pH 5); 0.2 M I with NaCl; 37°C) containing a varying amount of substrate. Enzyme concentration was 66 nM. Data given is the average ± standard deviation of three independent experiments.

Substrate	**K_m (μM)**	**k_{cat} (s^{-1})**	**Kcat/Km (s^{-1} μM^{-1})**
Ins(1,2,3,4,5,6)P_6	64.2 ± 0.61	122.1 ± 1.6	1902 ± 30
D-Ins(1,2,4,5,6)P_5	61.3 ± 0.57	134.5 ± 1.8	2194 ± 36
D-Ins(1,2,3,5,6)P_5	61.8 ± 0.52	135.3 ± 1.9	2189 ± 36
D-Ins(1,2,3,4,5)P_5	102.5 ± 0.67	78.4 ± 1.1	765 ± 12
InsP_5* - D/L-Ins(1,2,4,5,6)P_5	61.1 ± 0.49	133.9 ± 1.6	2192 ± 32
InsP_5* - D/L-Ins(1,2,3,4,5)P_5	61.5 ± 0.53	135.8 ± 1.7	2208 ± 34

*Generated by the PTP-like phytase from *M. elsdenii.*

Kinetic parameters were determined for the possible PhyAme Ins P_5 hydrolysis products in order to determine the specific Ins P_5 isomers generated from PhyAme catalyzed Ins P_6 hydrolysis (Table 4.4). The k_{cat} and K_m for the hydrolysis of the D/L-Ins(1,2,4,5,6)P_5 and D/L-Ins(1,2,3,4,5)P_5 produced by PhyAme are 133.9 s^{-1} and 61.1 μM and 135.8 s^{-1} and 61.5 μM, respectively. These values are most similar to the k_{cat} and K_m for the PhyAme catalyzed hydrolysis of D-Ins(1,2,4,5,6)P_5 (134.5 s^{-1} and 61.3 μM, respectively) and D-Ins(1,2,3,5,6)P_5 (135.3 s^{-1} and 61.8 μM, respectively).

4.4 DISCUSSION

Sequence analysis

We have cloned a gene (*phyAme*) encoding a PTP-like phytase from *Megasphaera elsdenii*. The deduced amino acid sequence of PhyAme shows similarity to the recently characterized PTP-like phytase from *S. ruminantium* (PhyAsr) (Chu *et al.*, 2004; refer, Chapter 2) and *S. ruminantium* subsp. *lactilytica* (PhyAsrl) (refer, Chapter 3), most notably in the PTP-like active site signature sequence. PhyAsr has a PTP-like core structure and catalytic mechanism similar to that of other members of the PTP superfamily (Chu *et al.*, 2004; refer, Chapter 2). The sequence identity, conservation of the active site signature sequence and similar ability to hydrolyze IPP substrates allows us to suggest that these enzymes may have a similar three-dimensional structure and a common mechanism of catalysis. Moreover, several bacterial putative PTPs have comparable sequence similarity to PhyAme (Table 4.2), but unknown enzymatic properties. It is possible that some of these enzymes also have the ability to hydrolyze IPPs.

Interestingly, a type III-secreted protein HopPtoD2 from *P. syringae* also shows sequence similarity to PhyAme. HopPtoD2 is made up of an N-terminal avirulence domain and a C-terminal PTP-like domain. It has been shown to dephosphorylate both pNPP and phosphotyrosine-containing peptides *in vitro* (Bretz *et al.*, 2003; Espinosa *et al.*, 2003), and has been linked to the modulation of a variety of plant defense responses to infection (Bretz *et al.*, 2003; Espinosa *et al.*, 2003). The exact biological substrates of most PTPs, including HopPtoD2, are unknown (Zhang, 2002). It is possible that, in light of its homology to the PTP-like phytases, HopPtoD2 also has the ability to dephosphorylate IPP substrates, which may contribute to its ability to moderate the plant cell-death defense response. An example of a similar function is seen in mammalian PTP-like PTEN. PTEN has significant structural similarity to PhyAsr (Chu *et al.*, 2004) and dephosphorylates the phosphoinositide PIP_3 and the cytosolic phosphoinositol Ins(1,3,4,5,6)P_5 *in vivo* (Caffrey *et al.*, 2001; Deleu *et al.*, 2006). The activity of PTEN has been implicated in the control of cellular growth, tumor suppression and the regulation of cellular IPP signaling molecules (Caffrey *et al.*, 2001; Deleu *et al.*, 2006). The biological importance of IPPs and phosphoinositides in mammalian cells has been established, and the physiological relevance of these molecules in plants has been recognized (Sasakawa *et al.*, 1995; Chi and Crabtree, 2000; Loewus and Murthy, 2000;

Shears, 2001; Raboy, 2003; Irvine, 2005). Although little is known of the IPP content of most prokaryotes, *myo*-inositol, the precursor of all inositol-containing compounds including phosphoinositides and inositol phosphates, is synthesized in Archaea (Chen *et al.*, 2000) and some bacteria (Bachhawat and Mande, 1999;2000). PTPs have been discovered in a range of prokaryotes, and most appear to serve roles which mimic their better-known eukaryotic counterparts as regulators of cellular function (Shi *et al.*, 1998; Kennelly and Potts, 1999). It is possible that PhyAme and its homologues make up a unique class of PTP-like IPPases, and in light of their homology to HopPtoD2 and PTEN, may be involved in modulating cellular functions. PhyAsr has been localized to the outer membrane of *S. ruminantium* (D'Silva *et al.*, 2000), and the presence of predicted signal peptides within its homologues, including PhyAme, indicates that these enzymes are excreted, and in turn, that they are active on extracellular IPPs. Preliminary binding assays done in our lab suggest that PhyAme can similarly associate with the outer membrane of *M. elsdenii*. The use of IPPs for prokaryotic inter- and intratracellular signal transduction has not yet been investigated.

Oligomeric nature of PhyAme

Results from gel-filtration, DLS and enzyme concentration dependence experiments are consistent with PhyAme existing and functioning as a monomer in our assay medium. The higher than expected Mr (~55 kDa) as determined by gel filtration and DLS under these conditions might suggest that PhyAme is not globular in shape under these conditions.

There is good evidence that the previously characterized PhyAsr exists as a dimer in solution, as it elutes from a gel filtration column consistently, with a position corresponding to 75 kDa (predicted M_r = 39 kDa) (Gruninger, R. J., personal communication). Additionally, all of the experimentally determined structures of PhyAsr found in the protein databank indicate similarly homo-dimerized protein under a variety of crystallization conditions (Gruninger, R. J., personal communication; PDB accession numbers: 1U24, 1U25, 1U26, 2B4U, 2B4P, and 2B4O). Further, a gene has been cloned in our lab whose gene product is homologous to this novel class of PTP and encodes the equivalent of a tandem repeat of PhyAsr. These facts suggest that there might be a functional significance to the dimer state of these enzymes. The presence of a gel filtration peak with a much higher than expected apparent M_r at higher pHs and with higher I suggests that the oligomeric state of this enzyme may be dynamic in vivo, perhaps dependent upon a co-factor or a controlled localized environment. As we expect that this enzyme associates with the outer membrane of the bacterial cell it is possible that these requirements are supplied by membrane components.

Substrate specificity

PhyAme had very little activity towards commonly used phosphatase substrates such as ρNPP and BCIP. PhyAsrl was previously shown to display similar low activity towards these substrates (refer, Chapter 3). Mammalian PTEN, a structural homologue of PhyAsr (Chu *et al.*, 2004), also displayed poor ability to dephosphorylate pNPP and other artificial protein substrates and showed preference for highly negatively charged, multiply phosphorylated polymers (Li and Sun, 1997; Myers *et al.*, 1997). Thus, all the characterized PTP-like IPPases seem to share this characteristic.

Hydrolysis pathway and kinetics

Based on the position of the first phosphate hydrolyzed, three types of phytases are recognized by the Enzyme Nomenclature Committee of the International Union of Biochemistry; *i.e.*, 3-phytase (EC 3.1.3.8), 6-phytase (EC 3.1.3.26) and 5-phytase (EC 3.1.3.72). To date, most of the known phytases are D-3-, D-6-, or L-6-phytases (Konietzny and Greiner, 2002). The PTP-like phytases PhyAsr and PhyAsrl were previously shown to have D-3 and 5-phytase activity respectively (refer, Chapter 2;Chapter 3). HPIC analysis have indicated that PhyAme predominantly hydrolyzes one of two phosphate positions of Ins P_6 first; *i.e.*, the D/L-3 or D/L-4 phosphate. It was concluded that the *myo*-inositol penta*kis*phosphate intermediates generated by PhyAme are D-Ins(1,2,4,5,6)P_5 (60%) and D-Ins(1,2,3,5,6)P_5 (30%), since the kinetic constants for the degradation of the major *myo*-inositol penta*kis*phosphates generated by PhyAme and D-Ins(1,2,4,5,6)P_5 and D-Ins(1,2,3,5,6)P_5 are almost identical (Table 4.4). Similar mixed position specificity has previously been identified for acid phytases cloned from the basidiomycete fungi *Agrocybe pediades*, *Ceriporia* sp. and *Trametes pubescens* (Lassen *et al.*, 2001), but no distinction was made between the enantiomers of their products of Ins P_6 hydrolysis. Of note, kinetic analysis with Ins P_6 and the Ins P_5s generated by PhyAme indicates that the enzyme has a slight catalytic preference for the penta*kis*phosphate substrate. Similar preference for a penta*kis*phosphate was displayed by PhyAsr (refer, Chapter 2).

Many acid phytases have been found to liberate all five equatorial phosphate groups of Ins P_6 (Konietzny and Greiner, 2002), including the PTP-like enzymes PhyAsr and PhyAsrl (refer, Chapter 2;Chapter 3). PhyAme displays the ability to cleave all five equatorial phosphates, resulting in a final product of Ins(2)P. HPIC and kinetic analysis indicate that following initial hydrolysis at the D-3- or D-4-phosphate positions, PhyAme follows distinct routes of hydrolysis with each subsequent product. PhyAme can produce Ins(2)P via the routes indicated in Figure 4.7. PhyAme predominantly degrades Ins P_6 to Ins(2)P via: (A) D-Ins(1,2,4,5,6)P_5, D-Ins(1,2,5,6)P_4, D-Ins(1,2,6)P_3 and D-Ins(1,2)P_2, and (B) D-Ins(1,2,3,5,6)P_5, D-Ins(1,2,3,6)P_4, Ins(1,2,3)P_3 and D/L-Ins(1,2)P_2 (60% and 30% respectively). The two major pathways are nearly identical except for the removal of the D-3 phosphate. The 'first' major pathway (60%) removes the D-3 phosphate first, whereas in the 'second' (30%), the D-3 phosphate is the fourth removed (3,4,5,6,1 vs. 4,5,6,3,1). The order in which PhyAme removes phosphate groups has little resemblance to that of PhyAsr or PhyAsrl. All characterized PTP-like enzymes to date utilize distinct, ordered and specific routes of Ins P_6 hydrolysis.

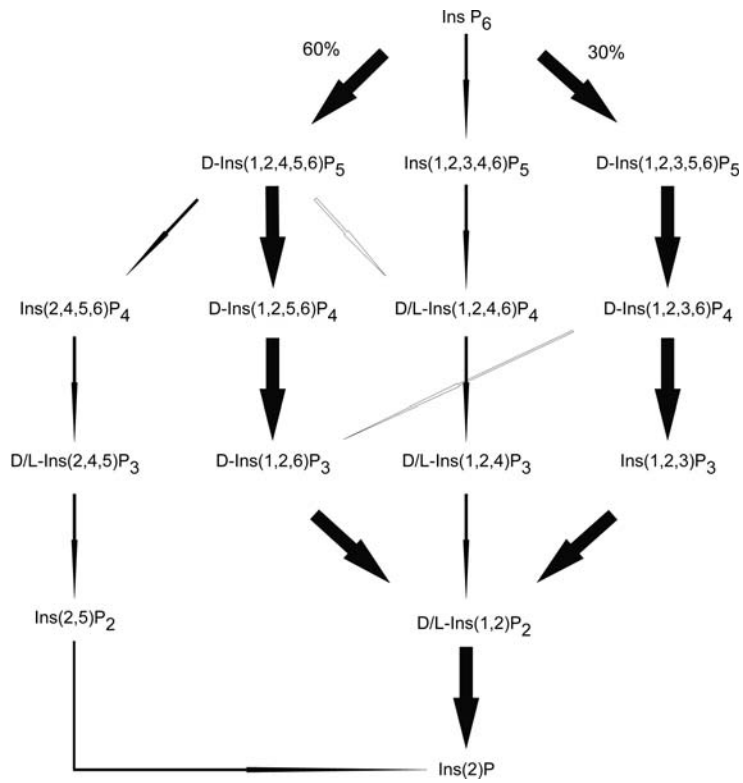

Figure 4.7. Degradation pathways of Ins P_6 by PhyAme. Larger arrows indicate major pathway, smaller arrows indicate minor pathways. Open arrows designate possible routes of hydrolysis as predicted from HPIC data, solid arrows represent routes verified by HPIC and kinetic data. Values (%) above respective major pathways indicate proportion of hydrolysis products generated by that route.

CHAPTER FIVE

Cloning and characterizing PhyAsl and PhyBsl from *Selenomonas lacticifex*, PTP-like 3-phytases

ABSTRACT

PhyAsl and PhyBsl from *Selenomonas lacticifex* are protein tyrosine phosphatase (PTP)-like phytases with a number of unique properties. In order to elucidate their substrate specificity and pathways of Ins P_6 dephosphorylation, a combination of kinetic and high-performance ion-pair chromatography studies have been conducted. The data indicate that both PhyAsl and PhyBsl have a general specificity for polyphosphorylated *myo*-inositol substrates *in vitro*. Both of these enzymes preferentially cleave Ins P_6 at the D-3-phosphate position (> 90%). Further, both enzymes have been shown to predominantly degrade Ins P_6 to Ins(2)P via: Ins P_6, D-Ins(1,2,4,5,6)P_5, D-Ins(1,2,5,6)P_4, D-Ins(1,2,6)P_3 and D-Ins(1,2)P_2, and do so with the most specific routes of Ins P_6 hydrolysis characterized to date. In addition, PhyBsl is shown to have a significant kinetic preference for the Ins P_4 intermediate in its Ins P_6 hydrolysis pathway, a unique characteristic among PTP-like phytases. Finally, a distant mammalian homologue has been identified using bioinformatic analysis within GeneBank.

5.1. INTRODUCTION

myo-inositol polyphosphates (IPPs) make up a group of phosphorylated inositols which are recognized as ubiquitous products of inositol metabolism (Sasakawa *et al.*, 1995). The most abundant IPPs in most cells are the higher inositol polyphosphates, *myo*-inositol hexa*kis*phosphate (Ins P_6) and *myo*-inositol penta*kis*phosphate (Ins P_5) (Sasakawa *et al.*, 1995). The biological importance of IPPs in eukaryotic cells has been well established (Sasakawa *et al.*, 1995; Chi and Crabtree, 2000; Shears, 2001; Raboy, 2003; Irvine, 2005). Moreover, IPPs have been recognized as having novel metabolic effects, and the growing list of research and pharmaceutical applications for specific IPPs has increased interest in the preparation of these compounds (Greiner *et al.*, 2002b).

Enzymes that can catalyze the release of orthophosphate from Ins P_6 have been grouped together as phytases (myo-inositol hexa*kis*phosphate phosphohydrolases) (Mullaney and Ullah, 2003). Four distinct classes of phosphatases have been characterized in the literature as having phytase activity, histidine acid phosphatases, ß-propeller phytases, purple acid phosphatases (Mullaney and Ullah, 2003) and most recently, protein tyrosine phosphatase-like phytases (Chu *et al.*, 2004; refer, Chapter 2;Chapter 3;Chapter 4). Based on the position of the first phosphate hydrolyzed, three types of phytases are recognized by the Enzyme Nomenclature Committee of the International Union of Biochemistry; *i.e.*, 3-phytase (EC 3.1.3.8), 6-phytase (EC 3.1.3.26) and 5-phytase (EC 3.1.3.72).

Protein tyrosine phosphatase (PTP) superfamily enzymes have been discovered in a range of prokaryotes, and most appear to serve roles which mimic their better-known eukaryotic counterparts as regulators of cellular function (Shi *et al.*, 1998; Kennelly and Potts, 1999). The recently described PTP-like phytases from *Selenomonas ruminantium* (PhyAsr), *S. ruminantium* subsp. *lactilytica* (PhyAsrl), and *Megasphaera elsdenii* (PhyAme) contain a PTP-like active site signature sequence (HCEAGVGR) that facilitates a classical PTP mechanism of dephosphorylation, but lack significant primary sequence identity with other known PTPs (< 20%). The X-ray crystallographic structure of PhyAsr reveals two domains, a PTP-like domain, and a partial β-barrel domain that is a unique feature of this enzyme (Chu *et al.*, 2004). The partial β-barrel domain, along with an extended C-terminal helix and an extended loop within the PTP-like domain contribute to the formation of a standby site within the binding pocket of PhyAsr that is believed to be involved with substrate recruitment (Chu *et al.*, 2004)(Mosimann, personal communication). While its biological function remains unclear, PhyAsr was the first example of a PTP-like enzyme with activity towards Ins P_6. Enzymes belonging to the recently described class of PTP-like phytases are all of bacterial origin, and no mammalian homologue has yet been identified (Chu *et al.*, 2004; refer, Chapter 2;Chapter 3;Chapter 4). A number of putative PTP-like PhyA homologues have been partially cloned from a range of bacteria isolated from the rumen and other anaerobic sources (Nakashima *et al.*, 2006). This chapter describes the cloning and sequencing of two full genes encoding novel PTP-like phytases from *Selenomonas lacticifex* (*phyAsl and phyBsl*), as well as the overexpression, purification, and detailed physicochemical characterization of the recombinant gene product.

5.2 MATERIALS AND METHODS

Gene cloning

Selenomonas lacticifex (ATCC 49690) was cultured anaerobically as described previously (refer, Chapter 3;Chapter 4). Isolation of total DNA was performed as previously detailed (Priefer *et al.*, 1984). Genomic DNA was digested with *Pst*I *(phyAsl) or Eco*RI *(phyBsl)*. The relative sizes of the fragments containing the genes coding for phytase were determined by Southern blot hybridization using the DIG DNA Labeling and Detection Kit (Boehringer; Mannheim, Germany) and a probe. The probe was a polymerase chain reaction (PCR) product corresponding to previously determined sequence fragments (GeneBank accession numbers DQ257450 and DQ257444; Nakashima *et al.,* 2006). Digested DNA corresponding to the approximate size of the *phy* containing fragments were gel purified (MinElute Gel Extraction Kit; Qiagen Inc.; Mississauga, ON). To clone *phyAsl*, gel purified subgenomic DNA was ligated into dephosphorylated *Pst*I pBluescript II SK (+) (Stratagene, La Jolla, CA). Inverse PCR primers (Table 5.1) were generated from the known internal *phyAsl* partial sequences (Nakashima *et al.*, 2006). These were used in conjunction with M13 and T7 universal primers to generate PCR products from the ligation products corresponding to regions of *phyAsl* straddling the known sequence (Figure 5.1). To clone *phyBsl*, gel purified subgenomic DNA was self-ligated to form circular products. The intramolecular ligation product was used as a template for inverse PCR with primers (Table 5.1) generated from the known, internal *phyBsl* partial sequences (Nakashima *et al.*, 2006). The PCR products from each *phy* gene were ligated into pGEM-T Easy (Promega Corp., Madison, WI) and sequenced by automated cycle sequencing at the University of Calgary Core DNA and Protein services facilities. Sequence data was analyzed with the aid of SEQUENCHER™ version 4.0 (Gene Codes Corp. Ann Arbor, MI) and MacDNAsis version 3.2 (Hitachi Software Engineering Co., Ltd., San Bruno, CA). Homology searches in GenBank (Fassler *et al.*, 2000; Benson *et al.*, 2006) were done using BLAST (Altschul *et al.*, 1990) and preliminary sequence alignments were generated using CLUSTAL W 1.82 (Higgins *et al.*, 1994; Chenna *et al.*, 2003). Alignment optimization was carried out with GeneDoc (Nicholas *et al.*, 1997) using methods for comparative structure-based sequence alignments (Greer, 1981) and the experimentally determined structure of the PTP-like phytate-degrading enzyme from *S. ruminantium* (PhyAsr; PDB accession: 1U24; Chu *et. al.*, 2004). Secondary structure predictions were generated with SSpro (Pollastri *et al.*, 2002) on the SCRATCH web server (Baldi and Pollastri, 2003; Cheng *et al.*, 2005).

Table 5.1. PCR and Inverse PCR primers used in this study. Restriction sites are underlined.

Gene	Primer Name	Primer Sequence
phyAsl	49690A For	GAT TAC GCA GGC AAT GAC AG
	49690A Rev	CGG GGC AAC ATA CTG GA
	49690A F Nest	TGA AGG CGC GAA GCA TCA
	49690A R Nest	CAG CTC ACG GCA TCA CCA TT
	*Nde*I ExpA	GCC ATA TGG CGG CTC AGG GGC AAA AG
	*Xho*I ExpA	GCC TCG AGA GAC GAT TCA GAC CTT TCC T
phyBsl	49690B For	GCA ACG GCT ACG GCT ATG TC
	49690B Rev	GGG ATG CTG TGC GAC TCA T
	*Nde*I ExpB	GCC ATA TGG CGG TGG CTT CCC AAT G
	*Xho*I ExpB	GCC TCG AGT TAA TGC CGG GCA AGC CA

Recombinant expression constructs

The regions coding for the mature *S. lacticifex* phytases (PhyAsl and PhyBsl; GeneBank accession numbers EF159976 and EF159975; residues 33-342 and 38-295) were amplified from genomic DNA using PCR. The predicted signal peptide sequences were determined with SIGNAL P 3.0 (Nielsen *et al.*, 1997; Bendtsen *et al.*, 2004). Both *phyAsl* and *phyBsl* expression primers (Table 5.1) included an *Nde*I (*Nde*I ExpA and B) and *Xho*I (*Xho*I ExpA and B) site and a 5' GC cap. The PCR products were double digested with *Nde*I and *Xho*I and ligated into a similarly digested pET28b vector (Novagen Inc., San Diego, CA). Constructs were verified with automated cycle sequencing.

Protein production and purification

Escherichia coli BL21 (DE3) cells (Novagen Inc.) were transformed with the *phyA* and *phyB* expression constructs. Over expression was carried out according to the instructions in the pET Systems Manual (Novagen Inc.). Cells were induced with the addition of IPTG to a final concentration of 1 mM and incubated for 6 hours at 37^{o}C (PhyAsl) or 25^{o}C for 4 hours (PhyBsl). Induced cells were harvested and resuspended in lysis buffer (20 mM PO_4 (pH 7), 600 mM NaCl, 1 mM β-mercaptoethanol (BME), and one Complete Mini, EDTA-free protease inhibitor tablet (Roche Applied Science; Laval, QC)). Cells were sonicated and debris was removed by centrifugation at 20 000 x g for 45 minutes. The protein was purified to homogeneity using Ni^{2+}-NTA spin columns according to the supplied protocol (Qiagen Corp.). Protein was washed on the column with lysis buffer containing 15 mM imidazole (wash buffer #1) and then with wash buffer #2 (20 mM PO_4 (pH 7), 300 mM NaCl, 10% glycerol, 15 mM imidazole, and 1 BME). Protein was subsequently eluted with lysis buffer containing 350 mM imidazole. Purified protein was dialyzed with three buffer changes into 20 mM Tris (hydroxymethyl) aminomethane (Tris; pH 7), 300 mM NaCl, 0.1 mM EDTA and 5 mM BME. The homogeneity of the purified protein was confirmed by

4/12% (w/v) SDS-polyacrylamide gel electrophoresis (SDS-PAGE) (Laemmli, 1970), and Coomassie Brilliant Blue R-250 staining. The theoretical M_r and extinction coefficient of the proteins were determined using PROT PARAM (Gasteiger *et al.*, 2005). Protein concentrations were determined by monitoring the A_{280}. For storage, purified protein was dialyzed into 50 mM ammonium bicarbonate (pH 8) with 3 buffer changes, lyophilized, and stored at -20^{o}C.

Assay of enzymatic activity

Activity measurements were carried out at 37°C. Enzyme reaction mixtures consisted of a 600 μl buffered substrate solution and 150 μl of a 0.5-1 μM enzyme solution. The buffered substrate solution contained 50 mM sodium acetate (pH 5) and 2 mM sodium phytate, or another of the substrates used in our study. I was held constant at 200 mM with the addition of NaCl. Following the appropriate empirically determined incubation period the reactions were stopped and the liberated phosphate was quantified with the ammonium molybdate methods described previously (refer, Chapter 2;Chapter 3). Profiling the dependence of enzyme activity on pH, temperature and I, as well as their substrate specificity was also done as described previously (refer, Chapter 3;Chapter 4). Activity (U) was expressed as μmol phosphate liberated per min. The steady-state kinetic constants (K_m, k_{cat}) for the hydrolysis of Ins P_6 and other IPPs by PhyAme were calculated from Michaelis-Menton plots. The data were analyzed with non-linear regression using SIGMA-PLOT 8.0 (Systat Software Inc.; Point Richmond, CA).

Preparation of individual myo-inositol phosphate isomers

Lyophilized PhyAsr was shipped to Dr. Ralf Greiner at the Centre for Molecular Biology of the Federal Research Centre for Nutrition and Food in Karlsruhe Germany where HPIC, production and isolation of lower IPPs and kinetic studies with lower IPPs was performed.

Phytases from *Aspergillus niger*, *Escherichia coli*, and rye were used to generate D-Ins(1,2,4,5,6)P_5, D-Ins(1,2,5,6)P_4, and D-Ins(1,2,6)P_3. These isomers and the Ins P_5 generated by PhyAsl and PhyBsl were prepared as described previously (Greiner *et al.*, 2002a; Greiner *et al.*, 2002b; refer, Chapter 2;Chapter 3). Sodium phytate (2.5 mmol) was incubated at 37°C in a mixture containing 50mM NH_4-acetate, pH 4.5 (*A. niger, E. coli* and PhyBsl), pH 5 (PhyAsl) or pH 6 (rye) and 10 U of the appropriate enzyme in a final volume of 500 mL.

Identification of enzymatically formed hydrolysis products

Standard phytase assays were run at 37°C by addition of 50 μl of a suitably diluted solution of enzyme to the incubation mixtures. Periodically stopped reactions were resolved on a High-Performance Ion Chromatography system (HPIC) using a Carbo Pac PA-100 (4 x 250 mm) analytical column (Dionex; Sunnyvale, CA) and a gradient of 5–98% HCl (0.5 M, 0.8 mL/min) as previously described (Skoglund *et al.*, 1998). The eluants were mixed in a post-column reactor with 0.1% $Fe(NO_3)_3$ in a 2% $HClO_4$ solution (0.4 mL/min) (Phillippy and Bland, 1988). The combined flow rate was 1.2 mL/min. *Myo*-inositol monophosphates were produced by incubation of 1.0 U of enzyme with a limiting amount (0.1 μmol) of Ins P_6 in a final volume of 500 μl of 50 mM NH_4-acetate. The end products were identified using a gas chromatograph coupled with a mass spectrometer as previously described (Greiner *et al.*, 2002a; Greiner *et al.*, 2002b; refer, Chapter 2).

5.3 RESULTS

Sequence analysis

Two separate sequence fragments were isolated from *Selenomonas lacticifex*, each containing a full open reading frame (ORF) with homologues in GeneBank that are PTP-like phytases and putative PTPs (Figure 5.1). The full ORFs have thus been designated *phyAsl* and *phyBsl* (GeneBank accession numbers DQ257450 and DQ257444 respectively). BLAST analysis has also indicated the presence of two partial ORFs adjacent to the sequence of *phyAsl*. The two partial ORFs (*orf*1 and *orf*2) have similarity to sequences in GeneBank that are: 1) putative TetR-family transcriptional regulators and 2) the ATPase component of ABC transporter systems, respectively.

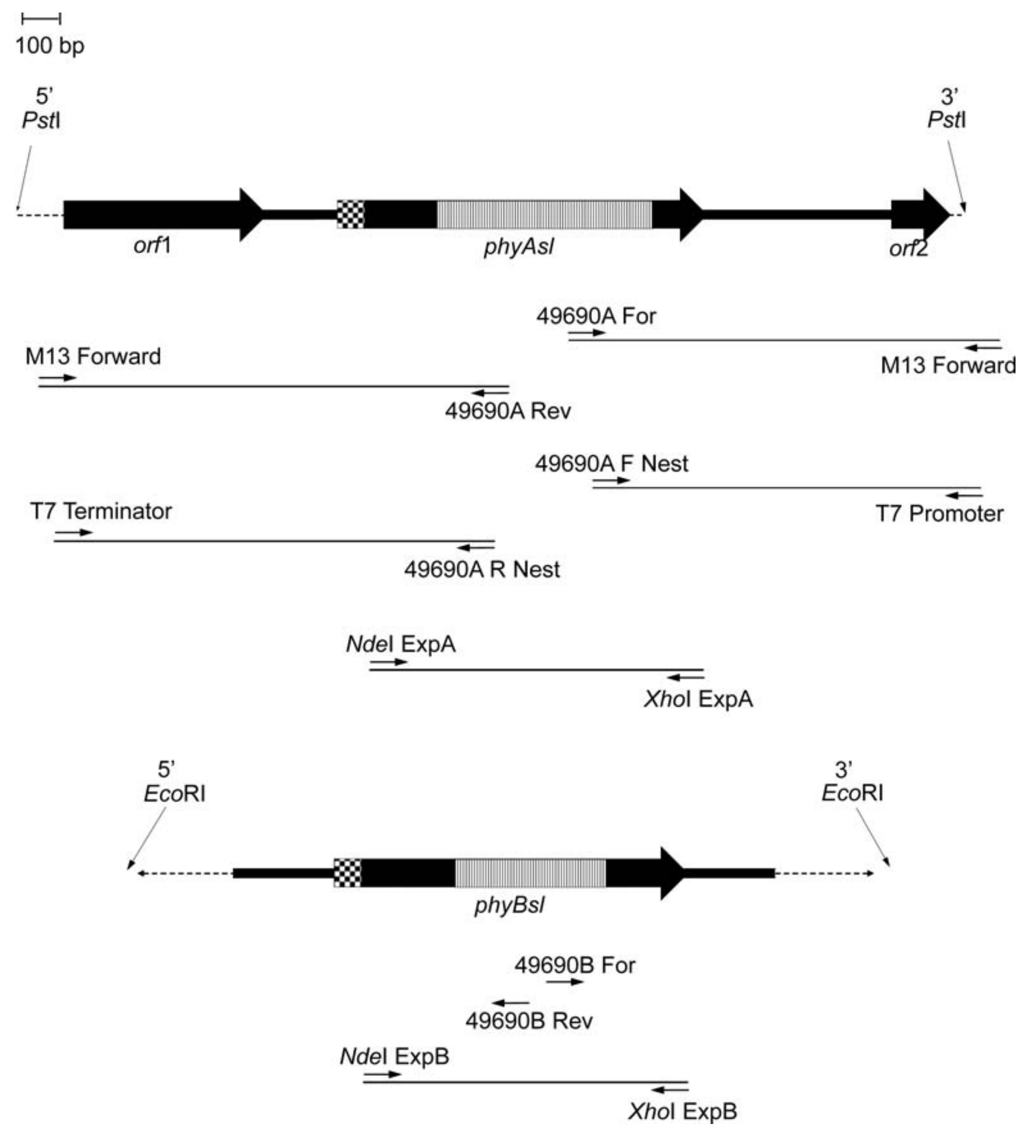

Figure 5.1. Schematic diagram representing *phyAsl* and *phyBsl* and the steps involved in their PCR/inverse PCR cloning. The relative positions of the primers used are indicated (detailed in '*Materials and Methods*'). The 620 and 380 bp fragments of *phyAsl* and *phyBsl*, respectively, cloned previously are presented as striped boxes. The predicted signal peptides are indicated by checkered boxes. A dashed line represents unsequenced regions.

The predicted gene products of *phyAsl* and *phyBsl* have 33% sequence identity with one another, and 54 and 31% sequence identity, respectively, with a characterized PTP-like phytase from *S. ruminantium* (PhyAsr) (refer, Chapter 2). PhyAsl has 46 and 35% sequence identity with the PTP-like phytases from *M. elsdenii* (PhyAme) and *S. ruminantium* subsp. *lactilytica* (PhyAsrl) respectively, whereas PhyBsl has 33 and 31% sequence identity respectively.

Interestingly, BLAST analysis with the sequence of PhyBsl has revealed a distant mammalian homologue; *i.e.*, paladin. Paladin (GeneBank Accession number NP_038781) is a putative PTP with unknown function and is broadly expressed (Benson *et al.*, 2006). Sequence analysis suggests that paladin contains two putative PTP domains, an uncharacterized PTP-like N-terminal domain and a C-terminal domain that shows low sequence similarity with PhyBsl (13% identity). A comparative structure-based sequence alignment was generated using the experimentally determined structure of PhyAsr (Chu *et al.*, 2004) and the amino acid sequences of all PTP-like phytases characterized to date as well as the homologous domain from paladin (Figure 5.2). Although the identities are low, sequence similarity with paladin is found in regions that are conserved amongst the characterized PTP-like phytases. Further, paladin's secondary structures were predicted using Recurrent Neural Networks (Baldi and Pollastri, 2003) and compared to the experimentally determined structure of PhyAsr on the sequence alignment. Paladins predicted secondary structures align well within the PTP-like domain of PhyAsr except for an insertion of three α-helices near the C-terminus. The predicted structures in the region corresponding to the partial β-barrel domain of PhyAsr have low similarity. Moreover, the structural alignment suggests that neither PhyBsl nor paladin have an extended loop located between β2 and β3 of PhyAsr (Chu *et al.*, 2004).

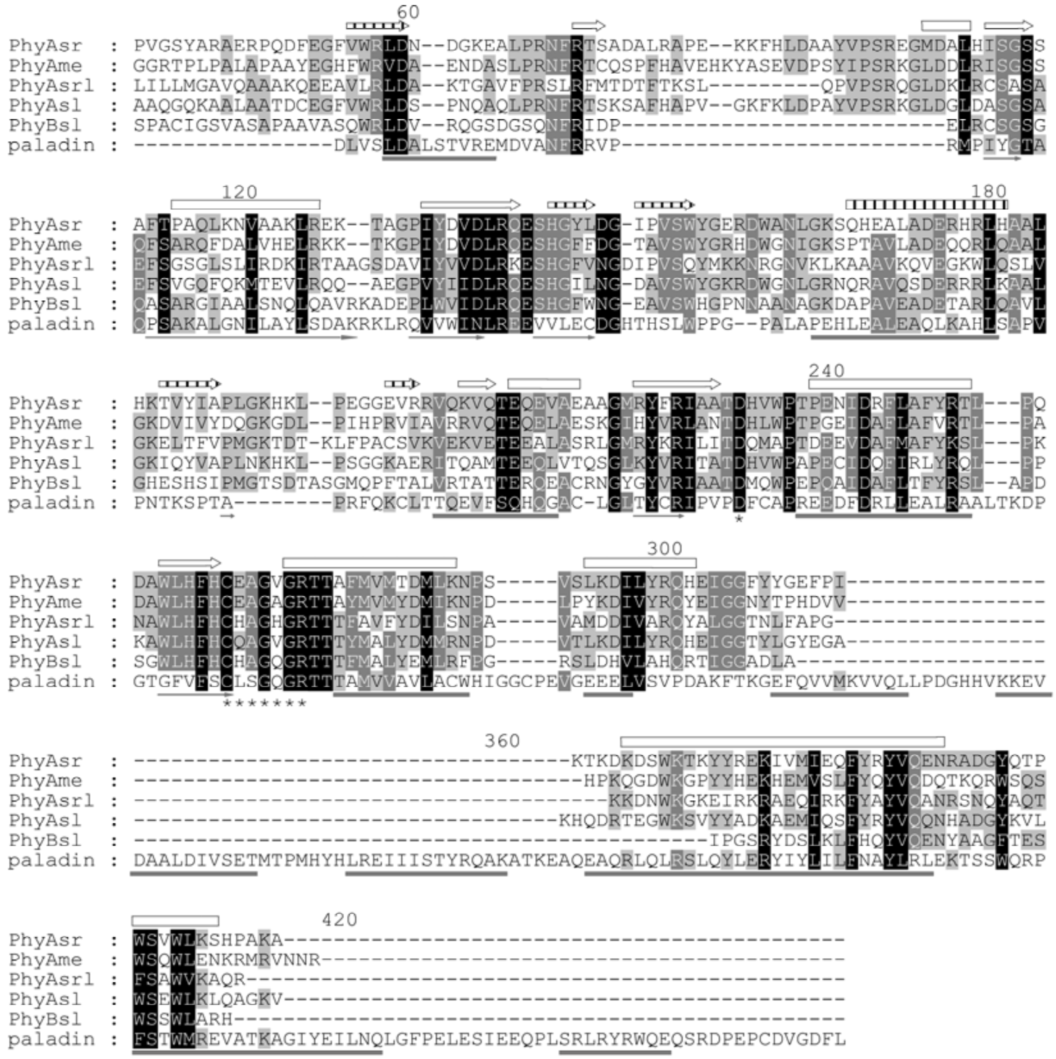

Figure 5.2. Comparative structure-based amino acid sequence alignment of the *S. lacticifex* PTP-like enzymes, their characterized PTP-like phytase homologues, and the distant mammalian homologue paladin. Shading is according to alignment consensus as given by GeneDoc (black = 100%; dark grey = 75%) with similarity groups enabled. The protein abbreviation, source, GenBank accession numbers, and residues included in the alignment are as follows: PhyAsr, *S. ruminantium* JY35, AAQ13669, 38-346; PhyAme, *M. elsdenii*, EF025174, 48-360; PhyAsrl, *S. ruminantium* subsp. *lactylitica*, EF016752, 23-321; PhyAsl, *S. lacticifex*, EF159976, 33-342; PhyBsl, *S. lacticifex*, EF159975, 33-342; 25-295; paladin, *Mus musculus*, BAC40433, 491-859. Numbering is according to the sequence of PhyAsr found in GeneBank. The PTP-like signature sequence and the conserved upstream aspartic acid are identified by *s. Secondary structures are identified for PhyAsr (PDB accession: 1U24) above the sequences with hollow arrows representing β-strands and hollow boxes indicating α-helices. The secondary structures corresponding to the partial β-barrel domain of PhyAsr (Chu *et al.*, 2004) are indicated by vertical stripes. Below the sequences are the predicted secondary structures for paladin according to Recurrent Neural Networks (Baldi and Pollastri, 2003), where solid arrows represent β-strands and solid boxes indicate α-helices.

The gene products of *phyAsl* and *phyBsl* contain predicted N-terminal signal peptide sequences, suggesting the enzymes are located extracellularly. To date, all PTP-like phytate-degrading enzyme genes cloned from anaerobic, ruminal bacteria have contained a predicted N-terminal signal peptide in their gene products (refer, Chapter 2;Chapter 3;Chapter 4).

Expression and purification

Following induction with IPTG, overexpression of polypeptides with M_r of about 35 kDa (PhyAsl) and 32 kDa (PhyBsl) was observed with SDS-PAGE. This is consistent with the mass predicted from the sequences of the recombinant proteins (predicted M_r = 35 and 31 kDa, respectively). The Ni^{2+}-NTA purification was able to produce purified PhyAsl and PhyBsl with > 95% homogeneity in a single step, as determined by SDS-PAGE and Coomassie Brilliant Blue R-250 staining (data not shown). The specific activity of the enzymes toward Ins P_6 as a substrate was examined. PhyAsl can hydrolyze Ins P_6 with a maximum specific activity of 440 U mg^{-1}. This activity is amongst the highest of the characterized PTP-like phytases. The highest specific activity towards Ins P_6 reported to date from a PTP-like enzyme is displayed by PhyAsr (668.11 U mg^{-1}) (refer, Chapter 2). PhyBsl can also dephosphorylate Ins P_6, and does so with a specific activity of 12 U mg^{-1}.

Biochemical profiles and substrate specificity

The pH, temperature, and I dependence of phytase activity were determined in order to establish the optimal conditions for Ins P_6 hydrolysis. Both PhyAsl and PhyBsl display pH dependence similar to other PTP-like phytases with optima at pH 4.5 (Figure 5.3A). Although they have the same pH optima, PhyAsl is active over a much wider pH range than PhyBsl. Previously characterized PhyAsr, PhyAme and PhyAsrl displayed optimal activity at pH 5, 5 and 4.5, respectively (refer, Chapter 2;Chapter 3;Chapter 4). Optimal phytase activity was displayed at 40°C and 37°C for PhyAsl and PhyBsl respectively (Figure 5.3B). This is lower than all previously characterized PTP-like enzymes that have optimal activity above

55^{o}C (refer, Chapter 3;Chapter 4). The effect of I on activity is presented in Figure 5.4, both PhyAsl and PhyBsl display an activity dependence on I with optimal activity at I = 100 mM.

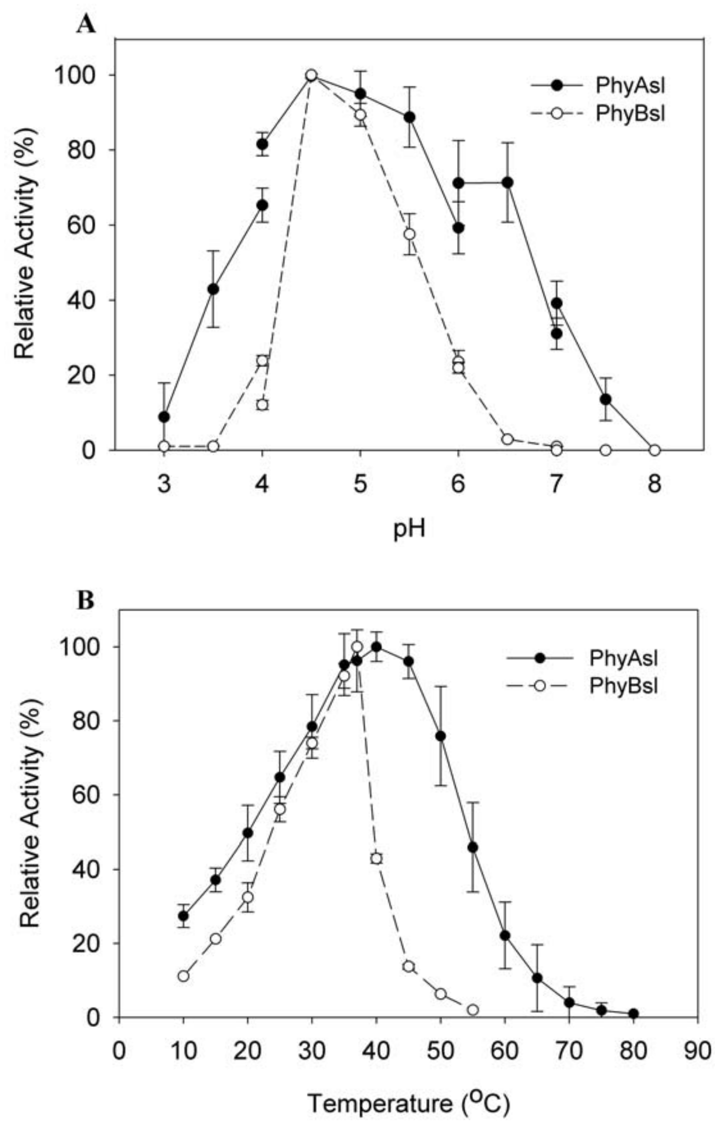

Figure 5.3. Effects of pH (A) and temperature (B) on PhyAsl and PhyBsl activity. (A) Standard phytase assays were performed with 2 mM sodium phytate over a pH range of 2 to 8. (B) To determine the optimum temperature for catalysis, standard phytase assays were performed with the temperature of the assays adjusted incrementally from 10 to 80 ^{o}C. The data presented in (A) and (B) are mean values with error bars representing the standard deviation between three independent experiments.

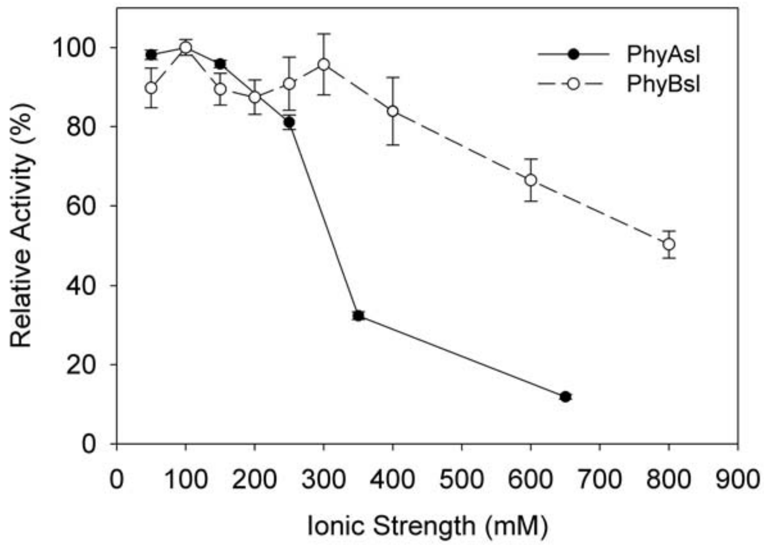

Figure 4.4. Effect of I on the activity of PhyAme. Standard assays were run under varying I controlled with NaCl. The data are mean values with error bars representing the standard deviations between three independent experiments. Values are normalized to 0.25 M.

We tested the ability of both PhyAsl and PhyBsl to hydrolyze various other phosphorylated compounds in order to characterize their specificity. The compounds that were hydrolyzed by the enzymes, and the rates of their hydrolysis, are given in Table 5.2. PhyAsl and PhyBsl exhibit relatively strict substrate specificity for IPP substrates, similar to other PTP-like phytases (refer, Chapter 3;Chapter 4). The enzymes displayed very little activity towards the commonly used phosphatase substrates pNPP and BCIP or towards the phosphorylated amino acids tested.

Pathway of dephosphorylation

Isomer-specific HPIC analysis was utilized to identify the IPP hydrolysis products generated by PhyAsl and PhyBsl catalyzed dephosphorylation of Ins P_6. Purified enzyme was incubated with excess sodium-phytate for 30 min., 60 min., and 24 hours; the stopped reaction was then resolved by HPIC (Figure 5.5). HPIC analysis suggests that PhyAsl and

PhyBsl follow identical major pathways of dephosphorylation. Following 30 min. of incubation with either enzyme, the quantity of Ins P_6 had decreased, and D/L-Ins(1,2,4,5,6)P_5 appeared as the major Ins P_5 degradation product (> 90%), along with trace amounts of Ins(1,2,3,4,6)P_5 and D/L-Ins(1,2,3,4,6)P_5. This indicates that PhyAsl and PhyBsl both initiate hydrolysis primarily at the D/L-3 phosphate position. Also found after 30 min. incubation were small amounts of D/L-Ins(1,2,5,6)P_4 and trace amounts of Ins(2,4,5,6)P_4, D/L-Ins(1,2,3,4)P_4, and D/L-Ins(1,2,4,6)P_4 . Interestingly, no Ins P_3 products were found after 30 min. incubation with PhyAsl, but large amounts of D/L-Ins(1,2,6)P_3; Ins(1,2,3)P_3 had been produced after 30 min. with PhyBsl.

Table 5.2. Substrates that were dephosphorylated by PhyAsl and PhyBsl. Hydrolysis rate of Ins P_6 was taken as 100% for determination of relative activity. All substrates were tested at 2 mM with the exception of PIP_3 which was tested at 500μM. A full list of substrates tested is presented in '*Materials and Methods*' of chapters 3 and 4.

	Specific Activity			
	PhyAsl		**PhyBsl**	
	U/mg	**(%)**	**U/mg**	**(%)**
Ins P_6	432.74	100	12.71	100
ATP	5.64	5.64	1.45	11.39
phospho (enol) pyruvate	4.23	0.98	0.49	3.89
α-naphthyl acid phosphate	2.5	0.58	0.26	2.07
pNPP	2.3	0.53	0.84	6.64
phenolphthalein diphosphate	2.14	0.49	0.87	6.83
α-naphthyl phosphate	2.04	0.47	0.28	2.23
BCIP	1.91	0.44	0.35	2.77
PIP_3	1.84	0.43	0.29	2.29
ADP	1.82	1.82	0.14	1.1
O-phospho-L-tyrosine	0	0	0.19	1.52

After 60 min. of incubation with PhyAsl, no Ins P6 remained, D/L-Ins(1,2,4,5,6)P_5 was the major Ins P5 product, and large amounts of D/L-Ins(1,2,5,6)P_4 and D/L-Ins(1,2,6)P_3; Ins(1,2,3)P3 had been produced. Following 60 min. incubation with PhyBsl, large amounts of

D/L-Ins(1,2,6)P_3; Ins(1,2,3)P_3 and D/L-Ins(1,2)P_2; Ins(2,5)P_2; D/L-Ins(4,5)P_2 had been produced, but there was no detectable Ins P_6, Ins P_5, or Ins P_4 products. Both PhyAsl and PhyBsl required extended incubation times (24 hours) to dephosphorylate Ins P_6 to predominantly Ins P_2 products.

There was no detectable Ins P_4 intermediate on the chromatograms generated by PhyBsl, so in an attempt to identify the major Ins P_4 intermediate generated shorter incubation times were attempted (10 and 20 min.). As illustrated in Figure 5.5, only small amounts of Ins P_4 products could be detected after any tested period of incubation. This suggests that PhyBsl can dephosphorylate the Ins P_4 intermediate of its pathway of Ins P_6 hydrolysis at a higher rate than the other IPP pathway intermediates.

The end products of Ins P_6 degradation were determined by incubating excess protein with a limiting substrate concentration. The results of a gas chromatography-mass spectrometry analysis revealed that the end product is Ins(2)P. At pH 5, Ins P_6 is expected to have 5 equatorial phosphates (positions 1,3,4,5,6) and 1 axial phosphate (position 2) (Isbrandt and Oertel, 1980), suggesting that these enzymes have the ability to cleave only equatorial phosphates from IPP substrates.

Kinetic properties

We determined the catalytic properties of the recombinant wild-type PhyAsl and PhyBsl with Ins P_6 and the other IPPs studied (D-Ins(1,2,4,5,6)P_5, D-Ins(1,2,5,6)P_4, D-Ins(1,2,6)P_3, and the major Ins P_5 generated by the enzymes under investigation) in an effort to elucidate the enzyme-substrate affinity and to determine the specific Ins P_5 isomers generated (Table 5.3). The rate of enzyme catalyzed phosphate release can be saturated by increasing the concentration of substrate, and remains linear over the time period of the assay (data not shown). The specific activities of the enzymes as a function of substrate concentration appear to be consistent with a classic Michaelis-Menton enzyme mechanism. The apparent k_{cat} and

K_m values for PhyAsl with Ins P_6 as a substrate were 256 s^{-1} and 309 μM respectively, and those of PhyBsl were 18 s^{-1} and 582 μM respectively. These values are within the characterized range of other PTP-like phytases (refer, Chapter 2;Chapter 3;Chapter 4).

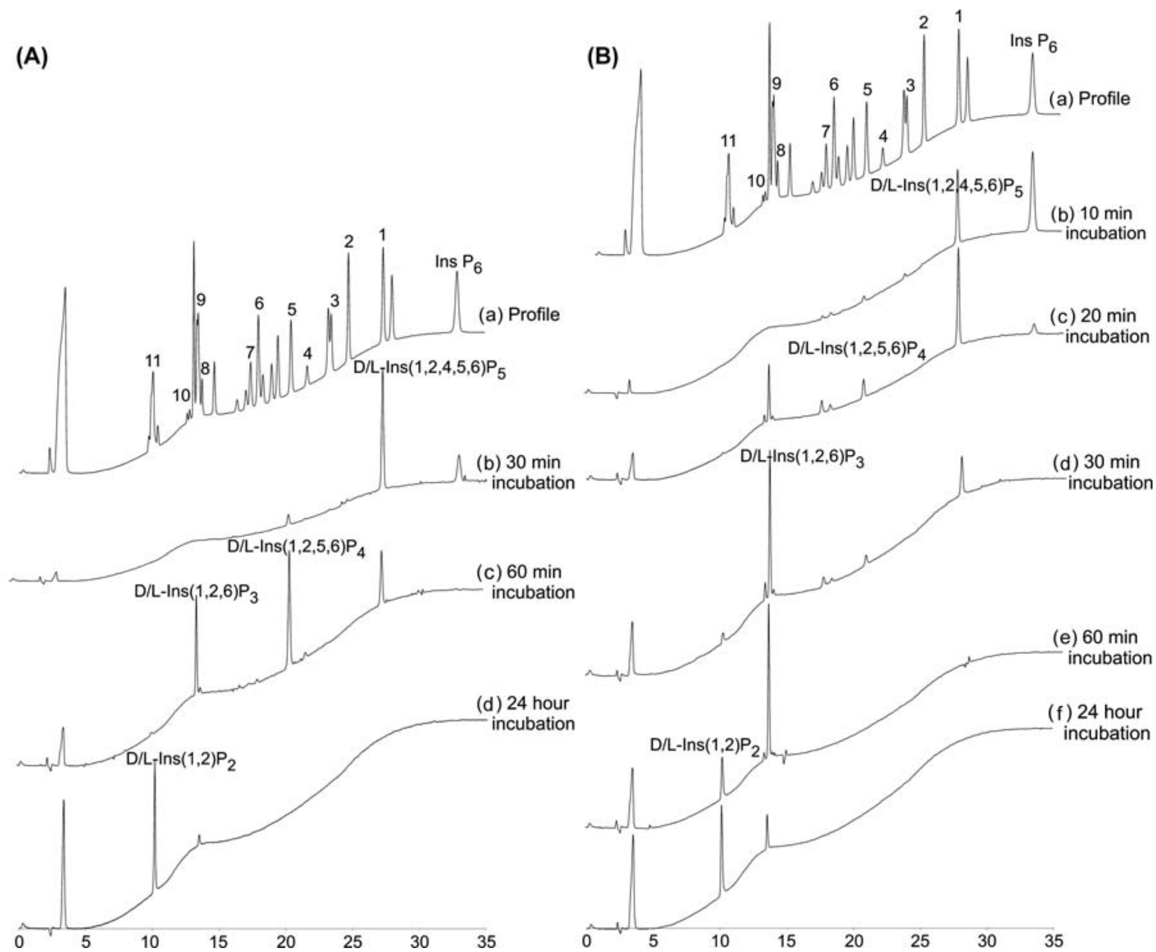

Figure 5.5**.** High-Perfomance Ion Chromatography analysis of hydrolysis products of *myo*-inositol polyphosphates by (A) PhyAsl and (B) PhyBsl. The source of the reference *myo*-inositol phosphates in the profile is as indicated in Skoglund *et al.* (1998); Peaks: Peaks: (1) D/L-Ins(1,2,4,5,6)P_5; (2) D/L-Ins(1,2,3,4,5)P_5; (3) Ins(1,2,3,4,6)P_5; (4) Ins(2,4,5,6)P_4; (5) D/L-Ins(1,2,5,6)P_4; (6) D/L-Ins(1,2,3,4)P_4; (7) D/L-Ins(1,2,4,6)P_4; (8) D/L-Ins(1,4,5)P_3, D/L-Ins(2,4,5)P_3; (9) D/L-Ins(1,2,6)P_3, Ins(1,2,3)P_3; (10) D/L-Ins(1,2,4)P_3, (11) D/L-Ins(1,2)P_2, Ins(2,5)P_2, D/L-Ins(4,5)P_2. Relative incubation times are indicated next to each chromatogram.

The k_{cat} and K_m for the hydrolysis of the D/L-Ins(1,2,4,5,6)P_5 produced by PhyAsl are 279 s^{-1} and 283 μM respectively. These values are nearly identical to the k_{cat} and K_m for the PhyAsl catalyzed hydrolysis of D-Ins(1,2,4,5,6)P_5 (272 s^{-1} and 278 μM respectively). Similarly, the k_{cat} and K_m for the hydrolysis of the D/L-Ins(1,2,4,5,6)P_5 produced by PhyBsl are 23 s^{-1} and 542 μM respectively. These values are nearly identical to the k_{cat} and K_m for the PhyBsl catalyzed hydrolysis of D-Ins(1,2,4,5,6)P_5 (21 s^{-1} and 533 μM respectively).

Table 5.3. Kinetic constants for enzymatic IPP dephosphorylation with recombinant PhyAsl and PhyBsl. Standard assays were run; *i.e.*, 50 mM NaAc (pH 5); 0.2 M I with NaCl; 37°C, containing a varying amount of substrate. Enzyme concentration was 66 nM. Data given is the average ± standard deviation of three independent experiments.

Enzyme	**Substrate**	**k_{cat} (s^{-1})**	**K_m (μM)**	**Kcat/Km (s^{-1} mM^{-1})**
	Ins(1,2,3,4,5,6)P_6	256 ± 7	309 ± 29	828 ± 81
PhyAsl	D-Ins(1,2,4,5,6)P_5	272 ± 14	278 ± 17	978 ± 78
	Ins P_5*	279 ± 16	283 ± 21	986 ± 92
	Ins(1,2,3,4,5,6)P_6	18 ± 1	582 ± 31	31 ± 2
	D-Ins(1,2,4,5,6)P_5	21 ± 2	533 ± 37	39 ± 5
PhyBsl	D-Ins(1,2,5,6)P_4	167 ± 16	105 ± 11	1590 ± 32
	D-Ins(1,2,6)P_3	15 ± 2	627 ± 41	24 ± 4
	Ins P_5*	23 ± 3	542 ± 28	42 ± 6

*Generated by the PTP-like phytase from *M. elsdenii*

HPIC analysis has suggested that PhyBsl can dephosphorylate its Ins P_4 intermediate at a much faster rate than its Ins P_5 or Ins P_3 intermediates. The Ins P_4 intermediate could not be isolated in sufficient amounts for kinetic studies, so the enzyme substrate affinity and maximal rates of hydrolysis were determined for the most probable Ins P_4 and Ins P_3 intermediates (Table 5.3). The k_{cat} and K_m for the enzymatic hydrolysis of D-

Ins(1,2,5,6)P_4 were 167 s^{-1} and 105 μM respectively. In comparison with Ins P_6, D/L-Ins(1,2,4,5,6)P_5, and D/L-Ins(1,2,6)P_3, the affinity of D-Ins(1,2,5,6)P_4 for PhyBsl and its maximal rate of hydrolysis were much higher.

5.4. DISCUSSION

Sequence analysis

We have cloned two genes (*phyAsl and phyBsl*) encoding PTP-like phytases from *S. lacticifex*. The deduced amino acid sequences show similarity to other recently characterized PTP-like phytases from *S. ruminantium* (PhyAsr) (Chu *et al.*, 2004; refer, Chapter 2), *S. ruminantium* subsp. *lactilytica* (PhyAsrl) (refer, Chapter 3), and *M. elsdenii* (PhyAme) (refer, Chapter 4). Sequence conservation is most notable in the region containing the PTP-like active site signature sequence. PhyAsr has a PTP-like core structure and catalytic mechanism similar to that of other members of the PTP superfamily (Chu *et al.*, 2004; refer, Chapter 2). The sequence identity, conservation of the active site signature sequence and similar ability to hydrolyze IPP substrates suggests that these enzymes may have a similar three-dimensional structure and a common mechanism of catalysis.

Interestingly, a widely expressed mammalian putative PTP; *i.e.*, paladin, shows some sequence similarity to PhyBsl. Paladin is made up of two putative PTP domains, and the C-terminal domain has sequence identities with PTP-like phytases. The biological function of paladin is unknown. This is the first mammalian homologue of PTP-like phytases, and it is possible that our growing knowledge regarding bacterial PTP-like phytases may contribute to an understanding of the function of paladin. PTPs have been discovered in a range of prokaryotes, and most appear to serve roles which mimic their better-known eukaryotic counterparts as regulators of cellular function (Shi *et al.*, 1998; Kennelly and Potts, 1999). It is possible that paladin can dephosphorylate IPPs, and this activity may contribute to its biological function. Mammalian PTP-like enzymes have already been identified that dephosphorylate IPP substrates, specifically PTEN. PTEN has significant structural similarity to PhyAsr (Chu *et al.*, 2004) and dephosphorylates the phosphoinositide PIP_3, and the cytosolic phosphoinositol Ins(1,3,4,5,6)P_5 *in vivo* (Caffrey *et al.*, 2001; Deleu *et al.*, 2006). The activity of PTEN has been implicated in the control of cellular growth, tumor suppression and the regulation of cellular IPP signaling molecules (Caffrey *et al.*, 2001; Deleu *et al.*, 2006). The biological importance of IPPs and phosphoinositides in mammalian cells has been well established (Sasakawa *et al.*, 1995; Chi and Crabtree, 2000; Shears, 2001; Raboy, 2003; Irvine, 2005).

Biochemical properties

The biochemical characteristics of both PhyAsl and PhyBsl were found to be consistent with other characterized PTP-like phytases. Despite only 25-50% sequence identity within this class, all display acidic pH optima, (*i.e.*, pH 4.5-5). Of note, the PTP from *Yersinia* and mammalian PTP1 display optimal activity at similar pHs (pH 5 and 5.5 respectively) towards the artificial phosphatase substrate ρ-nitrophenyl phosphate (ρNPP) (Zhang *et al.*, 1992; Zhang, 1995). In addition, similar to other characterized PTP-like phytases, PhyAsl and PhyBsl also display significant activity dependence on I of the reaction medium and a relatively strict specificity for IPP substrates. Mammalian PTEN, a structural homologue of PhyAsr (Chu *et al.*, 2004), also displayed poor ability to dephosphorylate pNPP and other artificial protein substrates and showed preference for highly negatively charged, multiply phosphorylated polymers (Li and Sun, 1997; Myers *et al.*, 1997).

Conversely, the thermostability of PhyAsl and PhyBsl is the weakest found amongst this class, and is a property shared by both enzymes despite only 33% sequence identity. As the biological function of these enzymes has not yet been determined it is difficult to speculate on the possibility of a functional significance for the relatively low stability seen with PhyAsl and PhyBsl, or alternatively, the relatively high stability of other PTP-like phytases.

Hydrolysis pathway and kinetics

Based on the position of the first phosphate hydrolyzed, three types of phytases are recognized by the Enzyme Nomenclature Committee of the International Union of Biochemistry; *i.e.*, 3-phytase (EC 3.1.3.8), 6-phytase (EC 3.1.3.26) and 5-phytase (EC 3.1.3.72). To date, most of the known phytases are D-3- or D-6-, or L-6-phytases (Konietzny and Greiner, 2002). It was concluded that the *myo*-inositol penta*kis*phosphate intermediate generated by PhyAsl is D-Ins(1,2,4,5,6)P_5 (>90%), since the kinetic constants for the degradation of the major *myo*-inositol penta*kis*phosphate generated by PhyAsl and D-Ins(1,2,4,5,6)P_5 are almost identical (Table 4.4). Similar analysis has indicated that the major *myo*-inositol penta*kis*phosphate generated by PhyBsl is also D-Ins(1,2,4,5,6)P_5. HPIC and kinetic analysis have thus indicated that PhyAsl and PhyBsl both predominantly hydrolyze the D-3-phosphate of Ins P_6. The PTP-like phytate-degrading enzymes PhyAsr and PhyAsrl display D-3 and 5-phytase activity, respectively (refer, Chapter 2;Chapter 3), and PhyAme has a mixed D-3- or D-6-phosphate position specificity.

Kinetic evaluation of the hydrolysis of different IPPs indicates that PhyBsl has a significant preference for the Ins P_4 intermediate over other IPP intermediates in its pathway of Ins P_6 dephosphorylation. PhyBsl has a specificity constant (kcat/Km) 40 fold higher for D-Ins(1,2,5,6)P_4 than for Ins P_6, D-Ins(1,2,4,5,6)P_5, and D-Ins(1,2,6)P_3. Other PTP-like phytases have commonly had a general affinity for all IPP intermediates in their pathways, often displaying only a slight preference for the more highly phosphorylated substrates.

To date, all characterized PTP-like phytases have the ability to liberate all five equatorial phosphate groups of Ins P_6 (refer, Chapter 2;Chapter 3;Chapter 4). PhyAsl and PhyBsl also display the ability to cleave all five equatorial phosphates, resulting in a final product of Ins(2)P, although it required long periods of incubation. HPIC and kinetic analysis indicate that PhyAsl and PhyBsl follow identical major routes of Ins P6 dephosphorylation to produce Ins(2)P; *i.e.*, D-Ins(1,2,4,5,6)P_5, D-Ins(1,2,5,6)P_4, D-Ins(1,2,6)P_3 and D-Ins(1,2)P_2 (Figure 5.6). With > 90% of the pathway intermediates produced via a single and specific route of hydrolysis, PhyAsl and PhyBsl have the most specific Ins P_6 degradation pathway characterized to date. The hydrolysis pathway displayed by these enzymes is similar to the major pathway of PhyAme (3,4,5,6,1) (refer, Chapter 4). All characterized PTP-like enzymes to date utilize ordered and specific routes of Ins P_6 hydrolysis.

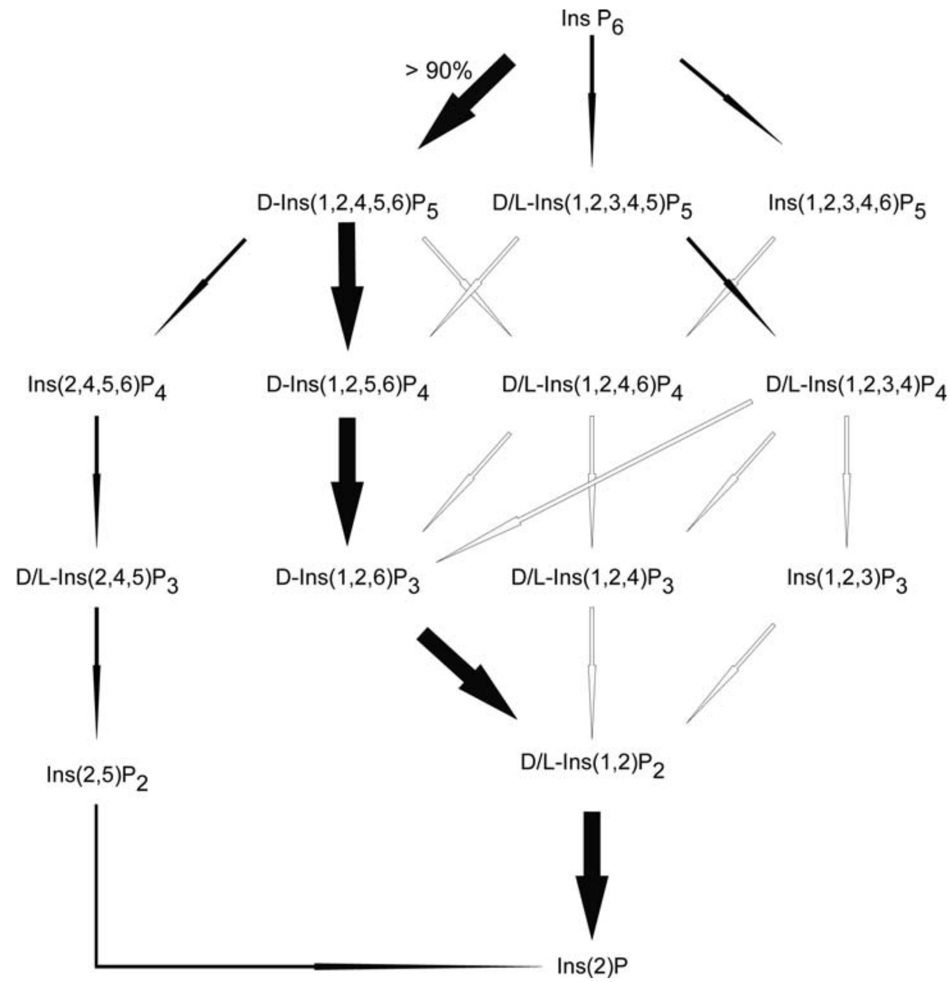

Figure 5.6. Degradation pathways of Ins P_6 by PhyAsl and PhyBsl. Larger arrows indicate the major pathway, smaller arrows indicate minor pathways. Open arrows designate possible routes of hydrolysis as predicted from HPIC data, solid arrows represent routes verified by HPIC and/or kinetic data. The proportion (%) of hydrolysis products generated by the major pathway is indicated.

GENERAL DISCUSSION

Protein tyrosine phosphatase (PTP) superfamily enzymes have been discovered in a range of prokaryotes, and most appear to serve roles which mimic their better-known eukaryotic counterparts as regulators of cellular function (Shi *et al.*, 1998; Kennelly and Potts, 1999). The work described in this thesis involved the cloning and sequencing of full genes encoding novel PTP superfamily phytases from *S. ruminantium* subsp. *lactilytica* (PhyAsrl), *M. elsdenii* (PhyAme), and *S. lacticifex*, as well as the overexpression, purification, and detailed physicochemical characterization of the recombinant gene products. The enzymes characterized in this study all contain a PTP-like active site signature sequence ($HC(X)_2G(X)GRTT$) that has been shown here to facilitate a classical PTP mechanism of dephosphorylation. While their biological function remains unclear, these enzymes differ considerably from other phytases as well as from other PTP superfamily enzymes.

Sequence Analysis

Comparison of the sequences of homologous proteins is an established method for studying enzymes with distinct differences in catalytic properties, and identification of the divergent residues responsible for those differences (Andersen *et al.*, 2005). The identification of residues that critically determine the catalytic properties is of primary interest when attempting to optimize an enzyme characteristic for a particular application. This has not been possible for PTP-like phytases because the number of cloned representatives belonging to this novel class was small prior to this study. The genes cloned in this study provide a basis for which to perform such a comparison, as their sequence identity and conservation of the active site signature sequence suggests that they have similar three-dimensional structures. Although the gene products characterized display only 30-55% sequence identity, the conserved regions are invariant between all of the enzymes studied.

The sequence segments that show the highest degree of variability are found in regions flanking the PTP-like domain, particularly areas that contribute structurally to the deep substrate binding pocket of PhyAsr as indicated by the X-ray structure; *i.e.*, the partial β-barrel domain, C-terminal helix, and extended loop (Chu *et al.*, 2004). Non-catalytic regions that flank the catalytic core of PTP superfamily enzymes often contribute to their diverse cellular functions (Mauro and Dixon, 1994; Andersen *et al.*, 2001b; Tonks and Neel, 2001). Future experiments using mutagenesis may clarify how these non-catalytic structures, and the sequence variability found therein, contribute to the functional variability observed within this novel class. Moreover, molecular models or X-ray structures of the individual proteins, in conjunction with molecular docking, could be used to elucidate how the sequence variability in these regions contributes to differences in substrate affinity, specificity, and other functional differences.

All of the cloned representatives of this class contain predicted N-terminal signal peptides. This suggests that these enzymes are secreted, and accordingly, PhyAsr has been localized to the outer membrane of *S. ruminantium* and phytase activity has been associated with the outer membrane of *M. multacida* (D'Silva *et al.*, 2000). Localization-function studies indicate that cellular localization of some PTPs may provide a molecular mechanism that determines substrate selectivity and isoform-specific function (Andersen *et al.*, 2001a). Is the biological function of PTP-like phytases subcellular-location specific? Future experiments examining the effect of membrane association on the functional characteristics of these enzymes may provide insight into the functional importance of membrane association.

Biochemical Characteristics

Despite only 30-55% sequence identity within the group, the PTP-like enzymes characterized in this study share some important biochemical characteristics. First, the enzymes all show preference for an acidic reaction medium *in vitro*. Optimal phytase activity is consistently observed at pH 4.5-5, with sharp drops in activity associated with pHs >6. The low pH optima displayed by these enzymes is inconsistent with what is expected of enzymes secreted by bacterial species commonly found in the digestive tract of animals where pHs are normally ≥ 6 (Garrett *et al.*, 1999). This could be explained by the possibility of a microenvironment produced by the outer cell membrane where these enzymes are located (D'Silva *et al.*, 2000). Alternatively, the low pH optima could be explained by the differences in reaction medium between our assays and that of the natural system. This suggestion is evidenced by the fact that other PTP superfamily enzymes have displayed similar low pH optima towards artificial substrates *in vitro* (Zhang *et al.*, 1992; Zhang, 1995). Future studies with an *in vivo* system may provide more insight.

A noted difference in the pH profiles of the enzymes characterized is the range of pHs at which they remain active. This is likely caused by variability in the magnitude of forces within each enzyme responsible for altering the pKa of key catalytic residues; *i.e.*, the general acid/base Asp, a key component of the mechanism of dephosphorylation of all PTP superfamily enzymes.

A second common characteristic among the enzymes studied is a common dependence of activity on the I of the reaction medium. This suggests that electrostatic interactions are important. The fact that both IPPs and the binding pocket of PhyAsr (Chu *et al.*, 2004) are highly, and oppositely charged suggests that enzyme-subtrate interactions contribute to this effect. The charge interactions could be involved in recruitment or catalytic orientation of substrate. The measure of I dependence is specific to each enzyme, and may indicate that not all of these enzymes rely on charge interactions to the same degree. Future pre-steady-state kinetic analysis may further elucidate the contribution of enzyme-substrate interactions to the I dependence of enzyme activity by determining binding constants at varying I.

Substrate Specificity and Ins P_6 Hydrolysis Pathways

All the PTP-like phytases characterized to date have displayed a relatively strict specificity for IPP substrates *in vitro*. Moreover, these enzymes have generally displayed a poor ability to dephosphorylate commonly used artificial phosphatase substrates such as pNPP. This could be due in part to a requirement for a highly negatively charged, multiply phosphorylated substrate. The PhyAsr structural homologue, mammalian PTEN, also displayed poor ability to dephosphorylate pNPP and other artificial protein substrates *in vitro* (Li and Sun, 1997; Myers *et al.*, 1997) but has activity towards IPPs and phoshoinositides. The activity of PTEN has been implicated in the control of cellular growth, tumor suppression and the regulation of cellular IPP signaling molecules (Caffrey *et al.*, 2001; Deleu *et al.*, 2006). Are these similarities in substrate preference a result of structural homology? Sequence identity with other PTP-like enzymes that function in the regulation of cellular function such as HopPtoD2 (Bretz *et al.*, 2003) seems to further support this suggestion. Substrate-trapping studies have been used to determine the exact biological substrate of other PTP superfamily enzymes, and may provide more insight into the function of these enzymes.

Perhaps the most striking feature of the enzymes characterized in this study is their exceptional pathways of Ins P_6 dephosphorylation. Similar to the stringent specificity by these enzymes for IPP substrates is a strict display of ordered and specific routes of Ins P_6 hydrolysis. All the enzymes characterized in this study have the ability to remove all five equatorial phosphates from Ins P_6, whereby a significant majority (> 85%) of the IPP intermediates are produced via a single, or two, major routes of hydrolysis. In contrast, kinetic constants determined in this study indicate that most of these enzymes have a general affinity and turnover capacity for all of the IPPs in their respective pathways. It is likely that the structural/electrostatic factors responsible for the stringent IPPase activity of these enzymes is also in part responsible for the strict preference for specific phosphate groups on each Ins P_6 dephosphorylation pathway intermediate. Many questions arise from these characteristics. Are the specific routes of Ins P_6 hydrolysis indicative of a function within a signaling pathway? Are the non-conserved regions of the primary structures responsible for the variability in stereospecificity displayed by individual enzymes? And what accounts for the preservation of such specific pathways? Further mutational, functional and structural studies may provide the answers.

Applications

The PTP-like phytases characterized in this study are interesting in the context of gaining a better understanding of this novel class of enzyme, but they are also interesting from an application perspective. Traditionally, phytases have been seen as a means for increasing nutrient bioavailability and reducing phosphate pollution on intensive livestock operations (Wodzinski and Ullah, 1996). A new and interesting application of phytases is in their use in the preparation of specific IPPs. The major role of IPPs in animals is in transmembrane signaling and mobilization of calcium from intracellular reserves (Sasakawa *et al.*, 1995; Shears, 1998;2001; Raboy, 2003). Therefore, these *myo*-inositol phosphates can be used as enzyme substrates for metabolic investigation, as enzyme inhibitors and therefore potentially as drugs (Laumen and Ghisalba, 1994). The chemical synthesis of these compounds is a very difficult process (Billington, 1993), and the separation of individual isomers is problematic with most analytical approaches (Greiner *et al.*, 2002b).

The phytases reported here display the most specific routes of Ins P_6 hydrolysis characterized to date, with > 85% of the hydrolysis products often generated via a single route of hydrolysis. Further, they dephosphorylate their IPP substrates with a relatively high turnover rate in comparison with other characterized phytases (Konietzny and Greiner, 2002). Some of the phytases characterized in this study even have the ability to produce IPPs not produced by any other characterized phytases, such as PhyAsrl which can generate Ins(1,2,3)P_3. Should these rare compounds become pharmaceutically important, as are other InsP_3 isomers, then these enzymes would offer a convenient means of producing them. Finally, further analysis of the relationship between specific residues or other structural features and the stereospecificity of these enzymes may lead to the ability to ‘build’ an enzyme that could dephosphorylate a position on Ins P_6 of our choosing.

REFERENCES

Altschul, S. F., W. Gish, W. Miller, E. W. Myers and D. J. Lipman (1990). Basic local alignment search tool. *Journal of Molecular Biology* **215**: 403-410.

Andersen, J. N., R. L. Del Vecchio, N. Kannan, J. Gergel, A. F. Neuwald and N. K. Tonks (2005). Computational analysis of protein tyrosine phosphatases: practical guide to bioinformatics and data resources. *Methods* **35**: 90-114.

Andersen, J. N., A. Elson, R. Lammers, J. Romer, J. T. Clausen, K. B. Moller and N. P. H. Moller (2001a). Comparative study of protein tyrosine phosphatase-epsilon isoforms: membrane localization confers specificity in cellular signalling. *Biochemical Journal* **354**: 581-590.

Andersen, J. N., O. H. Mortensen, G. H. Peters, P. G. Drake, L. F. Iversen, O. H. Olsen, P. G. Jansen, H. S. Andersen, N. K. Tonks and N. P. H. Moller (2001b). Structural and Evolutionary Relationships among Protein Tyrosine Phosphatase Domains. *Mol Cell Biol* **21**: 7117-7136.

Anderson, R. J. (1914). Concerning phytin in oats. *Journal of Biological Chemistry* **17**: 151-163.

Bachhawat, N. and S. C. Mande (1999). Identification of the INO1 gene of *Mycobacterium tuberculosis* H37Rv reveals a novel class of inositol-1-phosphate synthase enzyme. *Journal of Molecular Biology* **291**: 531-536.

Bachhawat, N. and S. C. Mande (2000). Complex evolution of the inositol-1-phosphate synthase gene among archaea and eubacteria. *Trends in Genetics* **16**: 111-113.

Baldi, P. and G. Pollastri (2003). The principled design of large-scale recursive neural network architectures-DAG-RNNs and the protein structure prediction problem. *Journal of Machine Learning Research* **4**: 575-603.

Barford, D., A. J. Flint and N. K. Tonks (1994). Crystal structure of human protein tyrosine phosphatase 1B. *Science* **263**: 1397-1404.

Barrientos, L., J. J. Scott and P. P. N. Murthy (1994). Specificity of hydrolysis of phytic acid by alkaline phytase from lily pollen. *Plant Physiology* **106**: 1489-1495.

Barrientos, L. G. and P. P. N. Murthy (1996). Conformational studies of myo-inositol phosphates. *Carbohydrate Research* **296**: 39-54.

Bartlett, G. R. (1976). Phosphate compounds in red cells of reptiles, amphibians and fish. *Comparative Biochemistry and Physiology* **55A**: 211-214.

Bartlett, G. R. (1978). Phosphate compounds in reptilian and avian red blood cells; developmental changes. *Comparative Biochemistry and Physiology* **61A**: 191-202.

Baten, A., A. Ullah, V. J. Tomazic and A. M. Shamsuddin (1989). Inositol-phosphate-induced enhancement of natural killer cell activity correlates with tumor suppression 10.1093/carcin/10.9.1595. *Carcinogenesis* **10**: 1595-1598.

Batten, G. D. and J. N. A. Lott (1986). The influence of phosphorus nutrition on the appearance and composition of globoid crystals in wheat aleurone cells. *Cereal Chemistry* **63**: 14-18.

Bendtsen, J. D., H. Nielson, G. Von Heijne and S. Brunak (2004). Improved prediction of signal peptides: SignalP 3.0. *Journal of Molecular Biology* **340**: 783-795.

Benson, D. A., I. Karsch-Mizrachi, D. J. Lipman, J. Ostell and D. L. Wheeler (2006). GenBank. *Nucleic Acids Research* **34**: D16-D20.

Billington, D. C. (1993). The inositol phosphates. chemical synthesis and biological significance. New York, NY, VCH Publishers.

Bitar, K. and J. G. Reinhold (1972). Phytase and alkaline phosphatase activities in intestinal mucose of rat, chicken, calf, and man. *Biochimica et Biophysica Acta* **268**: 442-452.

Blank, G., J. Pletcher and M. Sax (1971). Crystal structure of *myo*-inositol hexaphosphate dodecasodium salt octatriacontahydrate. *Abstracts of Papers of the American Chemical Society* 249-&.

Bliska, J., K. Guan, J. Dixon and S. Falkow (1991). Tyrosine phosphate hydrolysis of host proteins by an essential *Yersinia* virulence determinant. *Proceedings of the National Academy of Sciences USA* **88**: 1187-1191.

Brailoiu, E., M. D. Miyamoto and N. J. Dun (2003). Inositol derivatives modulate spontaneous transmitter release at the frog neuromuscular junction. *Neuropharmacology* **45**: 691-701.

Bretz, J. R., N. M. Mock, J. C. Charity, S. Zeyad, C. J. Baker and S. W. Hutcheson (2003). A translocated protein tyrosine phosphatase of *Pseudomonas syringae* pv. tomato DC3000 modulates plant defence response to infection. *Molecular Microbiology* **49**: 389-400.

Caffrey, J. J., T. Darden, M. R. Wenk and S. B. Shears (2001). Expanding coincident signaling by PTEN through its inositol 1,3,4,5,6-pentakisphosphate 3-phosphatase activity. *FEBS Letters* **499**: 6-10.

Caffrey, J. J., K. Hidaka, M. Matsuda, M. Hirata and S. B. Shears (1999). The human and rat forms of multiple inositol polyphosphate phosphatase: functional homology with a histidine acid phosphatase up-regulated during endochondral ossification. *Febs Letters* **422**: 99-104.

Caldwell, R. A. (1992). Effect of calcium and phytic acid on the activation of trypsinogen and the stability of trypsin. *Journal of Agricultural and Food Chemistry* **40**: 43-46.

Campbell, M., R. Dunn, R. Ditterline, S. Pickett and V. Raboy (1991). Phytic acid represents 10 to 15-percent of total phosphorus in alfalfa root and crown. *Journal of Plant Nutrition* **14**: 925-937.

Campbell, S., R. J. Fisher, E. M. Towler, S. Fox, H. J. Issaq, T. Wolfe, L. R. Phillips and A. Rein (2001). Modulation of HIV-like particle assembly *in vitro* by inositol phosphates. *The Proceedings of the National Academy of Sciences USA* **98**: 10875-10879.

Carrington, A. L., N. A. Calcutt, C. B. Ettlinger, T. Gustafsson and D. R. Tomlinson (1993). Effects of treatment with myo-inositol or its 1,2,6-trisphosphate (PP56) on nerve conduction in streptozotocin-diabetes. *European Journal of Pharmacology* **237**: 257-263.

Chatterjee, S., R. Sankaranarayanan and R. V. Sonti (2003). PhyA, a secreted protein of *Xanthomonas oryzae pv. oryzae*, is required for optimum virulence and growth on phytic acid as a sole phosphate source. *Molecular Plant-Microbe Interactions* **16**: 973-982.

Chen, L. J., C. Zhou, H. Y. Yang and M. F. Roberts (2000). Inositol-1-phosphate synthase from *Archaeoglobus fulgidus* is a class II aldolase. *Biochemistry* **39**: 12415-12423.

Chen, P. and J. N. A. Lott (1992). Studies of *Capsicum annuum* seeds: structure, storage reserves, and mineral nutrients. *Canadian Journal of Botany* **70**: 518-529.

Cheng, J., A. Z. Randall, M. J. Sweredoski and P. Baldi (2005). SCRATCH: a protein structure and structural feature prediction server. *Nucl Acids Res* **33**: W72-76.

Cheng, K.-J., L. B. Selinger, L. J. Yanke, H. D. Bae, L. Zhou and C. W. Forsberg (1999). DNA sequences encoding phytases of ruminal microorganisms.

Chenna, R., H. Sugawara, T. Koike, R. Lopez, T. J. Gibson, D. G. Higgins and J. D. Thompson (2003). Multiple sequence alignment with the Clustal series of programs. *Nucleic Acids Research* **31**: 3497-3500.

Chi, H. B., G. E. Tiller, M. J. Dasouki, P. R. Romano, J. Wang, R. J. O'Keefe, J. E. Puzas, R. N. Rosier and P. R. Reynolds (1999). Multiple inositol polyphosphate phosphatase: Evolution as a distinct group within the histidine phosphatase family and chromosomal localization of the human and mouse genes to chromosomes 10q23 and 19. *Genomics* **56**: 324-336.

Chi, H. B., X. N. Yang, P. D. Kingsley, R. J. O'Keefe, J. E. Puzas, R. N. Rosier, S. B. Shears and P. R. Reynolds (2000). Targeted deletion of Minpp1 provides new insight into the activity of multiple inositol polyphosphate phosphatase in vivo. *Molecular and Cellular Biology* **20**: 6496-6507.

Chi, T. H. and G. R. Crabtree (2000). Inositol phosphates in the nucleus. *Science* **287**: 1937-1938.

Chu, H. M., R. T. Guo, T. W. Lin, C. C. Chou, H. L. Shr, H. L. Lai, T. Y. Tang, K. J. Cheng, B. L. Selinger and A. H. J. Wang (2004). Structures of *Selenomonas ruminantium* phytase in complex with persulfated phytate: DSP phytase fold and mechanism for sequential substrate hydrolysis. *Structure* **12**: 2015-2024.

Cirri, P., P. Chiarugi, G. Camici, G. Manao, G. Raugei, G. Cappugi and G. Ramponi (1993). The role of Cys12, Cys17 and Arg18 in the catalytic mechanism of low-M(r) cytosolic phosphotyrosine protein phosphatase. *European Journal of Biochemistry* **214**: 647-657.

Claxson, A., C. Morris, D. Blake, M. Siren, B. Halliwell, T. Gustafsson, B. Lofkvist and I. Bergelin (1990). The anti-inflammatory effects of D-myo-inositol-1.2.6-trisphosphate (PP56) on animal models of inflammation. *Agents Actions* **29**: 68-70.

Copper, J. R. and H. S. Gowing (1983). Mammalian small intestine phytase. *British Journal of Nutrition* **50**: 673-678.

Cosgrove, D. J. (1966). The chemistry and biochemistry of inositol polyphosphates. *Review of Pure and Applied Chemistry* **16**: 209-224.

Cosgrove, D. J., G. C. J. Irving and Bromfiel.Sm (1970). Inositol phosphate phosphatases of microbiological origin - isolation of soil bacteria having inositol phosphate phosphatase activity. *Australian Journal of Biological Sciences* **23**: 339-&.

Costello, A. J., T. Glonek and T. C. Myers (1976). 31P nuclear magnetic resonance-pH titrations of myo-inositol hexaphosphate. *Carbohydrate Research* **46**: 159-171.

Cotton, F. A., E. E. j. Hazen, V. W. Day, S. Larsen, J. G. j. Norman, S. T. K. Wong and K. H. Johnson (1973). Biochemical importance of the binding of phosphate by arginyl groups. Model compounds containing methylguanidinium ion. *Journal of the American Chemical Society* **95**: 2367-2369.

Craxton, A., J. J. Caffrey, W. Burkhart, S. T. Safrany and S. B. Shears (1997). Molecular cloning and expression of a rat hepatic multiple inositol polyphosphate phosphatase. *Biochemical Journal* **328**: 75-81.

Cromwell, G. L. (1980). Biological availability of phosphorus for pigs. *Feedstuffs* **52**: 38.

Damen, J. E., L. Liu, P. Rosten, R. K. Humphries, A. B. Jefferson, P. W. Majerus and G. Krystal (1996). The 145-kDa protein induced to associate with Shc by multiple cytokines is an inositol tetraphosphate and phosphatidylinositol 3,4,5-trisphosphate 5-phosphatase. *Proceedings of the National Academy of Sciences USA* **93**: 1689-1693.

Deleris, P., S. Gayral and M. Breton-Douillon (2006). Nuclear Ptdlns(3,4,5)P-3 signaling: An ongoing story. *Journal of Cellular Biochemistry* **98**: 469-485.

Deleu, S., K. Choi, X. Pesesse, J. Cho, M. L. Sulis, R. Parsons and S. B. Shears (2006). Physiological levels of PTEN control the size of the cellular Ins(1,3,4,5,6)P-5 Pool. *Cellular Signalling* **18**: 488-498.

DeMaggio, A. E. and D. A. Stetler (1985). Mobilisation of storage reserves during fern spore germination. *Proceedings of the Royal Society of Edinburgh* **86B**: 195-202.

Denu, J. M. and J. E. Dixon (1995). A catalytic mechanism for the dual-specific phosphatases. *Proceedings of the National Academy of Sciences USA* **92**: 5910-5914.

Denu, J. M. and J. E. Dixon (1998). Protein tyrosine phosphatases: mechanisms of catalysis and regulation. *Current Opinion in Chemical Biology* **2**: 633-641.

D'Silva, C. G., H. D. Bae, L. J. Yanke, K. J. Cheng and L. B. Selinger (2000). Localization of phytase in *Selenomonas ruminantium* and *Mitsuokella multiacidus* by transmission electron microscopy. *Canadian Journal of Microbiology* **46**: 391-395.

Dunn, D., L. Chen, D. S. Lawrence and Z.-Y. Zhang (1996). The active site specificity of the *Yersinia* protein tyrosine Phosphatase. *J Biol Chem* **271**: 168-173.

Espinosa, A., M. Guo, V. C. Tam, Z. Q. Fu and J. R. Alfano (2003). The *Pseudomonas syringae* type III-secreted protein HopPtoD2 possesses protein tyrosine phosphatase activity and suppresses programmed cell death in plants. *Molecular Microbiology* **49**: 377-387.

Fassler, J., C. Nadel, N. Richardson, J. McEntyre, G. Schuler, S. McGinnis and S. Pongor (2000). NCBI website. National Center for Biotechnology Information. National Library of Medicine. National Institutes of Health. Bethesda, MD. http://www.ncbi.nlm.nih.gov/

Flint, A. J., T. Tiganis, D. Barford and N. K. Tonks (1997). Development of "substrate-trapping" mutants to identify physiological substrates of protein tyrosine phosphatases. *Proceedings of the National Academy of Sciences USA* **94**: 1680-1685.

Fredlund, K., M. Isaksson, L. Rossander-Hulthen, A. Almgren and A. S. Sandberg (2006). Absorption of zinc and retention of calcium: dose-dependent inhibition by phytate. *Journal of Trace Elements in Medicine and Biology* **20**: 49-57.

Freund, W. D., G. W. Mayr, C. Tietz and J. E. Schultz (1992). Metabolism of inositol phosphates in the protozoan *Paramecium* - characterization of a novel inositol-hexakisphosphate-dephosphorylating enzyme. *European Journal of Biochemistry* **207**: 359-367.

Fu, Y. and J. E. Galan (1998). The *Salmonella typhimurium* tyrosine phosphatase SptP is translocated into host cells and disrupts the actin cytoskeleton. *Molecular Microbiology* **27**: 359-368.

Fukuda, M. and K. Mikoshiba (1997). The function of inositol high polyphosphate binding proteins. *Bioessays* **19**: 593-603.

Funhoff, E. G., Y. Wang, G. Andersson and B. A. Averill (2005). Substrate positioning by His92 is important in catalysis by purple acid phosphatase. *Federation of European Biochemical Societies Journal* **272**: 2968-2977.

Gaidarov, I., M. E. Smith, J. Domin and J. H. Keen (2001). The class II phosphoinositide 3-kinase C2 alpha is activated by clathrin and regulates clathrin-mediated membrane trafficking. *Molecular Cell* **7**: 443-449.

Garrett, E. F., M. N. Pereira, K. V. Nordlund, L. E. Armentano, W. J. Goodger and G. R. Oetzel (1999). Diagnostic Methods for the Detection of Subacute Ruminal Acidosis in Dairy Cows. *J Dairy Sci* **82**: 1170-1178.

Gasteiger, E., C. Hoogland, A. Gattiker, S. Duvaud, M. R. Wilkins, R. D. Appel and A. Bairoch (2005). Protein Identification and Analysis Tools on the ExPASy Server. The Proteomics Protocols Handbook. J. M. Walker, Humana Press**:** 571-607.

Gibson, D. M. and A. H. J. Ullah (1988). Purification and characterization of phytase from cotyledons of germinating soybean seeds. *Archives of Biochemistry and Biophysics* **260**: 503-513.

Golovan, S., G. R. Wang, J. Zhang and C. W. Forsberg (2000). Characterization and overproduction of the Escherichia coli appA encoded bifunctional enzyme that exhibits both phytase and acid phosphatase activities. *Canadian Journal of Microbiology* **46**: 59-71.

Graf, E. and J. W. Eaton (1993). Suppression of colonic cancer by dietary phytic acid. *Nutrition and Cancer* **19**: 11-19.

Graf, E., K. L. Empson and J. W. Eaton (1987). Phytic acid - a natural antioxidant. *Journal of Biological Chemistry* **262**: 11647-11650.

Grases, F., A. Costa-Bauza and R. M. Prieto (2005). Intracellular and extracellular myo-inositol hexakisphosphate (InsP(6)), from rats to humans. *Anticancer Research* **25**: 2593-2597.

Grases, F., B. M. Simonet, I. Vucenik, J. Perello, R. M. Prieto and A. M. Shamsuddin (2002). Effects of exogenous inositol hexakisphosphate (InsP(6)) on the levels of InsP(6) and of inositol trisphosphate (InsP(3)) in malignant cells, tissues and biological fluids. *Life Sciences* **71**: 1535-1546.

Greer, J. (1981). Comparative model-building of the mammalian serine proteases. *Journal of Molecular Biology* **153**: 1027-1042.

Greiner, R. (2002). Purification and characterization of three phytases from germinated lupine seeds (*Lupinus albus var. amiga*). *Journal of Agricultural and Food Chemistry* **50**: 6858-6864.

Greiner, R. (2004). Purification and properties of a phytate-degrading enzyme from *Pantoea agglomerans*. *Protein Journal* **23**: 567-576.

Greiner, R. and M. L. Alminger (2001). Stereospecificity of myo-inositol hexakisphosphate dephosphorylation by phytate-degrading enzymes of cereals. *Journal of Food Biochemistry* **25**: 229-248.

Greiner, R., M. L. Alminger, N. G. Carlsson, M. Muzquiz, C. Burbano, C. Cuadrado, M. M. Pedrosa and C. Goyoaga (2002a). Pathway of dephosphorylation of *myo*-inositol hexakisphosphate by phytases of legume seeds. *Journal of Agricultural and Food Chemistry* **50**: 6865-6870.

Greiner, R., N. G. Carlsson and M. L. Alminger (2000a). Stereospecificity of *myo*-inositol hexakisphosphate dephosphorylation by a phytate-degrading enzyme of *Escherichia coli*. *Journal of Biotechnology* **84**: 53-62.

Greiner, R., A. Farouk, M. L. Alminger and N. G. Carlsson (2002b). The pathway of dephosphorylation of *myo*-inositol hexakisphosphate by phytate-degrading enzymes of different *Bacillus* spp. *Canadian Journal of Microbiology* **48**: 986-994.

Greiner, R., E. Haller, U. Konietzny and K. D. Jany (1997). Purification and characterization of a phytase from *Klebsiella terrigena*. *Archives of Biochemistry and Biophysics* **341**: 201-206.

Greiner, R., K. D. Jany and M. L. Alminger (2000b). Identification and properties of *myo*-inositol hexakisphosphate phosphohydrolases (Phytases) from barley (*Hordeum vulgare*). *Journal of Cereal Science* **31**: 127-139.

Greiner, R. and U. Konietzny (1996). Construction of a bioreactor to produce special breakdown products of phytate. *Journal of Biotechnology* **48**: 153-159.

Greiner, R., U. Konietzny and K. D. Jany (1993). Purification and characterization of two phytases from *Escherichia coli*. *Archives of Biochemistry and Biophysics* **303**: 107-113.

Greiner, R., U. Konietzny and K. D. Jany (1998). Purification and properties of a phytase from rye. *Journal of Food Biochemistry* **22**: 143-161.

Guan, K. L. and E. J. Dixon (1991). Evidence for protein tyrosine phosphatase catalysis proceeding via a cysteine-phosphate intermediate. *Journal of Biological Chemistry* **266**: 17026-17030.

Guan, K. L. and J. E. Dixon (1990). Protein tyrosine phosphatase activity of an essential virulence determinant in *Yersinia*. *Science* **249**: 553-556.

Guo, X. L., S. Kui, F. Wang, D. S. Lawrence and Z. Y. Zhang (2002). Probing the molecular basis for potent and selective protein-tyrosine phosphatase 1B inhibition. *Journal of Biological Chemistry* **277**: 41014-41022.

Ha, N. C., Y. O. Kim, T. K. Oh and B. H. Oh (1999). Preliminary X-ray crystallographic analysis of a novel phytase from a *Bacillus amyloliquefaciens* strain. *Acta Crystallographica Section D-Biological Crystallography* **55**: 691-693.

Ha, N. C., B. C. Oh, S. Shin, H. J. Kim, T. K. Oh, Y. O. Kim, K. Y. Choi and B. H. Oh (2000). Crystal structures of a novel, thermostable phytase in partially and fully calcium-loaded states. *Nature Structural Biology* **7**: 147-153.

Haefner, S., A. Knietsch, E. Scholten, J. Braun, M. Lohscheidt and O. Zelder (2005). Biotechnological production and applications of phytases. *Applied Microbiology and Biotechnology* **68**: 588-597.

Hanakahi, L. A., M. Bartlet-Jones, C. Chappell, D. Pappin and S. C. West (2000). Binding of inositol phosphate to DNA-PK and stimulation of double-strand break repair. *Cell* **102**: 721-729.

Harmer, A. R., D. V. Gallacher and P. M. Smith (2002). Correlations between the functional integrity of the endoplasmic reticulum and polarized Ca2+ signalling in mouse lacrimal acinar cells: a role for inositol 1,3,4,5-tetrakisphosphate. *Biochemical Journal* **367**: 137-143.

Haros, M., M. Bielecka and Y. Sanz (2005). Phytase activity as a novel metabolic feature in *Bifidobacterium*. *FEMS Microbiology Letters* **247**: 231-239.

Hawkins, P. T., D. R. Poyner, T. R. Jackson, A. J. Letcher, D. A. Lander and R. F. Irvine (1993). Inhibition of iron-catalyzed hydroxyl radical formation by inositol polyphosphates - a possible physiological function for *myo*-inositol hexakisphosphate. *Biochemical Journal* **294**: 929-934.

Hayakawa, T., K. Suzuki, H. Miura, T. Ohno and I. Igaue (1990). Myoinositol polyphosphate intermediates in the dephosphorylation of phytic acid by acid-phosphatase with phytase activity from rice bran. *Agricultural and Biological Chemistry* **54**: 279-286.

Hegeman, C. E. and E. A. Grabau (2001). A novel phytase with sequence similarity to purple acid phosphatases is expressed in cotyledons of germinating soybean seedlings. *Plant Physiology* **126**: 1598-1608.

Heinonen, J. K. and R. J. Lahti (1981). A new and convenient colorimetric determination of inorganic orthophosphate and its application to the assay of inorganic pyrophosphatase. *Analytical Biochemistry* **113**: 313-317.

Helsper, J., H. F. Linskens and J. F. Jackson (1984). Phytate metabolism in petunia pollen. *Phytochemistry* **23**: 1841-1845.

Heslop, J. P., R. F. Irvine, A. H. Tashjian and M. J. Berridge (1985). Inositol tetrakis- and pentakisphosphates in gh4 cells. *Journal of Experimental Biology* **119**: 395-401.

Higgins, D., J. Thompson and T. Gibson (1994). CLUSTAL W: improving the sensitivity of progressive multiple sequence alignment through sequence weighting, position-specific gap penalties and weight matrix choice. *Nucleic Acids Research* **22**: 4673-4680.

Houde, R. L., I. Alli and S. Kermasha (1990). Purification and characterization of canola seed(*Brassica* sp) phytase. *Journal of Food Biochemistry* **14**: 331-351.

Iijima, M., Y. E. Huang, H. R. Luo, F. Vazquez and P. N. Devreotes (2004). Novel mechanism of PTEN regulation by its phosphatidylinositol 4,5-bisphosphate binding motif is critical for chemotaxis. *Journal of Biological Chemistry* **279**: 16606-16613.

Irvine, R. F. (2005). Inositide evolution – towards turtle domination? *The Journal of Physiology* **566**: 295-300.

Irving, G. C. J. and D. J. Cosgrove (1972). Inositol phosphate phosphatases of microbiological origin: the inositol pentaphosphate products of *Aspergillus ficuum* phytase. *Journal of Bacteriology* **112**: 434-438.

Isaacks, R. E., D. R. Harkness and P. R. Witham (1978). Relationship between the major phosphorylated and metabolic intermediates and oxygen affinity of whole blood in the loggerhead (*Caretta caretta*) and the green sea turtle (*Chelonia mydas*) during development. *Developmental Biology* **62**: 344-353.

Isbrandt, L. R. and R. P. Oertel (1980). Conformational states of *myo*-inositol hexakis(phosphate) in aqueous solution. A 13C NMR, 31P NMR and Raman spectroscopy investigation. *Journal of the American Chemical Society* **102**: 3144-2148.

IUPAC-IUBMB (1992a). Nomenclature of cyclitols. Biochemical Nomenclature and Related Documents. C. Liébecq, Portland Press**:** 149-155.

IUPAC-IUBMB (1992b). Numbering of atoms in *myo*-inositol. Biochemical Nomenclature and Related Documents. C. Liébecq, Portland Press**:** 156-157.

Jackson, J. F. and H. F. Linskens (1982a). Conifer pollen contains phytate and could be a major source of phytate phosphorus in forest soils. *Australian Forest Research* **12**: 11-18.

Jackson, J. F. and H. F. Linskens (1982b). Phytic acid in *Petunia hybrida* pollen is hydrolyzed during germination by a phytase. *Acta Botanica Neerlandica* **31**: 441-447.

Jackson, T. R., T. J. Hallam, C. P. Downes and M. R. Hanley (1987). Receptor coupled events in bradykinin action: rapid production of inositol phosphates and regulation of cytosolic free Ca^{2+} in a neural cell line. *EMBO Journal* **6**: 49-54.

Jia, Z., D. Barford, A. J. Flint and N. K. Tonks (1995). Structural basis for phosphotyrosine peptide recognition by protein tyrosine phosphatase 1B. *Science* **268**: 1754-1758.

Johnson, L. F. and M. E. Tate (1969). Structure of 'phytic acids'. *Canadian Journal of Chemistry* **47**: 63.

Kennelly, P. J. and M. Potts (1999). Life among the primitives: protein o-phosphatases in prokaryotes. *Frontiers in Bioscience* **4**: d372-385.

Kerovuo, J., I. Lappalainen and T. Reinikainen (2000). The metal dependence of *Bacillus subtilis* phytase. *Biochemical and Biophysical Research Communications* **268**: 365-369.

Kerovuo, J., M. Lauraeus, P. Nurminen, N. Kalkkinen and J. Apajalahti (1998). Isolation, characterization, molecular gene cloning, and sequencing of a novel phytase from *Bacillus subtilis*. *Applied and Environmental Microbiology* **64**: 2079-2085.

Kim, Y. O., H. K. Kim, K. S. Bae, J. H. Yu and T. K. Oh (1998a). Purification and properties of a thermostable phytase from *Bacillus* sp. DS11. *Enzyme and Microbial Technology* **22**: 2-7.

Kim, Y. O., J. K. Lee, H. K. Kim, J. H. Yu and T. K. Oh (1998b). Cloning of the thermostable phytase gene (phy) from *Bacillus* sp. DS11 and its overexpression in *Escherichia coli*. *FEMS Microbiology Letters* **162**: 185-191.

Kimura, E. (2000). Dimetallic hydrolases and their models. *Current Opinion in Chemical Biology* **4**: 207-213.

Klabunde, T., N. Sträter, R. Fröhlich, H. Witzel and B. Krebs (1996). Mechanism of Fe(III)-Zn(II) purple acid phosphatase based on crystal structures. *Journal of Molecular Biology* **259**: 737-748.

Koba, K., J. W. Liu, E. Bobik, D. E. Mills, M. Sugano and Y. S. Huang (2003). Effect of phytate in soy protein on the serum and liver cholesterol levels and liver fatty acid profile in rats. *Bioscience Biotechnology and Biochemistry* **67**: 15-22.

Konietzny, U. and R. Greiner (2002). Molecular and catalytic properties of phytate-degrading enzymes (phytases). *International Journal of Food Science and Technology* **37**: 791-812.

Konietzny, U., R. Greiner and K. D. Jany (1995). Purification and characterization of a phytase from spelt. *Journal of Food Biochemistry* **18**: 165-183.

Kostrewa, D., F. G. Leitch, A. Darcy, C. Broger, D. Mitchell and A. vanLoon (1997). Crystal structure of phytase from *Aspergillus ficuum* at 2.5 angstrom resolution. *Nature Structural Biology* **4**: 185-190.

Kostrewa, D., M. Wyss, A. D'Arcy and A. van Loon (1999). Crystal structure of *Aspergillus niger* pH 2.5 acid phosphatase at 2.4 angstrom resolution. *Journal of Molecular Biology* **288**: 965-974.

Laboure, A. M., J. Gagnon and A. M. Lescure (1993). Purification and characterization of a phytase (*myo*-inositol-hexakisphosphate phosphohydrolase) accumulated in maize (*zea-mays*) seedlings during germination. *Biochemical Journal* **295**: 413-419.

Laemmli, U. K. (1970). Cleavage of structural proteins during the assembly of the head of bacteriophage T4. *Nature* **227**: 680–685.

Lassen, S. F., J. Breinholt, P. R. Ostergaard, R. Brugger, A. Bischoff, M. Wyss and C. C. Fuglsang (2001). Expression, gene cloning, and characterization of five novel phytases from four basidiomycete fungi: *Peniophora lycii, Agrocybe pediades, Ceriporia* sp., and *Trametes pubescens*. *Applied and Environmental Microbiology* **67**: 4701-4707.

Laumen, K. and O. Ghisalba (1994). Preparative-Scale Chemoenzymatic Synthesis of Optically Pure D-Myo-Inositol-1-Phosphate. *Bioscience Biotechnology and Biochemistry* **58**: 2046-2049.

Lee, J. O., H. J. Yang, M. M. Georgescu, A. Di Cristofano, T. Maehama, Y. G. Shi, J. E. Dixon, P. Pandolfi and N. P. Pavletich (1999). Crystal structure of the PTEN tumor suppressor: Implications for its phosphoinositide phosphatase activity and membrane association. *Cell* **99**: 323-334.

Leslie, N. R. and C. P. Downes (2004). PTEN function: how normal cells control it and tumour cells lose it. *Biochemical Journal* **382**: 1-11.

Leslie, N. R., X. Yang, C. P. Downes and C. J. Weijer (2005). The regulation of cell migration by PTEN. *Biochemical Society Transactions* **33**: 1507-1508.

Li, D. M. and H. Sun (1997). TEP1, encoded by a candidate tumor suppressor locus, is a novel protein tyrosine phosphatase regulated by transforming growth factor beta. *Cancer Research* **57**: 2124-2129.

Li, J., C. Yen, D. Liaw, K. Podsypanina, S. Bose, S. I. Wang, J. Puc, C. Miliaresis, L. Rodgers, R. McCombie, S. H. Bigner, B. C. Giovanella, M. Ittmann, B. Tycko, H. Hibshoosh, M. H. Wigler and R. Parsons (1997). PTEN, a putative protein tyrosine phosphatase gene mutated in human brain, breast, and prostate cancer. *Science* **275**: 1943-1947.

Lim, D., S. Golovan, C. W. Forsberg and Z. C. Jia (2000). Crystal structures of *Escherichia coli* phytase and its complex with phytate. *Nature Structural Biology* **7**: 108-113.

Liu, O., Q. Q. Huang, X. G. Lei and Q. Hao (2004). Crystallographic snapshots of *Aspergillus fumigatus* phytase, revealing its enzymatic dynamics. *Structure* **12**: 1575-1583.

Loewus, F. A. and P. P. N. Murthy (2000). *Myo*-inositol metabolism in plants. *Plant Science* **150**: 1-19.

Lohse, L. D., M. J. Denu, N. Santoro and E. J. Dixon (1997). Roles of aspartic acid-181 and serine-222 in intermediate formation and hydrolysis of the mammalian protein tyrosine phosphatase PTP1B. *Biochemistry* **36**: 4568-4575.

Lott, J. N. A. (1984). Accumulation of seed reserves of phosphorus and other minerals. Seed Physiology. D. R. Murray. Sydney, Academic Press. **1:** 139-166.

Lott, J. N. A. and M. S. Buttrose (1978a). Location of reserves of mineral elements in seed protein bodies: macadamia nut, walnut and hazel nut. *Canadian Journal of Botany* **56**: 2072-2082.

Lott, J. N. A. and M. S. Buttrose (1978b). Thin sectioning, freeze fracturing, energy dispersive x-ray analysis, and chemical analysis in the study of inclusions in seed protein bodies: almond, Brazil nut, and quandong. *Canadian Journal of Botany* **56**: 2050-2061.

Lott, J. N. A., I. Ockenden, V. Raboy and G. D. Batten (2000). Phytic acid and phosphorus in crop seeds and fruits: a global estimate. *Seed Science Research* **10**: 11-33.

Macbeth, M. R., H. L. Schubert, A. P. VanDemark, A. T. Lingam, C. P. Hill and B. L. Bass (2005). Inositol hexakisphosphate is bound in the ADAR2 core and required for RNA editing. *Science* **309**: 1534-1539.

Maehama, T. and J. E. Dixon (1998). The tumor suppressor, PTEN/MMAC1, dephosphorylates the lipid second messenger, phosphatidylinositol 3,4,5-trisphosphate. *Journal of Biological Chemistry* **273**: 13375-13378.

Maehama, T. and J. E. Dixon (1999). PTEN: a tumour suppressor that functions as a phospholipid phosphatase. *Trends in Cell Biology* **9**: 125-128.

Maenz, D. D., C. M. Engele-Schaan, R. W. Newkirk and H. L. Classen (1999). The effect of minerals and mineral chelators on the formation of phytase-resistant and phytase-susceptible forms of phytic acid in solution and in a slurry of canola meal. *Animal Feed Science and Technology* **81**: 177-192.

Maga, J. A. (1982). Phytate - Its chemistry, occurrence, food interactions, nutritional significance, and methods of analysis. *Journal of Agricultural and Food Chemistry* **30**: 1-9.

Maiti, I. B., A. L. Majumber and B. B. Biswas (1974). Purification and mode of action of phytase from *Phaseolus aureus*. *Phytochemistry* **13**: 1047-1051.

Mandel, N. C., S. Burman and B. B. Biswas (1972). Isolation, purification and characterization of phytase from germinating mung beans. *Phytochemistry* **11**: 495-502.

Mauro, L. J. and J. E. Dixon (1994). 'Zip codes' direct intracellular protein tyrosine phosphatases to the correct cellular 'address'. *Trends in Biochemical Sciences* **19**: 151-155.

McConnachie, G., I. Pass, S. M. Walker and C. P. Downes (2003). Interfacial kinetic analysis of the tumour suppressor phosphatase, PTEN: evidence for activation by anionic phospholipids. *Biochemical Journal* **371**: 947-955.

Mehtaa, B. D., S. P. Joga, S. C. Johnsona and P. P. N. Murthy (2006). Lily pollen alkaline phytase is a histidine phosphatase similar to mammalian multiple inositol polyphosphate phosphatase (MINPP). *Phytochemistry* In Press.

Michell, R. H. (2002). Inositol phosphates: a remarkably versatile enzyme. *Current Biology* **12**: R313-315.

Michell, R. H., N. M. Perera and S. K. Dove (2003). New insights into the roles of phosphoinositides and inositol polyphosphates in yeast. *Biochemical Society Transactions* **31**: 11-15.

Migita, K., L. Lu, Y. Zhao, K. Honda, T. Iwamoto, S. Kita and T. Katsuragi (2005). Adenosine induces ATP release via an inositol 1,4,5-trisphosphate signaling pathway in MDCK cells. *Biochemical and Biophysical Research Communications* **328**: 1211-1215.

Modlin, M. (1980). Urinary phosphorylated inositols and renal stone. *Lancet* **2**: 1113-1114.

Mullaney, E. J. and A. H. J. Ullah (1998). Conservation of the active site motif in *Aspergillus niger* (*ficuum*) pH 6.0 optimum acid phosphatase and kidney bean purple acid phosphatase. *Biochemical and Biophysical Research Communications* **243**: 471-473.

Mullaney, E. J. and A. H. J. Ullah (2003). The term phytase comprises several different classes of enzymes. *Biochemical and Biophysical Research Communications* **312**: 179-184.

Myers, M. P., I. Pass, I. H. Batty, J. Van der Kaay, J. P. Stolarov, B. A. Hemmings, M. H. Wigler, C. P. Downes and N. K. Tonks (1998). The lipid phosphatase activity of PTEN is critical for its tumor suppressor function. *Proceedings of the National Academy of Sciences USA* **95**: 13513-13518.

Myers, M. P., J. P. Stolarov, C. Eng, J. Li, S. I. Wang, M. H. Wigler, R. Parsons and N. K. Tonks (1997). P-TEN, the tumor suppressor from human chromosome 10q23, is a dual-specificity phosphatase. *Proceedings of the National Academy of Sciences USA* **94**: 9052-9057.

Nakano, T., T. Joh, K. Narita and T. Hayakawa (2000). The pathway of dephosphorylation of myo-inositol hexakisphosphate by phytases from wheat bran of *Triticum aestivum*. *Bioscience Biotechnology and Biochemistry* **64**: 995-1003.

Nakashima, B. A., T. A. McAllister, R. Sharma and L. B. Selinger (2006). Diversity of phytases in the rumen. *Microbial Ecology* In Press.

Nelson, T. S. (1967). Utilization of phytate phosphorus by poultry - a review. *Poultry Science* **46**: 862-871.

Nelson, T. S., McGilliv.Jj, T. R. Shieh, Wodzinsk.Rj and J. H. Ware (1968a). Effect of phytate on calcium requirement of chicks. *Poultry Science* **47**: 1985-1989.

Nelson, T. S., T. R. Shieh, Wodzinsk.Rj and J. H. Ware (1968b). Availability of phytate phosphorus in soybean meal before and after treatment with a mold phytase. *Poultry Science* **47**: 1842-1848.

Nicholas, K. B., N. H. B. Jr. and D. W. I. Deerfield (1997). GeneDoc: Analysis and visualization of genetic variation. EMBNEW.NEWS 4:14. http://www.psc.edu/biomed/genedoc

Nielsen, H., J. Engelbrecht, S. Brunak and G. Von Heijne (1997). Identification of prokaryotic and eukaryotic signal peptides and prediction of their cleavage sites. *Protein Engineering* **10**: 1-6.

Odom, A. R., A. Stahlberg, S. R. Wente and J. D. York (2000). A role for nuclear inositol 1,4,5-trisphosphate kinase in transcriptional control. *Science* **287**: 2026-2029.

Oh, B. C., B. S. Chang, K. H. Park, N. C. Ha, H. K. Kim, B. H. Oh and T. K. Oh (2001). Calcium-dependent catalytic activity of a novel phytase from *Bacillus amyloliquefaciens* DS11. *Biochemistry* **40**: 9669-9676.

Oh, B. C., W. C. Choi, S. Park, Y. O. Kim and T. K. Oh (2004). Biochemical properties and substrate specificities of alkaline and histidine acid phytases. *Applied Microbiology and Biotechnology* **63**: 362-372.

Ohkawa, T., S. Ebisuno, M. Kitagawa, S. Morimoto, Y. Miyazaki and S. Yasukawa (1984). Rice bran treatment for patients with hypercalciuric stones: experimental and clinical studies. *Journal of Urology* **132**: 1140-1145.

Ongusaha, P. P., P. J. Hughes, J. Davey and R. H. Michell (1998). Inositol hexakisphosphate in *Schizosaccharomyces pombe*: synthesis from Ins(1,4,5)P-3 and osmotic regulation. *Biochemical Journal* **335**: 671-679.

Onomi, S., Y. Okazaki and T. Katayama (2004). Effect of dietary level of phytic acid on hepatic and serum lipid status in rats fed a high-sucrose diet. *Bioscience Biotechnology and Biochemistry* **68**: 1379-1381.

Orchiston, E. A., D. Bennett, N. R. Leslie, R. G. Clarke, L. Winward, C. P. Downes and S. T. Safrany (2004). PTEN M-CBR3, a versatile and selective regulator of inositol 1,3,4,5,6-pentakisphosphate (Ins(1,3,4,5,6)P-5) - Evidence for Ins(1,3,4,5,6)P-5 as a proliferative signal. *Journal of Biological Chemistry* **279**: 1116-1122.

Ostanin, K., E. H. Harms, P. E. Stevis, R. Kuciel, M. M. Zhou and R. L. van Etten (1992). Overexpression, site-directed mutagenesis, and mechanism of *Escherichia coli* acid phosphatase. *Journal of Biological Chemistry* **267**: 22830-22836.

Ostanin, K. and R. L. van Etten (1993). Asp304 of *Escherichia coli* acid phosphatase is involved in leaving group protonation. *Journal of Biological Chemistry* **268**: 20778-20784.

Pannifer, A. D. B., A. J. Flint, N. K. Tonks and D. Barford (1998). Visualization of the cysteinyl-phosphate intermediate of a protein-tyrosine phosphatase by X-ray crystallography. *Journal of Biological Chemistry* **273**: 10454-10462.

Pasamontes, L., M. Haiker, M. Wyss, M. Tessier and A. vanLoon (1997). Gene cloning, purification, and characterization of a heat-stable phytase from the fungus Aspergillus fumigatus. *Applied and Environmental Microbiology* **63**: 1696-1700.

Pfeffer, W. (1872). Untersuchungen uiber die Proteinkdrner und die Bedentung des Asparagins beim Keimen der Sameni. *Jahrb F Wiss Bot* **8**: 429-571.

Phillippy, B. Q. and J. M. Bland (1988). Gradient ion chromatography of inositol phosphates. *Analytical Biochemistry* **175**: 162-166.

Phillipy, B. Q. and E. Graf (1997). Antioxidant functions of inositol 1,2,3-trisphosphate and inositol 1,2,3,6-tetrakisphosphate. *Free Radical Biology and Medicine* **22**: 939-946.

Piccolo, E., S. Vignati, T. Maffucci, P. F. Innominato, A. M. Riley, B. V. Potter, P. P. Pandolfi, M. Broggini, S. Iacobelli, P. Innocenti and M. Falasca (2004). Inositol pentakisphosphate promotes apoptosis through the PI 3-K/Akt pathway. *Oncogene* **23**: 1754-1765.

Pollastri, G., D. Przybylski, B. Rost and P. Baldi (2002). Improving the prediction of protein secondary structure in three and eight classes using recurrent neural networks and profiles. *Proteins* **47**: 228-235.

Pot, D. A. and J. E. Dixon (1992). Active site labeling of a receptor-like protein tyrosine phosphatase. *Journal of Biological Chemistry* **267**: 140-143.

Pot, D. A., T. A. Woodford, E. Remboutsika, R. S. Haun and J. E. Dixon (1991). Cloning, bacterial expression, purification, and characterization of the cytoplasmic domain of rat LAR, a receptor-like protein tyrosine phosphatase. *Journal of Biological Chemistry* **266**: 19688-19696.

Potter, B. V. L. (1990). Recent advances in the chemistry and biochemistry of inositol phosphates of biological interest. *Natural Product Reports* **7**: 1-23.

Priefer, U., R. Simon and A. Ptihler (1984). Cloning with cosmids. Advanced Molecular Genetics. A. Puhler and K. N. Timmis. New York, Springer-Verlag N.Y.**:** 190-201.

Quan, C. S., S. D. Fan and Y. Ohta (2003). Pathway of dephosphorylation of myo-inositol hexakisphosphate by a novel phytase from *Candida krusei* WZ-001. *Journal of Bioscience and Bioengineering* **95**: 530-533.

Quignard, J. F., L. Rakotoarisoa, J. Mironneau and C. Mironneau (2003). Stimulation of L-type Ca^{2+} channels by inositol pentakis- and hexakisphosphates in rat vascular smooth muscle cells. *The Journal of Physiology* **549**: 729-737.

Raboy, V. (2001). Seeds for a better future: 'low phytate', grains help to overcome malnutrition and reduce pollution. *Trends in Plant Science* **6**: 458-462.

Raboy, V. (2003). *Myo*-Inositol-1,2,3,4,5,6-hexakisphosphate. *Phytochemistry* **64**: 1033-1043.

Reddy, N. R., M. D. Pierson, S. K. Sathe and D. K. Salunkhe (1989). Phytates in cereals and legumes. Boca Raton, CRC Press, Inc.

Reddy, N. R., S. K. Sathe and D. K. Salunkhe (1982). Phytates in legumes and cereals. *Advances in Food Research* **28**: 1-92.

refer (Chapter 2). PhyAsr.

refer (Chapter 3). PhyAsrl.

refer (Chapter 4). PhyAme.

Rizzoli, S. O. and W. J. Betz (2002). Effects of 2-(4-morpholinyl)-8-phenyl-4H-1-benzopyran-4-one on synaptic vesicle cycling at the frog neuromuscular junction. *Journal of Neuroscience* **22**: 10680-10689.

Roberts, R. M. and F. Loewus (1968). Inositol metabolism in plants. VI. Conversion of myo-inositol to phytic acid in *Wolffiella floridana*. *Plant Physiology* **43**: 1710-1716.

Ruf, J. C., M. Ciavatti, T. Gustafsson and S. Renaud (1991). Effects of Pp-56 and vitamin-E on platelet hyperaggregability, fatty-acid abnormalities, and clinical manifestations in streptozocin-induced diabetic rats. *Diabetes* **40**: 233-239.

Ruf, J. C., M. Ciavatti, T. Gustafsson and S. Renaud (1994). In-vitro effect of D-myo-inositol 1,2,6-trisphosphate (Pp-56) on aggregation of platelets from normal and diabetic rats - relationship to malondialdehyde release and phosphoinositide pathway. *Canadian Journal of Physiology and Pharmacology* **72**: 644-649.

Sajidan, A., A. Farouk, R. Greiner, P. Jungblut, E. C. Muller and R. Borriss (2004). Molecular and physiological characterisation of a 3-phytase from soil bacterium *Klebsiella* sp ASR1. *Applied Microbiology and Biotechnology* **65**: 110-118.

Salvatore, S. and B. T. Chait (1998). Modification of cysteine residues by alkylation. A tool in peptide mapping and protein identification. *Analytical Chemistry* **70**: 5150-5158.

Sandberg, A. S. and R. Ahderinne (1986). HPLC method for determination of inositol tri-, tetra-, penta-, and hexaphosphates in foods and intestinal contents. *J Food Sci* **51**: 547-550.

Sandberg, A. S. and H. Andersson (1988). Effect of Dietary Phytase on the Digestion of Phytate in the Stomach and Small-Intestine of Humans. *Journal of Nutrition* **118**: 469-473.

Sasakawa, N., M. Sharif and M. R. Hanley (1995). Metabolism and biological-activities of inositol pentakisphosphate and inositol hexakisphosphate. *Biochemical Pharmacology* **50**: 137-146.

Schenk, G., Y. Ge, L. E. Carrington, C. J. Wynne, I. R. Searle, B. J. Carroll, S. Hamilton and J. deJersey (1999). Binuclear metal centers in plant purple acid phosphatases: Fe-Mn in sweet potato and Fe-Zn in soybean. *Archives of Biochemistry and Biophysics* **370**: 183-189.

Schneider, G., Y. Lindqvist and P. Vihko (1993). Three-dimensional structure of rat acid phosphatase. *EMBO Journal* **12**: 2609-2615.

Scott, H. W. and B. A. Dehority (1965). Vitamin requirements of several cellulolytic bacteria. *Journal of Bacteriology* **89**: 1169-1175.

Scott, J. J. (1991). Alkaline phytase activity in nonionic detergent extracts of legume seeds. *Plant Physiology* **95**: 1298-1301.

Scott, J. J. and F. A. Loewus (1986). A calcium-activated phytase from pollen of *Lilium-longiflorum*. *Plant Physiology* **82**: 333-335.

Selinger, L. B., L. J. Yanke, T. A. McAllister and K.-J. Cheng (2000). Is *Selenomonas ruminantium* phytaseA a protein tyrosine phosphatase. 50th Annual Meeting of the Canadian Society of Microbiologists, Winnipeg, MN.

Selinger, L. B., L. Zhou, H. D. Bae, L. J. Yanke and K.-J. Cheng (1999). Characterization of a novel phytase gene from the anaerobic bacterium *Selenomonas ruminantium*. Canadian Society of Microbiologists Meeting, Montreal, PQ.

Shamsuddin, A. M., I. Vucenik and K. E. Cole (1997). IP6: A novel anti-cancer agent. *Life Sciences* **61**: 343-354.

Shears, S. B. (1998). The versatility of inositol phosphates as cellular signals. *Biochimica Et Biophysica Acta-Molecular and Cell Biology of Lipids* **1436**: 49-67.

Shears, S. B. (2001). Assessing the omnipotence of inositol hexakisphosphate. *Cellular Signalling* **13**: 151-158.

Shi, L., M. Potts and P. J. Kennelly (1998). The serine, threonine, and/or tyrosine-specific protein kinases and protein phosphatases of prokaryotic organisms: a family portrait. *Fems Microbiology Reviews* **22**: 229-253.

Shimizu, M. (1992). Purification and Characterization of Phytase from Bacillus-Subtilis (Natto) N-77. *Bioscience Biotechnology and Biochemistry* **56**: 1266-1269.

Shin, S., N. C. Ha, B. C. Oh, T. K. Oh and B. H. Oh (2001). Enzyme mechanism and catalytic property of beta propeller phytase. *Structure* **9**: 851-858.

Singh, R. P. and R. Agarwal (2005). Prostate cancer and inositol hexaphosphate: Efficacy and mechanisms. *Anticancer Research* **25**: 2891-2903.

Skoglund, E., N. G. Carlsson and A. S. Sandberg (1998). High-performance chromatographic separation of inositol phosphate isomers on strong anion exchange columns. *Journal of Agricultural and Food Chemistry* **46**: 1877-1882.

Spiers, I. D., S. Freeman, D. R. Poyner and C. H. Schwalbe (1995). The first synthesis and iron binding studies of the natural product, myo-inositol 1,2,3-trisphosphate. *Tetrahedron Letters* **36**: 2125-2128.

Steger, D. J., E. S. Haswell, A. L. Miller, S. R. Wente and E. K. O'Shea (2003). Regulation of chromatin remodeling by inositol polyphosphates. *Science* **299**: 114-116.

Stewart, A. E., S. Dowd, S. M. Keyse and N. Q. McDonald (1999). Crystal structure of the MAPK phosphatase Pyst1 catalytic domain and implications for regulated activation. **6**: 174-181.

Strater, N., T. Klabunde, P. Tucker, H. Witzel and B. Krebs (1995). Crystal structure of a purple acid phosphatase containing a dinuclear Fe(III)-Zn(II) active site. *Science* **268**: 1489-1492.

Stuckey, J. A., H. L. Schubert, E. B. Fauman, Z.-Y. Zhang, J. E. Dixon and M. A. Saper (1994). Crystal structure of Yersinia protein tyrosine phosphatase at 2.5 A and the complex with tungstate. **370**: 571-575.

Sulis, M. L. and R. Parsons (2003). PTEN: from pathology to biology. *Trends in Cell Biology* **13**: 478-483.

Suzuki, V., K. Yoshimura and M. Takaishi (1907). Uber ein enzym "phytase" das anhydro-oxy-methylen diphosphorsaure. *Bull Coll Agric Tokyo* **7**: 503.

Takenawa, T. and T. Itoh (2001). Phosphoinositides, key molecules for regulation of actin cytoskeletal organization and membrane traffic from the plasma membrane. *Biochimica Et Biophysica Acta-Molecular and Cell Biology of Lipids* **1533**: 190-206.

Takenawa, T. and T. Itoh (2006). Membrane targeting and remodeling through phosphoinositide-binding domains. *IUBMB Life* **58**: 296-303.

Taylor, G. S. and J. E. Dixon (2003). PTEN and myotubularins: families of phosphoinositide phosphatases. *Methods in Enzymology* **366**: 43-56.

Tonks, N. K. and B. G. Neel (2001). Combinatorial control of the specificity of protein tyrosine phosphatases. *Current Opinion in Cell Biology* **13**: 182-195.

Truong, N. T., J. I. Naseri, A. Vogel, A. Rompel and B. Krebs (2005). Structure-function relationships of purple acid phosphatase from red kidney beans based on heterologously expressed mutants. *Archives of Biochemistry and Biophysics* **440**: 38-45.

Turk, M., A. S. Sandberg, N. G. Carlsson and T. Andlid (2000). Inositol hexaphosphate hydrolysis by baker's yeast. Capacity, kinetics, and degradation products. *Journal of Agricultural and Food Chemistry* **48**: 100-104.

Turner, B. L., M. J. Paphazy, P. M. Haygarth and I. D. McKelvie (2002). Inositol phosphates in the environment. *Philosophical Transactions of the Royal Society of London Series B-Biological Sciences* **357**: 449-469.

Tye, A. J., F. K. Y. Siu, T. Y. C. Leung and B. L. Lim (2002). Molecular cloning and the biochemical characterization of two novel phytases from *Bacillus subtilis* 168 and *Bacillus licheniformis*. *Applied Microbiology and Biotechnology* **59**: 190-197.

Ullah, A. H. J., K. Sethumadhavan, X. G. Lei and E. J. Mullaney (2000). Biochemical characterization of cloned Aspergillus fumigatus phytase (phyA). *Biochemical and Biophysical Research Communications* **275**: 279-285.

van Etten, R. L. (1982). Human prostatic acid phosphatase: a histidine phosphatase. *Annals of the New York Academy of Sciences* **390**: 27-51.

Vats, P. and U. C. Banerjee (2004). Production studies and catalytic properties of phytases (myo-inositolhexakisphosphate phosphohydrolases): an overview. *Enzyme and Microbial Technology* **35**: 3-14.

Wada, T. and J. N. A. Lott (1997). Light and electron microscopic and energy dispersive X-ray microanalysis studies of globoids in protein bodies of embryo tissues and the aleurone layer of rice (*Oryza sativa L.*) grains. *Canadian Journal of Botany* **75**: 1137-1147.

Wodzinski, R. J. and A. H. J. Ullah (1996). Phytase. <u>Advances in Applied Microbiology</u>. **42:** 263-302.

Wu, L. and Z. Y. Zhang (1996). Probing the function of Asp128 in the low molecular weight protein-tyrosine phosphatase-catalyzed reaction. A pre-steady-state and steady-state kinetic investigation. *Biochemistry* **35**: 5426-5434.

Wyss, M., R. Brugger, A. Kroenberger, R. Remy, R. Fimbel, G. Osterhelt, M. Lehmann and A. van Loon (1999). Biochemical characterization of fungal phytases (*myo*-inositol hexakisphosphate phosphohydrolases): Catalytic properties. *Applied and Environmental Microbiology* **65**: 367-373.

Yang, W. J., Y. Matsuda, S. I. Sano, H. Masutani and H. Nakagawa (1991). Purification and characterization of phytase from rat intestinal-mucosa. *Biochimica Et Biophysica Acta* **1075**: 75-82.

Yanke, L. J., H. D. Bae, L. B. Selinger and K. J. Cheng (1998). Phytase activity of anaerobic ruminal bacteria. *Microbiology-Uk* **144**: 1565-1573.

Yanke, L. J., L. B. Selinger and K. J. Cheng (1999). Phytase activity of Selenomonas ruminantium: a preliminary characterization. *Letters in Applied Microbiology* **29**: 20-25.

York, J. D., A. R. Odom, R. Murphy, E. B. Ives and S. R. Wente (1999). A phospholipase C-dependent inositol polyphosphate kinase pathway required for efficient messenger RNA export. *Science* **285**: 96-100.

Yu, J., B. Leibiger, S. N. Yang, J. J. Caffery, S. B. Shears, I. B. Leibiger, C. J. Barker and P. O. Berggren (2003). Cytosolic multiple inositol polyphosphate phosphatase in the regulation of cytoplasmic free Ca^{2+} concentration. *Journal of Biological Chemistry* **278**: 46210-46218.

Yuvaniyama, J., J. M. Denu, J. E. Dixon and M. A. Saper (1996). Crystal structure of the dual specificity protein phosphatase VHR. *Science* **272**: 1328-1331.

Zhang, X. and P. W. Majerus (1998). Phosphatidylinositol signalling reactions. *Seminars in Cell and Developmental Biology* **9**: 153-160.

Zhang, Z. (1995). Kinetic and mechanistic characterization of a mammalian protein-tyrosine phosphatase, PTP1. *J Biol Chem* **270**: 11199-11204.

Zhang, Z., J. Clemens, H. Schubert, J. Stuckey, M. Fischer, D. Hume, M. Saper and J. Dixon (1992). Expression, purification, and physicochemical characterization of a recombinant *Yersinia* protein tyrosine phosphatase. *J Biol Chem* **267**: 23759-23766.

Zhang, Z., R. Poorman, L. Maggiora, R. Heinrikson and F. Kezdy (1991). Dissociative inhibition of dimeric enzymes. Kinetic characterization of the inhibition of HIV-1 protease by its COOH-terminal tetrapeptide. *J Biol Chem* **266**: 15591-15594.

Zhang, Z., Y. Song and X. L. Wang (2005). Inositol hexaphosphate-induced enhancement of natural killer cell activity correlates with suppression of colon carcinogenesis in rats. *World Journal of Gastroenterology* **11**: 5044-5046.

Zhang, Z., Y. Wang and J. Dixon (1994a). Dissecting the catalytic mechanism of protein tyrosine phosphatases. *Proceedings of the National Academy of Sciences USA* **91**: 1624-1627.

Zhang, Z. Y. (1998). Protein-tyrosine phosphatases: biological function, structural characteristics, and mechanism of catalysis. *Critical Reviews in Biochemistry and Molecular Biology* **33**: 1-52.

Zhang, Z. Y. (2002). Protein tyrosine phosphatases: Structure and function, substrate specificity, and inhibitor development. *Annual Review of Pharmacology and Toxicology* **42**: 209-234.

Zhang, Z. Y. (2003). Mechanistic studies on protein tyrosine phosphatases. *Progress in Nucleic Acid Research and Molecular Biology* **73**: 171-220.

Zhang, Z. Y. (2005). Functional studies of protein tyrosine phosphatases with chemical approaches. *Biochimica Et Biophysica Acta-Proteins and Proteomics* **1754**: 100-107.

Zhang, Z. Y. and E. J. Dixon (1993). Active site labeling of the *Yersinia* protein tyrosine phosphatase: The determination of the pK_a of the active site cysteine and the function of the conserved histidine 402. *Biochemistry* **32**: 9340-9345.

Zhang, Z. Y., Y. Wang and J. E. Dixon (1994b). Dissecting the catalytic mechanism of protein-tyrosine phosphatases. *Proceedings of the National Academy of Sciences USA* **91**: 1624-1627.

Zhang, Z. Y., Y. Wang, L. Wu, B. E. Fauman, A. J. Stuckey, L. H. Schubert, A. M. Saper and D. E. J. (1994c). The $Cys(X)_5Arg$ catalytic motif in phosphoester hydrolysis. *Biochemistry* **33**: 15266-15270.

Zhou, G., J. M. Denu, L. Wu and J. E. Dixon (1994). The catalytic role of Cys124 in the dual specificity phosphatase VHR. *Journal of Biological Chemistry* **269**: 28084-28090.